Connecting the Dots: Linking White Matter Hyperintensity Patterns to Longitudinal Cognitive Changes in Ageing in The Irish Longitudinal Study on Ageing (TILDA)

Michael Courtney
MB, BCh, BAO

A thesis submitted in fulfilment of the requirements for the degree of Doctor of Medicine

Trinity College Dublin, the University of Dublin
2025

Declaration

I declare that the work in this thesis is entirely my own, except where credit is given in the acknowledgements.
The study was approved by the Faculty of Health Sciences Research Ethics Committee at Trinity College Dublin, and all participants provided written informed consent. All experimental procedures adhered to the Declaration of Helsinki.
I declare that this thesis has not been submitted as an exercise for a degree at this or any other university and it is entirely my own work. I agree to deposit this thesis in the University's open access institutional repository or allow the Library to do so on my behalf, subject to Irish Copyright Legislation and Trinity College Library conditions of use and acknowledgement. I consent to the examiner retaining a copy of the thesis beyond the examining period, should they so wish (EU GDPR May 2018).

Signed _____ Michael Courtney

Acknowledgements

Table of contents

List of Figures and Tables

Page #

Thesis list of Abbreviations

ACE	Angiotensin Converting Enzyme
ADEM	Acute Disseminated Encephalomyelitis
AD	Alzheimer's Dementia
AGT	Angiotensinogen
AGTR1	Angiotensin II Receptor Type 1
AMNCH	Adelaide and Meath National Children's Hospital
BMI	Body Mass Index
CAA	Cerebral Amyloid Angiopathy
CAPI	Computer Assisted Personal Interviews
CAR-T	Chimeric Antigen Receptor T-Cell
CGAS	Candidate Gene Association Studies
CSF	Cerebrospinal Fluid
CT	Computed Tomography
CVDE	Cardiovascular Disease Event
DNA	Deoxyribonucleic Acid
DSA	Digital Subtraction Angiography
DTI	Diffusion Tensor Imaging
DWI	Diffusion Weighted Imaging
EPI	Echo Planar Imaging
FA	Fractional Anisotropy
FLAIR	Fluid Attenuation Inversion Recovery
GWAS	Genome-Wide Association Studies
HIV	Human Immunodeficiency Virus
IPAQ	International Physical Activity Questionnaire
JVR	Jugular Venous Reflux
LADIS	Leukoaraiosis and Disability
LME	Linear Mixed Effects
LPA	Lesion Prediction Algorithm
LST	Lesion Segmentation Tool
MD	Mean Diffusivity
MMSE	Mini Mental State Examination
MOCA	Montreal Cognitive Assessment
MRI	Magnetic Resonance Imaging
MS	Multiple Sclerosis
MTR	Magnetisation Transfer Ratio
NAWM	Normal Appearing White Matter
NFT	Neurofibrillary Tangle
NMO	Neuromyelitis Optica
NP	Neuritic Plaques
NT	Neuropil Threads
PET	Positron Emission Tomography
PML	Progressive Multifocal Leukoencephalopathy
PRES	Posterior Reversible Encephalopathy Syndrome
ROI	Region of Interest
SCQ	Self-Completed Questionnaire
SJH	St James Hospital
SLE	Systemic Lupus Encephalopathy
SNP	Single Nucleotide Polymorphism

TE	Time to Echo
TILDA	the Irish Longitudinal Study on Ageing
TR	Time to Repetition
TRIM65	Tripartite Motif Containing 65
VCAM	Vascular Cell Adhesion Molecule
WMH	White Matter Hyperintensity

Abstract

INTRODUCTION

White matter hyperintensities (WMHs) are known to correlate with cognitive decline, stroke, and dementia. Previous research has explored the independent effects of white matter macrostructure, microstructure, and spatial distribution on cognitive function, yet a comprehensive analysis combining these elements is limited. This thesis stratifies WMHs into six distinct phenotypes based on location, volume, and microstructural properties in order to assess their association with cognitive decline over a six-year period.

METHODS

Data was obtained from The Irish Longitudinal Study on Ageing (TILDA), including MRI scans and cognitive performance scores from 497 community-dwelling older adults. WMHs were segmented using the Lesion Prediction Algorithm (LPA) and analysed with fractional anisotropy (FA) and mean diffusivity (MD). K-means clustering identified three primary WMH phenotypes, further stratified by periventricular and deep white matter location, resulting in six lesion phenotypes. Linear mixed effect models were used to assess the relationship between these phenotypes and cognitive decline, adjusting for demographic and health-related variables.

RESULTS

High-volume, low FA WMHs in both deep ($p=0.05$) and periventricular ($p=0.004$) white matter were significantly linked to cognitive decline over six years ($X=12.0$, $P=0.004$). Deep lesions, irrespective of FA or volume, were linked to poorer cognitive performance. Small periventricular lesion with near normal microstructural properties do not predict cognitive decline

CONCLUSIONS

This study provides evidence that WMHs manifest as diverse phenotypes, with specific lesion types associated with cognitive decline. High-volume, low FA lesions in both periventricular and deep white matter are particularly predictive of cognitive deterioration. Identifying WMH phenotypes may inform early intervention strategies and improve patient outcomes by targeting individuals at higher risk of cognitive decline.

Lay Abstract

INTRODUCTION

Thinking, remembering and learning are all a part of what we call cognition. As people get older, these abilities may sometimes deteriorate. For some, the changes are mild, while for others the decline can be more severe. We are interested in why this happens and why it affects people differently. One way to investigate these changes is by using new technology to examine the brain. As we age, tiny blood vessels in the brain may not work as well as they used to and this can leave small spots on brain scans which appear as "white spots". These white spots are common, but we do not fully understand what they mean for memory and thinking. New types of MRI scans allow us to look more closely at these white spots and how they affect the brain. At the same time, new tests of memory and thinking skills make it possible to track how a person's abilities change over time. By bringing these two approaches together, brain scans and cognitive testing, we can learn more about how ageing affects the brain and what these white spots mean for future brain health. Our study shows that not all white spots are the same and bigger, more damaged areas matter the most for future memory problems, while smaller changes don't seem to have much impact.

MD Hypothesis

My hypothesis is that white matter hyperintensities which vary in size, location and microstructural properties are not all the same, and which, depending on size, location and microstructure may correlate with decline in cognitive function.

To test this hypothesis, I investigated the possibility that WMHs visible on MRI scans from the TILDA population can be stratified into coherent groups and correlated the findings with cognitive data from the same cohort.

Outputs

Publications:

Connecting the dots: microstructural properties of white matter hyperintensities predict longitudinal cognitive changes in ageing
Michael Courtney, Daniel Carey, Stephen Murphy, Silvin Knight, James F Meaney, Rose Ann Kenny, Celine De Looze
Frontiers Aging Neuroscience Feb 2025

Presentations:
Connecting the dots: microstructural properties of white matter hyperintensities predict longitudinal cognitive changes in ageing
Michael Courtney
Oral Presentation
European Society of Radiology 2025 Congress

SECTION ONE: GENERAL INTRODUCTION

Chapter 1: History of White Matter Hyperintensities

'White-matter changes are indeed associated with intellectual impairment and somewhat, but not exclusively, with vascular disease' – Vladimir Hachinski.

The debate began and the stage was set by Hachinski in 1987 in the landmark paper which first coined the term "Leuko-araiosis" (1). This initial paper ignited a discourse which has yet to reach its conclusion, which has seen significant evolution and multiple iterations over the decades. With the advances in medical imaging of the time, clinicians were faced with a novel, but increasingly common dilemma encountered in clinical medical and radiological practice; 'It is more likely that we are witnessing the unfounded attribution of a specific pathologic cause to increasingly more sensitive images of the brain'(1). At this time, the periventricular changes identified on computed tomography (CT) and magnetic resonance imaging (MRI) were becoming commonly attributed to Binswanger's Disease (2), an obscure disorder unfamiliar to the great majority of neurologists of the time(3), despite the patients' clinically presenting without any physical signs or symptoms to suggest this diagnosis(4). Binswanger was a prominent German neuropathologist at the time whose original article appeared in a weekly medical newspaper and although further reports were promised, none were ever forthcoming(5). In short order, the phenomenon of leuk-araiosis was described and the community at large trended away from attributing these lesions to Binswanger's Disease.

Once a consensus term was defined to describe the white matter lesions, the work began and the question was posed; what are they? The finding of altered areas of white matter (hypo)attenuation on CT were found to be more obvious, and indeed more extensive, as abnormal areas of signal intensity on MRI due to the latter's better sensitivity for soft tissue changes, particularly for subtle changes in water content, especially once the FLAIR (Fluid Attenuation Inversion Recovery) sequence was introduced(6,7). The lesions were seen to predominate in the periventricular areas and deep white matter and, as they were best seen on FLAIR MRI sequences, the term "white matter lesions" was introduced and remains a common descriptor to this day(8). With the proliferation of MRI during the 1990's, and the replacement of low field strength (0.02 – 0.5 Tesla) scanners with 1.5T MRI scanners which became the industry norm, the WMHs, now more obvious with improvements in contrast and spatial resolution, were encountered with increasing frequency(9). Rapidly CT and MRI employing T1 and T2 weighted sequences were superseded by the FLAIR sequence (T1 being of similar sensitivity to subcortical changes as modern CT scanners, while T2 had improved sensitivity to white matter lesions, but all were less sensitive than FLAIR(10). Thus, the advent of FLAIR sequence revolutionised the evaluation of WMHs and provided an approach that ultimately became available on all MRI scanners, and which would provide the industry standard. Therefore, it is important to consider that the reporting of early scientific findings in relation to WMHs was significantly hindered by the lack of sensitivity of CT and earlier MRI approaches.

The imaging and ageing communities rapidly realised that Hachinski's WMHs, which correlate with areas of leuko-ariosis, were present in a large portion of the population, and were therefore a non-specific sign(11). In the early 1990's, the role of leuko-araiosis in dementia and cognitive decline became established(12) and the nomenclature shifted from leuko-araiosis to cerebral white matter hyperintensities which were easy to visualise employing virtually all standard MRI scanners. Lesions with similar appearances on MRI

were appreciated in stroke(13), therefore a vascular pathogenesis came to the forefront. Diffusion weighted imaging (DWI) was first used in the evaluation of the human brain by Le Bihan in 1986(14) and rapidly became a cornerstone of the evaluation of stroke as it allowed the differentiation of acute stroke (with restricted diffusion) from remote stroke (without restricted diffusion).

Both DWI and FLAIR sequences became central to studies of cerebral WMHs and resulted in significant acceleration in the investigation of cerebral WMHs relative to that seen by Hachinski and their contemporaries in the 1980's.

A variant of DWI, Diffusion Tensor Imaging (DTI) described in 1996 by Pierpaoli, soon followed and allowed understanding of the microstructural properties of tissue and specifically the orientation and integrity of neuronal pathways(15).

Before the advent of cross-sectional imaging, WMHs were not a recognised phenomenon in the world of histopathology(16,17). At the time, the focus of pathological examination centred on small CSF-containing cavities termed "lacunes", which were easier to detect pathologically compared to the subtle changes of WMHs(18,19). The changes of WMHs can be difficult to visualise even on histopathological cross-sectional specimens unless they are particularly advanced(20). When the changes of WMHs are subtle, as in the typical specimen, the full extent of these changes can be challenging to appreciate on histological analysis unless they are specifically sought(21) and differentiated from the multiple processes occurring in the aged specimen or other diseases which can complicate the examination(22).

As technological advancements progressed, novel imaging modalities gave a deeper understanding of the cerebral microstructure and knowledge of white matter hyperintensities has significantly expanded. As early as the year 1990, it was recognised that increasing age correlated with the extent of periventricular WMHs, however no correlation was yet established between the supposed severity of WMHs and the risk of Alzheimer's Dementia (AD) as demonstrated by an early though small investigation by Kozachuk(23). This was one of the first papers to use a semi-quantitative method of lesion analysis which correlated the extent of WMHs based on quantitative assessment. By the mid 1990's authors were investigating WMHs with regard to the size and location of the lesions in an effort to establish a link between cognitive impairment and WMHs. In their 1995 paper, Ylikoski examined large numbers of WMHs using the Helsinki Aging Brain Study in what was a sophisticated analysis for the time. The WMHs were subjectively scored on a scale of 0 – 3 for eight anatomical positions(24). Ylikoski found a positive link between WMHs and vascular risk factors. However, the authors acknowledged that in neurologically healthy elderly individuals, WMHs were also associated with age and other factors. Despite this, these factors only partially explained their development. Their study revealed different patterns in younger and older elderly groups, leading them to suggest that WMHs in the elderly may be influenced by other, yet unidentified, age-related factors(24).

In 1998 Guttmann described the patterns of decreasing normal white matter volume and increasing cerebrospinal fluid (CSF) space in normal ageing(25). As one millennium rolled into the next, the significance of WMHs association with normal and accelerated cognitive decline in ageing became clearer and a broad heterogeneity of WMHs, varying vastly in size and location, became clearer despite the varied landscape of available

technologies across the globe. Importantly, the vast majority of studies agreed that WMHs were positively correlated with advanced age and vascular risk factors. Additionally, the association of WMHs with mild cognitive impairment, dementia, depression, and hypertension became universally accepted.

Chapter 2: White Matter Hyperintensities In Depth

2.1 White Matter Hyperintensity (WMH) definition

The term "white matter hyperintensity" is a descriptor used in the MRI lexicon for a hyperintense lesion on T2/FLAIR imaging in the cerebral or cerebellar white matter(26). These lesions are typically present in the periventricular white matter and deep cortical white matter. One can approach the assessment of WMHs by classifying the lesions into vascular and non-vascular WMHs. While vascular WMHs are far more common, one of the most clinically and academically relevant non-vascular subgroups is the WMHs seen in multiple sclerosis (MS), typically termed MS "plaques". The relevance of MS and the studies of MS plaques will be discussed separately.

2.2 Epidemiology of White Matter Hyperintensities

WMHs are age related and present in approximately 10% to 20% of subjects aged sixty years old and with prevalence approaching 100% in persons aged ninety years and older(27). WMHs have been reported in the Japanese, Chinese, Caucasian, African-American and Caribbean Black demographics, with increasing incidence across all ethnicities with age(28).

2.3 Symptoms of White Matter Hyperintensities

White matter hyperintensities may be symptomatic or asymptomatic. If asymptomatic, this reflects the underlying pathological process and functionality of the lesion location. The lesions are often incidentally detected during routine imaging and are often considered "silent" entities. Typically, small WMHs in the elderly are asymptomatic, but these lesions can progress to large confluent lesions which may be associated with cognitive impairment, dementia, functional decline, urinary incontinence, balance and gait impairment and neuropsychiatric disorders(29).

2.4 Aetiology of White Matter Hyperintensities

Increasing age is the best-known risk factor for cerebral white matter hyperintensities. Other common risk factors include hypertension, diabetes mellitus, hyperlipidaemia, and hyperhomocysteiaemia(28). A number of genetic factors have been identified which suggests a genetic factor to the development of WMHs. Twin studies have suggested a 60% to 80% heritability(30,31).

2.5 Vascular White Matter Hyperintensities

Vascular WMHs are the most common type of WMHs and are typically seen in elderly patients. Vascular WMHs can be organised into periventricular and deep or subcortical WMHs. Periventricular WMHs are the smooth caps around the frontal horns and the linear halo like lesions around the bodies of the lateral ventricles which are commonly seen on MR studies in the aging population(32). The periventricular white matter is accepted to lie within 15mm of the ventricles(33). Lesions classified as deep WMHs are the punctate or more confluent lesions which are more distant from the lateral ventricles and occupy the subcortical white matter. The underlying pathophysiology of these lesions is thought to relate to chronically reduced blood flow, though the exact mechanism depends on the cause.

Imaging Findings of Cerebral White Matter Hyperintensities
Cerebral white matter hyperintensities appear as areas of increased signal intensity on T2-weighted and FLAIR imaging sequences. The size and morphology of these lesions can vary greatly and the absence of additional imaging features such as associated mass effect, necrosis/cavitation, enhancement, diffusion restriction and susceptibility on gradient imaging helps differentiate vascular WMHs from those related to specific pathological entities. The anatomical distribution of these changes is noteworthy with most authors agreeing that the white matter of the corpus callosum, the temporal lobe and the cerebellum are normally spared from typical vascular white matter changes(34). The periventricular white matter is most commonly involved. The subcortical band of white matter containing arcuate fibers is not altered in age related white matter disease, supposedly due to the dense capillary network in this region and lesions in these areas are typically secondary to pathological processes such as immune mediated systemic diseases. White matter hyperintensities may be graded using a four-point Leukoaraiosis And DISability (LADIS) scale as follows; grade 0: no changes, grade 1: punctate lesions, grade 2: early confluent, grade 3: confluent(35–37).

Periventricular and Deep White Matter Anatomical Supply
Chronic small vessel disease or cerebral microangiopathy are terms frequently ascribing the underlying cause of periventricular white matter lesions. Diminished blood flow is commonly cited as the leading cause of WMHs. The periventricular cerebral white matter is supplied by the long perforating branches of the relevant cerebral arteries, boosted by supply from the ventriculofugal vessels, the terminal branches of the subependymal arteries, which in turn arise from the anterior choroidal artery, a branch of the internal carotid artery(38). The terminal long perforators and the ventriculofugal vessels do not anastomose (i.e. they are end arteries), and the periventricular white matter is therefore a watershed/borderzone area(39). Watershed or border zone areas of the cerebral parenchyma are vulnerable to ischaemic or hypoperfusion injuries due to the vulnerable nature of their blood supply. Studies using PET/CT and digital subtraction angiography (DSA) have revealed increased oxygen demand of watershed regions in ischaemia relative to other areas implying further susceptibiltiy. Hypertension causes arteriosclerotic changes of the terminal subependymal arteries leading to susceptibility to hypoperfusion and eventual ischaemic damage in the periventricular white matter(40).

The deep white matter is vulnerable to hypoperfusion from anatomical factors for different reasons. The cerebral deep white matter is supplied by the cerebral arteries which terminate with the short branches of the long perforating arteries. These perforators follow a long winding course and provide the only avenue for the terminating short vessels to deliver blood to the deep white matter. Further evidence to the vulnerable nature of this route of supply comes from the cortical U-fibers which receive supply from the separate nutrient branches as well as the short branches(38). As a result, WMHs are rarely if ever seen in the U-fibers.

Animal studies have demonstrated that cerebral hypoperfusion directly leads to ischaemic damage to the watershed areas, suggesting WMHs originate from ischaemia(41).

Cerebral Blood Flow Autoregulation
The causes of ischaemia are more complex and multifactorial than purely mechanical/anatomical blood supply. Dynamic changes in cerebral blood flow can cause

ischaemia and impaired cerebral blood flow autoregulation is the most common type of haemodynamic abnormality(42). Haemodynamic changes have been found to play an important role in the pathogenesis of ischaemic changes.

Dynamic cerebral autoregulation plays a role in the aetiology of ischaemic stroke but has varied characteristics depending on the type of stroke(47). Autoregulation processes in large vessel atherosclerosis and small vessel occlusion differ greatly. Static cerebral autoregulation refers to the overall efficiency of cerebral blood flow overall, while dynamic cerebral autoregulation refers to the ability to restore cerebral blood flow in the event of sudden changes in perfusion(48). Cerebral autoregulation manifests via the ability of the artery to modulate arterial wall smooth muscle tone and stiffness, thereby maintaining cerebral blood flow(49). For example, it has been proposed that in the case of aortic stenosis, deficits in large vessel autoregulatory are associated with angiectasis and impaired smooth muscle tone of large vessels causing impaired vessel expansion and resultant hypoperfusion(50). In contrast, in cerebral small vessel disease, impaired dynamic cerebral autoregulation is present and implicated in the development of WMHs. The pathological mechanism of the global impairment may relate to arteriosclerosis, characterised by the loss of smooth muscle cells from the tunica media, luminal stenosis, fibro-hyaline deposition and inflammation or thickening of the vessel wall(51). These processes coalesce and result in increased vessel stiffness and impaired elasticity which culminate in reduced compliance and impaired systolic and diastolic functions of the vessels(45,52). These factors lead to diffuse small vessel impaired dynamic autoregulatory function which has been shown to lead to the inhibition of the clearance of emboli, unregulated cerebral blood flow and eventually embolisms to tiny terminal cerebral vessels(53,54). Impairment of cerebral small vessel dynamic autoregulation has been shown to be a global process with diffuse impact on small arteries, arterioles, capillaries and venules, culminating in periventricular and deep white matter ischaemia, directly leading to the formation of WMHs(55).

The Relationship of WMHs and Alzheimer's Disease

WMH burden is closely associated with Alzheimer's disease(56,57). Alzheimer's disease is associated with progressive neuronal death which is primarily attributed to the deposition of toxic intracellular tau proteins and extracellular amyloid-beta proteins(58). Impaired small vessel dynamic cerebral autoregulation promotes the deposition of amyloid-beta and leads to poor clearance of amyloid-beta(59,60). Amyloid-beta deposition damages endothelial cell function leading to increased vascular wall stiffness(61,62). Importantly, amyloid accumulation alone may not directly cause neuronal death or dementia; increasing evidence suggests a synergistic interaction of amyloid pathology with tau pathology and neuroinflammatory responses driving disease progression. Therefore, while amyloid deposition, particularly in the setting of cerebral amyloid angiopathy (CAA) is central to the vascular component of Alzheimer's disease, it should be considered just one element of a broader cascade including tau pathology and inflammation. An overall larger volume of cerebral WMHs is seen in individuals with AD than the general population(63). WMHs in posterior brain regions predict progression to AD and the number increase several years before symptom onset in autosomal-dominant AD(64). A detailed discussion of tau pathology is provided below in the histopathology section.

Venous Ischaemia and The Pathophysiology of WMHs.

A potential role for venous ischaemia in WMH formation has gained traction in contemporary literature. Collateral venous outflow from the brain has important pathophysiological consequences and occlusion of the principal outflow from the internal jugular veins can be compensated almost completely by the large vertebral plexuses. Outflow from the deep venous system via the great vein of Galen, when occluded, can be substituted by the choroidal, thalamic and striate anastomoses to the basal vein. However, intracerebral venous anastomoses through the centrum semiovale (the deep white matter) are non-existent, resulting in an extensive venous watershed in the periventricular and deep white matter(65). Venous occlusion results in vasogenic oedema and disruption of the blood brain barrier, rather than direct hypoperfusion(66). Venous ischaemia is purported to be a more chronic, indolent process and aligns with the changes seen in WMHs and cognitive impairment. While not disagreeing with the earlier claim of Andeweg et Al that jugular outflow can be replaced entirely, later studies have demonstrated that unilateral jugular venous outflow obstruction results in limited drainage via the bilateral deep vein system and watershed area due to venous reflux into the superior sagittal sinus or transverse sinus, resulting in bilateral WMHs with clinical findings typical of other causes of WMHs(67). This contrasts with the outcomes seen in unilateral carotid arterial disease which are more commonly associated with the symptoms of classic territorial stroke rather than chronic small vessel disease.

Jugular venous reflux (JVR) occurs when there is an abnormal pressure gradient, the extent of which is greater than the competence of the jugular valves(68), a phenomenon commonly seen in the Valsalva manoeuvre. In the event of downstream venous occlusion or obstruction, the elevated jugular pressure gradient would result in baseline JVR. Sustained JVR results in elevated pressure across the sigmoid sinus into the deep cerebral venous system which results in decreased cerebral perfusion and consequent cerebral ischaemia(69). The pathophysiological changes seen in persistent JVR include blood brain barrier dysfunction, venule collagenosis, cerebral blood flow autoregulation impairment and endothelial cell dysfunction(70–72). Another relevant concept in venous dysfunction is that of pulse wave encephalopathy, whereby vascular dysfunction and increasing arterial stiffness with advancing age is associated with increased systolic pressure transmitted to the brain, damaging the relatively fragile cerebral microcirculation, leading to abnormal cerebral perfusion(73).

The Blood Brain Barrier and Vascular White Matter Hyperintensities

Several studies have confirmed the association between blood brain barrier disruption and cerebral WMHs. The blood brain barrier consists of fenestration free endothelial cells with tight junctions, a basement membrane and a perivascular end-feet of astrocytes(74). The barrier provides a safe environment for the central nervous system and maintains neuronal stability. Histopathological studies have shown an association between white matter disease and diffuse abnormalities of cerebral blood vessel outer membrane and smooth muscle layers resulting in breakdown of the blood brain barrier(19).

Permeability of the blood brain barrier is implicated in the pathogenesis of WMHs. The entry of potentially noxious substances including serum proteins, complement and fibrinogen into the cerebral white matter following damage to the blood brain barrier contributes to WMHs. There is greater leak of contrast agents in the perforating arterial watershed areas of patients with WMHs than patients without WMHs(75). Increased permeability of the blood brain barrier is present in diabetes mellitus and hypertension, common risk factors for WMHs. Acute cerebral ischaemic events in the brain are

associated with cerebral oedema on MRI indicating disruption of the blood brain barrier, with imaging findings persisting for weeks. Blood brain barrier permeability can be quantified using the ratio of CSF albumin to serum albumin as a surrogate marker and by dynamic MRI perfusion(76). Increased permeability of the blood brain barrier is short lived in acute stroke, but, in contrast, permanently elevated permeability of the blood brain barrier has been identified in individuals with vascular dementia compared to control groups(77). Therefore, WMHs are associated with permeability of the blood brain barrier. Histopathological studies have demonstrated the presence of blood brain barrier damage in both WMHs and surrounding normal appearing white matter, thereby positing that blood brain barrier disruption is a cause of WMHs, and does not occur because of WMHs(78). Animal studies have demonstrated the presence of blood brain barrier damage before subcortical ischaemic changes(79) and have shown that with increasing duration of hypertension there is decreased expression of molecular constituents of the blood brain barrier and subsequent worsening of WMHs(80).

Hypertension and White Matter Hyperintensities

Hypertension is the leading preventable cause of cardiovascular disease and is currently estimated to affect one in three adults worldwide(81). Hypertension is one of the strongest and most consistently reported risk factors for the development and progression of white matter hyperintensities(80,82). Chronic elevation of blood pressure contributes to small vessel disease through arteriolosclerosis, impaired autoregulation, and disruption of the blood–brain barrier. These processes result in reduced perfusion of periventricular and deep white matter, making these regions particularly vulnerable to ischaemic injury.

Several large population studies, including the work of Wardlaw et al.(9), have demonstrated both the association between hypertension and WMH burden and the potential modifying effect of antihypertensive treatment. Previous studies have demonstrated that even in people with well controlled hypertension, increased systolic blood pressure is associated with clinically silent brain injury such as brain atrophy(83,84). More novel techniques have demonstrated subtle microstructural changes are associated with hypertension, for example altered fractional anisotropy in the anterior corpus callosum has been associated with hypertension in multiple studies, notable as altered fractional anisotropy in this region is associated with cognitive decline and dementia(85–87). These findings highlight the importance of recognising hypertension not only as a risk factor for WMHs, but also as a potential target for intervention to slow their progression and reduce associated cognitive decline.

Genetic Factors in Vascular White Matter Hyperintensities

Genetic factors have been shown to play a role in the development of WMHs. Framingham study subset analysis found high heritability of WMH overall and similar heritability for both men and women in a family-based study comprising generally healthy individuals(88). Genome-wide linkage analysis has demonstrated WMHs are linked to chromosomes 1(89), 4(90), 5 and 11(91). Two fields of research have emerged exploring the genetic impact on WMHs, these are candidate gene association studies (CGAS) and genome-wide association studies (GWAS). Genetic studies on WMHs suggest that their pathogenesis involves the activation of multiple cellular pathways and molecular mechanisms such as inflammatory cascades and oxidative stress mechanisms(92). CGAS led to the discovery of multiple genes related to WMHs which are associated with biological processes including ApoE regulation of cholesterol(93), AGT, ACE and AGTR1 regulating blood pressure and cerebral blood flow(94,95).

GWAS have revealed WMH susceptibility genes but have also informed research into the molecular mechanism of WMHs. In a genome wide association study to search for gene mutations in 9361 individuals with WMHs, a single nucleotide polymorphism on the second intron (a non-coding sequence of DNA) of human TRIM65 gene locus was significantly associated with WMHs(31). TRIM65 is a physiological E3 ubiquitin ligase of vascular cell adhesion molecule 1(VCAM-1) and is expressed in human vascular endothelial cells(96). TRIM65 plays a role in the inflammatory cascade in vascular endothelial cells and the expression of this single-nucleotide polymorphism (SNP) likely predicts the development of cerebral WMHs(97). It should be noted however that there are few large-scale studies examining the genetic basis of cerebral WMH and of the available data in the literature the associations suggested in CGAS are not reproduced in the GWAS studies. Further research into the genetic basis of WMHs is needed.

2.6 Non-Vascular White Matter Hyperintensities

WMHs of non-vascular aetiology are less common than typical vascular WMHs. In clinical practice, these lesions are typically regarded simply as 'lesions,' rather than being described as white matter 'changes'; a term often used for WMHs of vascular or age-related origin. Compared with vascular diseases, other pathological processes resulting in cerebral WMHs tend to result in a greater variety of clinical symptoms and signs, often related to the underlying aetiology and spatial distribution of the lesions. Typical vascular WMHs are felt ultimately to be the result of chronic ischaemia and small vessel disease. Risk factors such as hypertension, impaired cerebral autoregulation and blood-brain barrier dysfunction act upstream, promoting arteriosclerosis and vessel wall changes. These processes converge on a final common pathway of reduced perfusion and chronic ischaemia driving the development of WMHs. Non-vascular WMHs typically arise from demyelination, inflammation and metabolic disorders, though inflammation is a complex topic with focal and systemic processes discussed in detail separately. In these non-vascular cases, the clinical manifestation of the disease entity often prompts neurological investigations, rather than the typical course in vascular WMHs, which tend to be incidentally detected. The non-vascular causes of cerebral WMHs can be classified as follows; toxic or metabolic, leukodystrophy or mitochondriopathy, infectious, neoplastic and immune mediated.

The following lesions differ from the typical vascular age-related WMHs in their imaging characteristics in several ways. These non-vascular entities tend to be symmetric and widespread, with many entities demonstrating characteristic anatomical distributions, such as the posterior cerebral hemisphere distribution seen in heroin and cocaine inhalation(98), the midline crossing butterfly glioma or the mass-like, enhancing soft tissue which intensely restricts diffusion seen in lymphoma.

Toxic White Matter Disease

A wide variety of substances can result in cerebral WMHs spanning banned substances, medications and environmental toxins. These chemicals produce WMHs by a different mechanism, acting on the myelin, oligodendroglia, axons and astroglia of the white matter inducing toxic leukoencephalopathy with demyelination as the common histopathological endpoint(99). An increasingly common contemporary cause of toxic neurological insult presenting with subtle WMHs is inhalation of nitrous oxide(100). Another cause of toxic leukoencephalopathy is the so-called post hypoxic demyelination observed after carbon monoxide poisoning. Toxic insults tend to cause diffusion restriction and may be seen to affect the corpus callosum. The rare Marchiafava-Bignami

disease is a nutritional form of a metabolically induced leukoencephalopathy associated with malnutrition in the setting of severe alcohol disease which localises to the splenium of the corpus callosum, resulting in diffusion restriction and axonal necrosis in severe cases(101). Other causes of toxic WMHs include B12 and copper deficiency. The inherited autosomal dominant disorder of acute intermittent porphyria may manifest large subcortical white matter lesions which may demonstrate postcontrast enhancement. A novel cause is the newly described immune effector cell-associated neurotoxicity syndrome (ICANS) which is seen as an adverse effect following administration of a novel chimeric antigen receptor T-cell (CAR-T) form of immunotherapy for the treatment of haematological malignancies, primarily lymphoma and manifest radiologically as FLAIR signal white matter hyperintensities in a variable distribution(102–104).

Leukodystrophies and Mitochondriopathies

The leukodystrophies and mitochondriopathies are inborn errors of metabolism which can occur sporadically or manifest in a heritable fashion. While typically manifesting at a young age, although some of these diseases may present later in life. Even in cases of a single well-defined disorder, the lesion pattern in these entities may vary depending on the age of onset. The leukodystrophies tend to affect subcortical white matter, while the mitochondriopathies affect grey matter(105).

Infectious Causes of White Matter Hyperintensities

The neurotoxic HIV often affects the white matter resulting in cognitive impairment and, in up to 20%, dementia. HIV encephalitis is characterised by widely disseminated lesions of astrogliosis, nodules of microgliosis, white matter loss and characteristic multinucleated giant cells of HIV encephalopathy(106). In cases of HIV encephalopathy MRI reveals confluent and nearly homogenous WMHs predominantly in the centrum semiovale sparing the subcortical U-fibers. Histopathological cross section in these cases shows diffuse and symmetrical pallor of the myelin corresponding to the spatial described on MRI(107).

Progressive multifocal leukoencephalopathy (PML) occurs in approximately 5% of HIV patients and is occasionally seen in other immune-deficient states. PML, caused by the JC polyomavirus, infects and destroys oligodendrocytes and produces intranuclear inclusions resulting in severe demyelination. MRI features are characteristic showing multifocal and asymmetric non-enhancing lesions in the subcortical white matter, including the U-fibers. The lesions are hyperintense on FLAIR sequences and, unlike vascular WMHs, are most pronounced in the grey-white matter junction, spreading along fiber tract without associated mass effect(108).

Other pathogens such as cytomegalovirus, human-simplex virus, neurosyphilis and many fungi all result in hyperintense white matter lesions. The lesions tend to enhance and have a significantly more diverse range of imaging distribution compared to typical vascular WMHs(109).

Neoplastic White Matter Lesions

Typical adult brain tumours originate from astrocytes as glial tumours with local mass effect, diffusely infiltrating along white matter fiber tracts of white matter, manifesting as hyperintense signal on T2-weighted imaging and FLAIR sequences(110). These lesions are readily distinguished from vascular WMHs in a number of ways. Brain tumours, being highly cellular may be associated with restricted diffusion, which is not present in

vascular WMHs. Additionally, tumours result in mass effect as they grow, resulting in oedema of the surrounding brain parenchyma, a phenomenon not observed in vascular WMHs. Primary CNS lymphoma is typically a diffuse large B-cell tumour in immunocompetent individuals which demonstrates restricted diffusion and enhancement(111).

Immune Mediated White Matter Lesions

Multiple sclerosis is the most common immune mediated cause of white matter hyperintensities. Other inflammatory or autoimmune cause such as acute disseminated encephalomyelitis (ADEM), neuromyelitis optica (NMO) and systemic lupus erythematosus (SLE) produce similar WMHs but are less common causes of immune mediated white matter disease(112).

Multiple sclerosis is of particular interest as the diagnostic criteria of MS, which have seen several iterations over time, have placed consistent emphasis on the dissemination of white matter lesions with regards to time and space. White matter lesions in MS are characteristically seen in the juxtacortical, periventricular and infratentorial white matter with frequent cord involvement(113). MS plaques sometimes have a unique, disease specific distribution and are important for disease monitoring. Assessing the impact of disease modifying treatments has influenced the development of software which specifically isolates and measures white matter hyperintensities. Some of the first software packages developed to automatically segment WMHs used young patients with known MS plaques as subjects in software trails. The tools developed were later found to be effective in segmenting WMHs of presumed vascular aetiology in older populations, which speaks to the similar imaging properties of these lesions.

While most basic automatic lesion segmentation algorithms typically will not discriminate between MS plaques and WMHs of other aetiologies, it is usually possible to discern an MS plaque from a vascular WMH by evaluating the lesion location and assessing for lesion specific signs seen in MS. MS plaques may demonstrate lesion specific characteristics such as the central vein sign or a paramagnetic rim lesion, features which are helpful biomarkers of MS plaques(114,115). The central vein sign is the imaging manifestation of the perivenular nature of demyelinating plaques and appears as a vein coursing centrally through a demyelinating plaque. While not pathognomonic, the central vein sign is useful in differentiating MS plaques from mimics. Paramagnetic rim lesions, sometimes called iron rim lesions, are typically seen in relapsing or progressive MS and are highly specific for MS. These lesions reflect chronic or low-grade inflammation and iron accumulation within macrophages at the edge of lesions. The paramagnetic properties of iron result in a hypointense rim on susceptibility weighted sequences resulting in the typical imaging appearance. As well as these morphological findings, the location of MS plaques can be helpful in distinguishing the lesions from typical WMHs. MS plaques may occur in the cortical white matter and the spinal cord, whereas vascular WMHs most often affect the deep and periventricular white matter and are not seen in the spinal cord.

2.7 Histopathological Findings of Age-Related White Matter Hyperintensities

Post-mortem histopathological studies have repeatedly demonstrated arteriosclerosis and small vessel ischaemic disease as the pathological correlates of typical vascular WMHs and disruption of white matter integrity in aging(116). For example, one cross sectional study examined the pathological correlates of white matter hyperintensity burden in 93

subjects and found arteriolosclerosis was independently strongly correlated with WMH volume(117).

In older individuals, the presence of extensive neurofibrillary tangle pathology is associated with WMH accumulation over time(118). One of the most conspicuous brain related changes seen in Alzheimer's Disease is the development of intraneuronal cytoskeletal changes partly formed of abnormally phosphorylated tau protein. This material develops in the form of neurofibrillary tangles (NFTs), neuropil threads (NTs) and argyrophilic components of neuritic plaques (NPs). NFTs develop within the nerve cell body while NTs are found in the distal dendritic processes(119).

Neurofibrillary tangles are composed of bundles of abnormal filaments accumulating in neuronal perikarya, dendrites and axons. When viewed under electron microscope, these filaments show regular constrictions or can appear straight having been described as two filaments helicoidally twisted around each other, lending credence to the term "paired helical filaments"(120). Neuropil threads are composed of small curled dystrophic neurites dispersed in the neuropil and containing abnormal filaments. Classical NFTs are composed of tightly packed bundles filling a part of the cell body and extending into the dendrites. Neuronal death is accompanied by a partial disaggregation of the NFT(121).

Possible explanations for the association between more advanced NFTs and WMH accumulation have been proposed. These include NFT-induced Wallerian degeneration of myelinated axons, leading to white matter disruption manifesting as WMHs on MRI. Another potential explanation is ischaemic necrosis of axons leading to NFT formation and neuronal degeneration, again manifesting as WMHs on MRI. Evidence from traumatic brain injury research suggests that axonal injury may cause disorganisation of the cell cytoskeleton triggering tau phosphorylation and aggregation(122). It has been suggested that the correlation between NFTs and WMHs may stem from a shared underlying pathological mechanism contributing to both. In this eventuality, ischaemia may lead both to changes in the white matter as well as trigger processes that lead to neurodegeneration of AD such as abnormal tau protein synthesis, tau hyperphosphorylation and subsequent aggregation (123,124). In animal studies, reduced cerebral blood flow has been demonstrated to lead to the accumulation of amyloid beta oligomers and increase both neuronal amyloid beta levels and neuronal tau phosphorylation(125).

Observational studies in humans have demonstrated a strong association between cerebrovascular disease risk factors and both a clinical diagnosis of AD, as well as the neuropathological changes that accompany AD(126). A Korean population-based study demonstrated an association between coronary artery calcification, a surrogate for atherosclerosis, and cerebral WMHs(127). High levels of atherosclerosis have been shown to be associated with increased NFTs. An autopsy study examining the frequency and severity of cerebral atherosclerosis found atherosclerosis to be present to a significantly higher degree in individuals with AD when compared to the normal control group and individuals with other neurodegenerative disease. Across the entire study population and within individual sub-groups, atherosclerosis ratings were highly correlated with NP, NFT and cerebral amyloid angiopathy ratings using the circle of Willis atherosclerosis scoring system(128).

Chapter 3: White Matter Hyperintensities and Ageing

3.1 White Matter Hyperintensities in the Ageing Population

Ageing is a complex, heterogenous and multifaceted process that is characterised by "intrinsic deterioration with time that causes decreases in strength, endurance and fecundity, and increases in disease susceptibility and likelihood of death"(129). The underlying cause of ageing remains unclear and there is a wealth of theories proposed across multiple different categories including evolutionary, molecular, cellular and systemic causes(130). The cardiovascular effects of ageing include endothelial cell dysfunction, increased arterial stiffness, increased left ventricular stiffness and decreased autonomic function(131). Multimorbidity becomes increasingly more prevalent with ageing. Barnett et al found increased rates of multimorbidity (at least two chronic conditions) in a cross-sectional study of Scottish community dwelling adults - 30.4% in adults aged 45-64 years and increasing to 64.9% at age 65-84 years, and to >80% for adults over 85 years(132).

WMHs increase with age, as previously discussed, likely due to a combination of factors including increased burden of chronic disease, higher incidence of cardiovascular conditions such as hypertension with increasing age and reduced cerebral blood flow with age(133). One of the primary causes of WMHs is cerebral small vessel disease referring to damage of the small blood vessels in the brain. As age increases, the small blood vessels undergo arteriosclerosis, vessel wall thickening and impaired elasticity which leads to reduced blood flow and chronic low-grade ischemia. This reduced perfusion results in ischemia causing demyelination and neuroaxonal damage, which underlie the structural damage seen in WMHs(134).

The chronic low-grade activation of the innate immune system that accompanies ageing, sometimes referred to as "inflammageing" is proposed to contribute to the development of cerebral WMHs through a series of pathogenic cascades triggered by dysfunction of the circadian clock, gut dysbiosis, immunosenescence or impaired cholinergic signalling(135). The systemic, cellular and molecular characteristics of ageing identified by López-Otín et Al. include mitochondrial dysfunction, cellular senescence and chronic inflammation(136,137). Sustained inflammation has been shown to lead microglial activation with resultant weakening of the blood brain barrier(138), a known cause of WMHs. Chronic inflammation in ageing is also associated with neuronal loss, disruption of myelin sheaths and axonal injury(139), pathological processes which lead to the development of WMHs. Although the brain has long been considered an immune-privileged organ with limited exposure to peripheral immune challenges, in the context of "inflammaging" and the dysregulation of the neuro-immune axis, the brain becomes increasingly vulnerable(140). The sequalae of these vulnerabilities manifests as cerebral atrophy, grey and white matter loss, increase in extracellular water, demyelination and the accumulation of cerebral WMHs(141). This low-grade activation of the innate immune system seen in ageing differs from the focal, adaptive immune-driven demyelination seen in MS. While both processes feature white matter injury with inflammatory components and blood brain barrier disfunction, the lesions seen in age related changes are associated more typically with chronic microvascular damage. These lesion typically manifest as non-enhancing lesions in the vulnerable periventricular area, while the pathognomonic MS plaques are associated with focal (T- and B- cell mediated demyelination) immune processes, resulting in lesions disseminated in time and space with frequent enhancement.

3.2 White Matter Hyperintensities and Hospital Presentations

Reflecting the demographics of an increasing ageing population and the association of WMHs with ageing, WMHs are increasingly identified on brain MRI in hospital inpatients. In 2004 in the United States of America, there was an admission rate of 36 hospitalisations per 100,000 US adults per year, but this figure increased to 233 per 100,000 when adjusted for adults aged 75 years and older(142). Therefore, whilst cerebral WMHs per se are asymptomatic and not a direct cause of hospital admission, hospitalisation of older adults in whom decline of global and domain specific cognitive domains is to be expected WMHs may be a surrogate for mental decline. The clinical impact of this accelerated decline will depend on the individuals baseline cognitive reserve and expected longevity, factors upon which WMHs bear influence(143).

3.3 White Matter Hyperintensities and Mortality

There is a clear association between WMH burden and mortality in particular due to cardiovascular disease and dementia related complications. The relationship between WMH burden and death rates remains significant even after adjusting for traditional vascular risk factors such as hypertension and diabetes. In a large population-based study involving 2229 Framingham Offspring Study participants, Debette et al found that increasing WMH volume was associated with an increased risk of death independent of vascular risk factors and of interim stroke and dementia(144).WMHs may therefore serve as a biomarker to identify individuals at adverse risk of healthcare outcomes, prompting detection and management of risk factors and important step in reducing mortality of these patients(145).

3.4 Evaluation of Patients with Cerebral White Matter Hyperintensities

The work up of patients with cerebral WMHs includes a standard medical history and physical examination. Evaluation should be broad with the goal of uncovering the presence of hypertension, diabetes mellitus, dyslipidaemia, current or previous smoking history and quantification of alcohol use. Laboratory investigation centres around screening for vascular risk factors with relevant laboratory tests including a complete metabolic panel, fasting lipid profile and HbA1c. The clinician should clarify the patient's cognitive status, using any number of clinical cognitive assessment tools including but not limited to the Mini-Mental State Examination (MMSE) and Montreal Cognitive Assessment (MoCA)(146,147). Imaging plays an important role in excluding other causes of cognitive or neurological disorder. CSF analysis may be required in atypical cases where the presence of oligoclonal bands would suggest multiple sclerosis or acute disseminated encephalomyelitis (ADEM), and antiviral antibodies might suggest an infectious demyelinating cause. In cases where an underlying neurological cause is identified, MR imaging is useful to monitor the burden of cerebral WMHs(148) with a higher burden of WMHs indicating more advanced disease and increased likelihood to progress to cognitive impairment.

3.5 Treatment of Vascular WMHs

While the understanding of the pathophysiology of WMHs and their relationship to cognitive decline has improved in recent times, treatment of the lesions is usually confined to patients with identifiable underlying neurological conditions such as MS. In patients without underlying neurological diseases in whom the WMHs are silent biomarkers of the underlying disorder, little attention has been given to the treatment of

lesions. Nonetheless, understanding of the underlying aetiology of white matter disease allows clinicians and researchers to focus effort on effective treatment strategies of the associated condition(149,150).

Traditional dogma states that white matter disease once established is inert or progressive, however novel research has demonstrated restorative properties and plasticity attributable to cerebral white matter. A particularly interesting study by Wardlaw et Al of patients who presented with minor stroke demonstrated a reduction in WMH volume at 1 year following initiation of medical therapy targeted at vascular risk factors. Their patients strictly adhered to treatment algorithms according to UK guidelines (antiplatelet therapy, statins, antihypertensive medication, anticoagulation in cases of atrial fibrillation and cessation of smoking). Patients were encouraged to exercise and address other relevant lifestyle factors. Specifically, the authors found that reduction in blood pressure was significantly associated with decrease in WMH volume at one year follow up. Interestingly they also found that the mean diffusivity of normal appearing white matter also reduced in the individuals in which WMH volume was decreased, an expected finding countering the belief that WMHs are simply inert end products of damaged brain(151). While Wardlaw's study did not highlight a single treatment to account for the reduction in mean diffusivity, other authors showed that modification of vascular risk factors leads to improved cognitive outcomes in elderly populations with a significant burden of white matter disease(152). Histopathological studies have demonstrated that recovery of white matter is more likely when neuronal axons are preserved as myelin can be restored if the axonal cylinders remain intact, but the opposite is not the case(153). WMHs seen in typical vascular white matter disease, rather than autoimmune demyelinating or metabolic disease, are characterised by ischaemic demyelination with relative axonal preservation(154), indicating the potential to regress with treatment.

The ability of WMHs to regress is explained by the concept of neuronal plasticity. Plasticity is a property of both grey and white matter and refers to the capacity of the brain to change with experience(155). In cerebral white matter, plasticity is attributed to myelin and refers to enhanced myelination with experience(156). The concept is well established in nonhuman animal models in which the formation of myelin has been identified as a mechanistic basis of learning, complementing grey matter via traditional synaptic function. In essence, activity dependent myelination is the ability to lay down new myelin in the distal axon as a function of proximal electrical activity(157). This phenomenon means that environmental experience, which increases the electrical activity of axons, can influence myelination of distal axonal segments, improving neural circuit plasticity. Studies of white matter plasticity in cognitively normal individuals have demonstrated that white matter microstructure can be altered by a range of activities, generally activities which are mentally stimulating such as piano practice, physical exercise and memory training(158). White matter changes have been shown to occur in as little as two hours in young adults. In this study, healthy adult subjects were trained in a spatial learning exercise for two hours, with diffusion tensor MRI performed between training exercises demonstrating alteration in diffusion indices of the hippocampus and parahippocampal gyri(159). The relevant literature is sparse in disease states; however, the concept has been proven in individuals with Broca's aphasia following left sided infarction who underwent melodic intonation therapy resulting in an increase in the size of the right arcuate fasciculus with resultant language improvement(160). Neuronal plasticity is a characteristic of cerebral white matter which should be exploited in the treatment of cerebral WMHs.

Treatment of WMHs is dependent on brain plasticity and centred on controlling vascular risk factors. Education about risk factors with early intervention aimed at preventing the development or progression of WMHs is appropriate. Incidental detection of WMHs on imaging of older patients this should prompt management of vascular risk factors through control of hypertension, tight glycaemic control, management of dyslipidaemia, promotion of physical fitness, smoking cessation/avoidance and alcohol reduction/avoidance. Antiplatelet therapy has been shown to improve outcomes in vascular disease(161).

The findings of Wardlaw et Al were reproducible in a number of large cohort studies, with the key factor of regression of WMHs being the control of hypertension(162–164). A consistently noteworthy outcome in these analyses, was the finding that intensive treatment of hypertension reduced conversion from normal cognition to mild cognitive impairment(165).

SECTION TWO: ADVANCED IMAGING OF WHITE MATTER HYPERINTENSITIES

Chapter 4: Imaging of White Matter Hyperintensities

4.1 Introduction to Magnetic Resonance Imaging.

Magnetic resonance imaging is a relatively young imaging modality compared to its counterparts in the Radiology Department, yet has its roots firmly set in the 19th century when one Nicola Tesla devised the first rotating magnetic field in 1882. In the present day we measure magnetic field strength in units derived from his name. Despite these seemingly archaic origins, it took almost one hundred years for the first magnetic resonance images to be successfully produced when Lauterbur overcame the problem of spatial localisation(166). By contrast, many of the other imaging modalities employed in the Radiology department had already been firmly established by this point, with the first radiograph produced by Rontgen in 1895(167), ultrasound images arrived in the 1940's(168) and of course the advent of computed tomography in the 1960's due to the efforts of Godfrey Hounsfield(169).

MR imaging is founded on the principle of Spin. In classical physics, a rotating object possesses the property of angular momentum, a form of inertia. This property of inertia is based on the object's shape, mass and rotational velocity. Atomic and subatomic particles, from which MR images are derived, possess a corresponding property known as Spin. The property of Spin was first exploited in 1938 by Isidor Rabi who successfully passed a particle beam through a magnetic field and demonstrated that the particles could be made to emit radio-waves at a frequency which depended on the particle charge and strength of the magnetic field(170). In short order, the same principle was applied to solids and liquids. Spin theory is applied to human biology as the human body is 70% composed of water and therefore hydrogen molecules, which due to their proton number being higher and different to their neutron number possess a net dipole moment allowing hydrogen atoms to precess or "spin" on its own axis, producing a small magnetic field. When hydrogen protons are exposed to a strong external magnetic field, all of the "spinning" protons will align in a parallel or antiparallel line to the applied magnetic field. Slightly more protons will align in the parallel direction, also known as a low energy state, compared to the antiparallel direction, also known as the high energy state (Figure 1)(171). The net magnetic vector produced by the small number of extra protons aligned in the parallel direction is the source of the MR signal and is used to produce MR images. Protons "Spin" around this parallel longitudinal axis at a precession rate known as the Larmor frequency, which is directly proportional to the magnetic field strength(172). Subsequent application of a radio-frequency pulse wave to the hydrogen atoms causes the nuclei to undergo a process releasing or absorbing energy which induces a voltage that can be detected, measured and recorded. The water molecules, and thus the hydrogen atoms, in the human body have different energy states, depending on their chemical composition with the result that the relaxation times of these different tissues will be different when the same radio-frequency wave is applied, and subsequently switched off. Therefore, the resultant induced signal is unique to each individual soft tissue structure based on chemical composition. This is the principle that underlies magnetic resonance imaging(173).

When the radiofrequency pulse is switched off, protons will begin to realign to equilibrium state, i.e. the magnetic field direction, in a process termed relaxation. Relaxation occurs in two ways known as T1 relaxation and T2 relaxation. In T1 relaxation, protons exchange energy with surroundings to return simply to their low energy state along the longitudinal axis. T1 is the time taken for 63% of the longitudinal

magnetization to be restored. Different molecules in the body have characteristically different T1 relaxation times which are related to how tightly bound the hydrogen atom is to a certain molecule. For example, water has a long T1 relaxation time, producing a dark signal on T1 weighted imaging, while fat has a short T1 relaxation, resulting in a bright signal. T1 weighted images are particularly useful for anatomical demonstration. T1 images alone, prior to the administration of contrast media, are generally of little utility for pathological investigations, particularly in imaging of the brain.

T2-weighted images are of particular interest in neurological disease states, as pathology typically presents as T2 hyperintense. When the radiofrequency pulse is switched off, transverse magnetization starts to disappear as protons fall out of phase with the X-Y plane, returning to the longitudinal plane. T2 time is the time when just 37% of the original transverse magnetization remains present. There are many causes of the loss of coherence of protons, chief among which is the inhomogeneity within local tissue caused by neighbouring protons influencing small magnetic fields in adjacent molecules. This effect is termed spin-spin relaxation or more commonly T2 relaxation. Free water displays characteristically relatively far apart molecules and hence has longer T2 times compared to larger macromolecules and thus free water typically appears bright on T2 weighted sequences.

An important concept in the generation of MR images are the concept of Time to Echo (TE) and Time to Repetition (TR). TE is the time between the peak of the 90-degree radiofrequency pulse and the peak of the echo formed while TR is the time taken to run a pulse sequence. TE and TR are the parameters which determine whether an imaging sequence will be T1-weighted or T2-weighted. T1 images typically have a short TE and long TR, while T2 images are formed when a short TE and short TR are employed(174)(Figure 2).

4.2 Fluid-Attenuated Inversion Recovery Imaging

The fluid-attenuated inversion recovery (FLAIR) sequence was first described in 1992 and is firmly established as one of the cornerstones of neuroimaging. FLAIR is an inversion recovery sequence with a long time to repetition (TR) and a long time to echo (TE) and an inversion time that is specifically tailored to null the signal from cerebrospinal fluid(175). Most pathological processes demonstrate increased signal intensity on T2 weighted images, but lesions that are located close to CSF interfaces between brain parenchyma can appear relatively occult on standard T2 weighted images. In addition to low lesion visibility in the vicinity of the CSF containing spaces, the increased signal of CSF can render differentiation of perivascular spaces from true lesions difficult. FLAIR sequences are heavily T2 weighted with CSF signal suppression, highlighting hyperintense lesions and improving their visibility even when located adjacent to CSF containing spaces(176). These properties render FLAIR the standard sequence of choice in the assessment of periventricular and deep white matter disease, which classically appear as T2/FLAIR signal hyperintensities.

FLAIR is a T2 weighted sequence that includes an inversion pulse followed by a delay before the image is acquired. The sequence begins with a 180-degree inversion pulse which inverts the magnetic spin of the tissue, flipping them to the opposite direction. Following this inversion pulse, the spins begin to relax back to their equilibrium state at variable rates depending on the inherent T1 relaxation time specific to each tissue. The inversion time is specifically chosen to suppress the signal from the CSF. This inversion

time is the time when the longitudinal magnetisation of CSF crosses zero during its relaxation back to equilibrium. At this specific time, the CSF's signal intensity is zero, meaning it produced no signal when the image is acquired. The typical inversion time for suppressing CSF in FLAIR is around 2000 to 2500 milliseconds depending on the magnetic field strength. Following the inversion time, the FLAIR sequence applies a 90-degree excitation pulse which generates the MR signal which is measured and used to produce the image. As such, since the CSF intensity is zero, it appears dark on the resultant image, while tissues such as normal brain parenchyma retain their signal(177)(Figure 3).

4.3 Diffusion Weighted Imaging and Diffusion Tensor Imaging

Diffusion weighted imaging (DWI) is a type of sequence or a variant of traditional magnetic resonance imaging based on the tissue diffusion rate of water(14,178). Advanced imaging techniques in diffusion weighted imaging have attempted to resolve the microstructural integrity of the cerebrum, and while many challenges remain, the eventual and realistic goal of diffusion imaging is to make the MRI scanner a genuine in vivo microscope(179). DWI is a non-invasive imaging technique which boasts unparalleled sensitivity to water movement within the architecture of tissue and is available as a standard component of MRI without the need for additional equipment, contrast agents or chemicals. This specialised MR technique is of particular importance in the detection of acute stroke, brain tumours, infections and white matter disease.

In biological tissues, water molecules are constantly in motion due to thermal energy, a process termed Brownian motion, named after the 19th century Scottish botanist. In an unrestricted environment, for example, pure water, water molecules will move freely in all directions. This entirely free movement is known as isotropic diffusion. However, in practice and in human tissues, structures including cell membranes, myelin fibers and myelin sheaths restrict the movement of water causing anisotropic diffusion or diffusion that is variable depending on the directions (Figure 4)(180). DWI exploits these properties to determine how freely water molecules can move in different tissue(181).

DWI employs diffusion-sensitising gradients to detect the movement of water molecules. This involves the application of two strong magnetic field gradients before and after a standard imaging pulse sequence. The first gradient labels the position of water molecules at a specific point in time and the second gradient applied after a short delay detects any displacement of those water molecules. If water molecules have not moved significantly between the two gradients their signals will remain coherent and result in a high signal intensity on the image (Figure 5)(182). If the molecules have moved significantly the signal becomes incoherent resulting in a lower signal intensity. The diffusion gradients can be applied at different strengths, with higher strength gradients resulting in increased sensitivity to diffusion. Gradients are measured in b-values and in s/mm^2. The b-value is determined by the duration for which the gradient is applied and the time between the gradients. The higher the b-value, the more sensitive the sequence is to diffusion(183).

Conventional DWI may utilise as few as 3 or 6 directions across which to apply the gradients, however more advanced imaging techniques including diffusion tensor imaging (DTI) may use in excess of 48 directions to increase the sensitivity of the sequence to diffusion. In standard practice a DWI sequence may take anywhere from 1 to 5 minutes to complete depending on the selected parameters, however a DTI sequence may take 5 to 15 minutes(184).

DWI is an inherently low resolution and low signal to noise ratio technique with issues exacerbated by its high sensitivity to motion. A small amount of patient motion, even cardiac pulsation, may cause significant signal phase shift, negatively affecting image quality(185). It is difficult to overemphasise the inherently noise-sensitive and artefact-prone nature of DWI and the importance of rigorous image quality assurance and stringent image analysis.

The advent of the diffusion tensor model enables indirect measurement of the degree of anisotropy and structural orientation that characterises diffusion tensor imaging(15). DWI refers to the contrast of the acquired images, diffusion tensor imaging is a specific type of modelling of the diffusion datasets. The introduction of the diffusion tensor model provides an elegant approach to quantify information related to the microstructure of complex tissues(186). Using DTI analysis, it is possible to infer in each voxel properties including the molecular rate of diffusion or the mean diffusivity (MD), the directional preference of diffusion (Fractional Anisotropy), the axial and the radial rates of diffusion (diffusion rates along the main and transverse axis of direction respectively). Diffusion in normal white matter is less restricted along the axon tending to be anisotropic (direction dependent) whereas the diffusion observed in grey matter is generally less anisotropic(187). Based on these initial observations, Basser et Al modelled the diffusion process on an ellipsoid mathematically represented by a 3 x 3 matrix, also referred to as a "tensor", thus the name Diffusion Tensor Imaging.

DTI is in essence, an advanced extension of DWI which informs the user as to the direction and integrity of water diffusion in tissues. DTI itself is not a sequence but a mathematical model applied to a multidirectional DWI dataset. From the directionally sampled diffusion signals, a symmetric 3x3 diffusion tensor is estimated per voxel. Eigen-decomposition of this tensor yields three eigenvalues and three orthogonal eigenvectors which represent the principal diffusivities and principal directions respectively. This is of particular application in the brain's white matter tracts. While DWI measures overall diffusion of water molecules, DTI quantifies diffusion anisotropy, that is, the directionality of water diffusion. Similar to DWI, DTI utilises the application of multiple gradients, often in excess of 36 gradients to achieve higher levels of accuracy. By measuring how water diffusion varies along these different eigenvectors, the model is able to construct a diffusion tensor for each voxel. While DTI can be used to generate images of neuronal pathways, the primary research output of DTI is a number of key metrics including Fractional Anisotropy (FA) and Mean Diffusivity (MD). FA is a measure of the degree of the degree of anisotropy or directionality of molecular diffusion within a voxel. The values of FA range from 0 (completely isotropic diffusion such as seen in free water) to 1 (completely anisotropic diffusion, such as a tightly packed highly cellular structure or white matter tract. Higher values of FA indicate well organised white matter, while low FA is suggestive of damage, degeneration or demyelination. MD measures the average rate of diffusion in all directions within a voxel. Increasing MD is often associated with tissue damage or increased extracellular space seen in oedema or neurodegeneration(188,189).

DTI has many practical and research applications and is predominantly used in the evaluation of white matter architecture. DTI has found utility in the detection of microstructural abnormalities and the task of mapping neural pathways. However, the process of acquiring and analysing images for DTI studies is complex, necessitating a

working knowledge of image artefacts, MRI protocols, neuroanatomy and the rigorous software processes involved in image pre and post processing(190).

4.4 Data Acquisition, Quality Control and Processing.

Artefacts in DWI datasets are typically related to the gradient system hardware, pulse sequence, acquisition technique and motion. DWI data is generally collected over the entire brain by repeating the acquisition over various orientations and magnitude gradients(191). One technique used to reduce the effect of motion artefact is to reduce the scan time by employing single shot echo planar imaging (EPI)(192). The EPI technique is the most commonly used approach; however, it is not without drawbacks. EPI is susceptible to artefacts related to the EPI characteristics such as field inhomogeneities which are more pronounced at higher field strengths, image blurring and poor resolution due to signal decay(193). The usual diffusion limitations such as eddy current-induced distortions and general MRI artefacts of B0 susceptibility apply to EPI also(194). Reducing the readout time is a commonly employed strategy to increase signal to noise ratio and is achieved by using a phased array head coil which allows parallel imaging, an important technique at higher field strengths.

The principal artefacts seen in DTI which can render acquired images non-diagnostic are eddy current distortions and head motion. The strong gradients used for diffusion encoding create eddy currents in the conductive parts of the magnet which cause geometric distortion in the diffusion images which depend on the amplitude and direction of the gradients(195). Naturally these distortions are greater at higher field strengths. The eddy currents can be retrospectively corrected by registering the strongly distorted diffusion images to the less distorted images acquired during non-diffusion sequences such as T1 or T2 weighted sequences. Retrospective correction has some limitations in that the eddy currents cannot be entirely retrospectively removed; thus, residual artefacts will persist and reduce comparability of the dataset(196). Novel strategies to eliminate eddy current artefacts based on twice refocused spin echo pulse, bipolar gradients, field maps and pre-processing techniques are commonly employed in modern software packages(197).

DWI is profoundly sensitive to motion and as such suffers from motion artefacts more so than other techniques. As with other artefacts, the degree of image quality degradation increases with field strength. Motion artefacts can be caused by microscopic processes such as phase shifts induced microscopically driven by physical displacement of water molecules and macroscopically by head motion, cardiac pulsation and respiratory motion(198). Vibration from the MRI machine has been reported as a cause of motion artefact. Vibration of the patient table as a result of low frequency mechanical resonances of the machine cause brain tissue movement which manifests as signal loss which the brain movement occurs in the direction of the diffusion encoding gradient(199). While it is possible to correct motion artefacts using pre and postprocessing techniques, the gold standard technique remains appropriate position and padding of the patient's head.

If images are significantly degraded and efforts to remedy or correct the signal loss, many studies advocate exclusion of the subject. Alternatively, it may be possible to limit analysis to brain regions unaffected by the artefact. The distortions caused by eddy currents and motion are typically corrected in the pre-processing stage with affine registration to the b0 image and rigid body registration, with both procedures consisting

of registration processes, most software packages implement these corrections in a single step and typically have built in applications to execute these commands(200).

Chapter 5: Imaging Quantification of White Matter Hyperintensities

5.1 Evaluation of White Matter Hyperintensities

The assessment of white matter hyperintensities on MRI typically involves measuring a number of quantifiable factors, chief among which is the size of the lesions. Historically, both qualitative and quantitative techniques have been used to measure WMHs(201). The main qualitative visual rating scales documented in the literature include the Fazekas scale(202), the Rotterdam Scan Study scale(203) and the Scheltens Scale(204). While these qualitative rating scales have several advantages, particularly their ease of use and insensitivity to artefacts which facilitate their application to large cohort-based studies(205), there are a number of significant drawbacks associated with this approach which has seen quantitative methods largely eclipse their application. Perhaps most important among these limitations is the constraint of a predefined scale and categorical rating. For example, in longitudinal studies, lesions which have been categorised in the most severe level of the scale on initial or early assessment, cannot achieve a higher score on follow-up analyses, even though the lesion may have increased in size. This limitation and the poor discrimination of absolute lesion volume, are significant limitations quoted against the qualitative approach(36). Qualitative scales have received scrutiny due to the subjective nature of their interpretation with studies showing poor reliability in longitudinal studies(206). One analysis of 13 different visual rating scales concluded that the heterogenous properties of the scales resulted in inconsistencies among previously published studies(207).

As an example of the previously common qualitative methods of lesion quantification, the Scheltens Scale is explained here in detail. The Scheltens Scale is a visual rating scale that includes anchored, 7-point (0–6) severity ratings in periventricular (i.e., frontal horn, occipital horn, lateral bands), cortical (i.e., frontal lobe, temporal lobe, parietal lobe, occipital lobe), subcortical (i.e., caudate, putamen, globus pallidus, internal capsule, thalamus), and infratentorial (i.e., mesencephalon, pons, medulla, cerebellum) regions. The scale was derived in 1992 and sought to build upon the older Fazekas Scale (1987) in an effort to improve upon this scale, citing the limitation of "providing only global information on the presence of periventricular and deep white matter hyperintensities" as a drawback of the older scale. The Fazekas system received criticism for a lack of information regarding anatomical distribution of lesions and a poor intra- and inter-rater agreement(208).

In quantitative analyses, measurements are generally expressed as a measure of volume, and denoted in mm^3. These methods typically use computer-based techniques to obtain volumetric measurements(209). These methods include manual outlining techniques to fully automatic WMH detection. The gold standard of lesion quantification remains manual segmentation(210), however the method is time consuming and for large cohorts requires multiple reviewers and subspecialist training to reduce inter and intra-reviewer variability(206). Manual segmentation involves a region-of-interest methodology in which the reviewer manually traces out the WMH on a computer using the mouse and the cursor, typically over several image slices. After an ROI is traced, the computer will calculate a volume of the region derived from the selected region. Volumetric accuracy is a strength of this method however the technique is limited by the required time investment and need for a well-trained investigator.

Fully automated techniques have gained popularity in the literature for large studies with evidence proving these methods to be non-inferior to manual segmentation(211). Automated techniques are computer algorithms which isolate WMHs based on the intensity of each voxel. These algorithms typically use a predefined threshold of intensity and count all voxels exceeding this threshold to calculate WMH volume. The lesion threshold determination of these algorithms is typically what separates them, with determinations varying from relatively straightforward to sophisticated computations derived from global and local intensity histograms(212).

5.2 Lesion Segmentation

Many of the initial tools for lesion segmentation were developed on the back of clinical trials in multiple sclerosis. The assessment of lesion volume change in MS is considered a relevant marker of disease progression(213) and has been used as a significant outcome measure and a marker of potential disease-modifying treatments(214). The algorithms developed for segmenting WMHs in multiple sclerosis have been proven effective for segmentation of vascular WMHs(215). General principles apply across the board to many of these algorithms. An algorithm developed by Paul Schmidt, the Lesion Segmentation Tool Lesion Prediction Algorithm (LST-LPA) has been cited amongst the best performing and most consistent freely available WMH segmentation algorithms(216). A review by Heinen et al. of five freely available and fully automated lesion segmentation tools compared LST-LPA, Cascade, K-Nearest Neighbour with tissue type priors (KNN-TTP), Lesion-Topology-preserving Anatomical Segmentation (Lesion-TOADS) and the Lesion Segmentation Tool Lesion Growth Algorithm (LST-LGA) against manually segmented lesions by a trained rater. In this review the KNN-TTP and LST-LPA were the top performers, with similar Dice's similarity coefficients and comparable outcomes across different scanners. The LST-LPA had some advantage in that the overall volume error was relatively small though a negligible lesion underestimation compared to the competition at higher volume loads. The LST-LGA demonstrated larger absolute volume error and more pronounced error at higher volumes, Lesion-TOADS again tended to underestimate volumes at higher loads with poorer performance overall while Cascade had the worst reported performance. Schmidt's LST-LPA was chosen as the segmentation tool used in later sections of this thesis due to its reported performance and compatibility with other software (MRIcron and ExploreDTI).

Lesion segmentation algorithms rely on signal intensity, spatial information and other factors to define regions of interest. Challenges for these algorithms include false positives produced by artefacts and infarctions and false negatives, typically punctate spurious hyperintensities. Other challenges include coexisting pathologies such as extensive cerebral atrophy.

In order to minimise the effects of some of these challenges, the images to be quantified typically undergo a number of pre-processing steps. One key step is image noise reduction using a technique called Gaussian smoothing or Gaussian blurring. This technique works by transforming the image to a Gaussian function which applies a weighted average value to the pixels in the image emphasising the central pixel and diminishing the impact of surrounding pixels. This function results in a smoothed image where rapid changes in intensity, termed noise, are reduced, while important features are preserved. This process increasing the accuracy of segmentation where tasks such as segmentation, edge detection and feature extraction are important. The process used a

Gaussian function, a mathematical formula which includes a standard deviation to control the spread of the function. Excessive application of the function can blur fine details which can limit the detection of miniscule abnormalities. Therefore, choosing the right standard deviation is essential to not excessively smooth the image(217,218).

The LST-LPA algorithm operates a three-step process. The first step involves pre-processing of the images which corrects MR field inhomogeneity, registration to native space and noise reduction techniques. Following standardised corrections, voxels are classified into grey matter, white matter and cerebrospinal fluid using standard software(219). After applying additional refining applications, the FLAIR sequence is co-registered to the native T1 weighted image. A tissue probability map of FLAIR white matter (as well as grey matter and CSF) is able to be generated using this co-registration and spatial probability tools. With this FLAIR white matter map generated the second step involves the generation of a "lesion belief map". This process involves a mathematical computation which calculates the average intensity of grey matter, white matter and CSF on FLAIR images. Outliers of intensity within the white matter are calculated and this generates an initial lesion map. Once generated, this initial belief map is used in the third step which is the lesion growth algorithm. The lesion growth algorithm analyses each voxel in the neighbourhood of the initial lesions and uses information obtained from the T1 and FLAIR sequences combined with a mathematical formula to classify the surrounding voxels as either "lesion" or grey matter, white matter or CSF(220).

The generated map of segmented lesions provides accurate measurements of WMH volume, as well as the location of the lesion in native space. The generated map can be exported to other applications, such as MRIcron to generate a lesion atlas detailing the anatomical location of the WMH. The lesion map can be used in ExploreDTI, a diffusion tenor analysis program used to acquire diffusion metrics including FA and MD of the target WMHs. These applications used in tandem produce the volume of a lesion in mm^3, the location of the lesion, the FA and MD (as well as a number of additional diffusion metrics).

CHAPTER 6: THE IRISH LONGTITUDINAL STUDY ON AGEING (TILDA)

6.1 The Irish Longitudinal Study on Ageing (TILDA)

TILDA is a prospective nationally representative study of community dwelling adults in the Republic of Ireland aged 50 years and over(221). TILDA participants were selected using multi-stage, stratified random sampling that identified 640 geographical areas, stratified by socio-economic characteristics, and selected 40 households within each area(222). The Irish GeoDirectory listing of all residential addresses provided the sampling frame. Details of the sample maintenance strategies used by TILDA are available elsewhere(223).

The first Wave of data collection took place between the years 2009 – 2011, with subsequent waves collected biennially (Wave 2 in 2012, Wave 3 in 2014, etc)(224). TILDA collects information on its participants in three separate ways: computer-assisted personal interviews (CAPI), self-completion questionnaires (SCQ), and a comprehensive health assessment by a trained nurse. The information collected by TILDA at each Wave covers a wide range of topics involving health, economic, social and family circumstances. The CAPI and SCQ are repeated at each Wave and the health assessments were repeated at Wave 3 and again at Wave 6 in 2021(225).

6.2 Ethics

Ethical approval for each wave of TILDA is obtained from the Faculty of Health Sciences Research Ethics Committee in Trinity College Dublin. Participants are provided with enough information to make an informed decision about their participation including advance notice of the study. Written consent is obtained for separate components of the study (i.e. interview, health assessment, blood samples); participants may refuse to take part in or withdraw at any time without justification.

CHAPTER 7: MD Hypothesis

The primary hypothesis of this MD is that microstructural changes detected on MR imaging in at risk populations can predict which individuals progress to cognitive impairment. As part of this hypothesis, I also wanted to explore whether it was useful to categorise WMHs into specific phenotypes based on their location, size and microstructural properties and examine the effects of these phenotypes on cognitive states over time.

My secondary hypothesis was that individuals with large volume lesions with microstructural properties most removed from that of normal appearing white matter i.e. lower average fractional anisotropy and higher mean diffusivity, would be associated with accelerated cognitive impairment over time.

Finally, I hypothesised that identification of specific phenotypes could provide information related to the underlying mechanism of the development of cerebral WMHs.

SECTION THREE: LINKING WHITE MATTER HYPERINTENSITIES TO LONGITUDINAL CHANGES IN AGEING

CHAPTER 8: Introduction

The association between white matter integrity and adverse brain health outcomes is well-established. Increased white matter lesion burden has consistently been linked to higher risk of stroke, cognitive impairment, dementia, and mortality in cross-sectional and longitudinal studies involving diverse patient populations and healthy older adult cohorts(149,226,227). Assessment of white matter microstructural integrity using Diffusion Tensor Imaging (DTI) has revealed robust association with cognitive performance in both healthy older adults and various patient groups in cross-sectional and longitudinal designs(144,228,229). White matter hyperintensities (WMHs), initially localised to periventricular regions but progressing into deep white matter with increasing lesion number, play a crucial role in these associations.

WMH is a descriptive term used in MRI interpretation. A WMH is best described as a hyperintense lesion on T2/FLAIR sequencing in the cerebral white matter. These lesions are typically present in the periventricular white matter and deep cortical white matter. Typical age related vascular white matter hyperintensities are seen in the general population in approximately 10 – 20% of subjects aged sixty years old and with prevalence approaching 100% in persons aged ninety years and older(27). WMHs are reportedly common in the Japanese, Chinese, Caucasian, African-American and Caribbean Black demographics, increasing across all ethnicities with age(28). Typically, small WMHs in the elderly are asymptomatic, but these lesions can progress to large confluent lesions which can present with cognitive impairment, dementia, functional decline, urinary incontinence, balance and gait impairment and neuropsychiatric disorders(29).

While previous research has independently explored the impact of white matter macrostructure, microstructure, and spatial distribution on cognitive function, a comprehensive understanding of their cumulative and interconnected effects on cognitive decline is currently lacking. Previous investigations into the microstructural nature of WMHs, utilising fractional anisotropy (FA), mean diffusivity (MD), and magnetization transfer ratio (MTR), have demonstrated reduced white matter integrity in those with WMHs compared to those without (normal appearing white matter - NAWM). Specifically, FA and MTR values are significantly lower, while MD values are significantly higher in WMHs compared to NAWM(230,231). Histopathological studies suggest ischemia as the primary underlying process in the development of WMHs, but the process of microstructural damage is likely more complex and multifactorial(45,232–234).

Our hypothesis posits that heterogeneity in white matter integrity, as measured by MRI, may correlate with cognitive function. In this study, we categorise WMHs into six lesion phenotypes based on their location (periventricular or deep white matter), size (low/high volume), and microstructural properties (FA, MD). Using a large MRI sample of community-dwelling healthy older adults from The Irish Longitudinal Study on Ageing, a nationally-representative population-based study, we examined the effects of these phenotypes on cognitive decline over a six-year period. Our primary hypothesis was is that due to a diverse combination of causative factors, WMHs manifest as variable phenotypes, and that different phenotypes are associated with cognitive decline. Specifically, we anticipated that large-volume deep white matter hyperintensities demonstrating significantly lower average FA and higher MD values are linked to accelerated cognitive decline over time. We believe that the characterisation of both

macro- and microstructure of WHM lesions, and their spatial distribution, is critical for understanding their impact on cognitive decline and the associated risk of dementia.

The identification of WMH phenotypes associated with accelerated cognitive decline might impact clinical practice and aid in early detection of individuals at higher risk of progression from cognitive impairment to dementia, and could potentially lead to early implementation of intervention strategies which could improve patient outcomes.

CHAPTER 9: Methods

Sample

The Irish Longitudinal Study on Ageing (TILDA) is a large population-based study of a nationally-representative sample of community-dwelling older adults aged 50 years and over, resident in the Republic of Ireland. TILDA's random sampling procedure and study design have been described elsewhere(222). Briefly, participants have been followed biennially from Wave 1 (data collection baseline: 2009-2011; N=8,504) and this analysis includes data from Wave 3 (2014-2015), Wave 4 (2016-2016), Wave 5 (2018-2018) and Wave 6 (2021-2021). Macro- and micro-structural measures of WMHs at Wave 3 and cognitive data (Wave 3 - 6) were available for 497 participants (see Figure 6 for a detailed breakdown)). At each wave, participants took part in a computer assisted personal interview (CAPI) and completed a questionnaire (SCQ). At Wave 3, participants were also invited to take part in a health assessment and a sub sample of those who completed the health assessment were randomly selected to undergo magnetic resonance imaging (MRI). Ethical approval was granted by the Trinity College Faculty of Health Sciences Research Ethics Committee, Dublin, Ireland. Protocols conformed with the 1964 Declaration of Helsinki and its later amendments. Signed informed consent was obtained from all respondents prior to participation. Additional ethics approval was received for the MRI sub-study from the St James's Hospital/Adelaide and Meath Hospital, Inc. National Children's Hospital, Tallaght (SJH/AMNCH) Research Ethic Committee, Dublin, Ireland. Those attending for MRI were also required to complete an additional MRI-specific consent form.

MRI data acquisition and processing

The MRI sampling procedure has been previously described in detail(235). In brief, MRI scanning was completed at the Thomas Mitchell Centre for Advanced Medical Imaging (CAMI), St. James' Hospital, Dublin, (3T Philip's Achieva system and 32-channel head coil). The study protocol included T1, fluid attenuation inversion recovery (FLAIR) and diffusion weighted imaging (DWI) sequences. T1-weighted scans were acquired using a 3D Magnetisation Prepared Rapid Gradient Echo (MP - RAGE) sequence (FOV (mm): 240x240x162; SENSE factor: 2; TR: 6.7ms; TE: 3.1ms; flip angle: 8°; voxel size (mm): 0.8x0.8x0.9). FLAIR images were acquired using a 2D turbo spin-echo sequence (FOV (mm): 230x230; TR: 11000ms; TE: 125ms; TI: 2800ms; flip angle: 90°; number of slices: 30; slice thickness: 4 mm; slice gap: 1 mm; voxel size(mm): 0.45x0.45). DWI images were acquired using a high spatial (1.9 mm3) and high angular resolution (61-direction) protocol with a high diffusion sensitivity (b = 1200 s/mm2; TR: 2885ms; TE: 64ms; flip angle: 90°; number of slices: 30; slice thickness: 4mm; slice gap 1mm: voxel size (mm): 0.96x0.96).

Images were pre-processed using SPM12 (University College London, London, UK) and ExploreDTI(236). All images were reorientated to a canonical SPM template. The dataset was inspected for appropriate orientation and any gross artefacts before processing and segmentation. DWI preparation included correcting multiple prerequisite parameters in the ExploreDTI software toolbox for MATLAB (https://www.mathworks.com/products/matlab.html). The entire standardised dataset was converted to ExploreDTI compatible diffusion files, corrected for signal drift(237), Gibbs Ringing artefact(238), head motion and eddy current artefact with registration to the B0

reference image(239) and EPI deformation correction via registration to the T1 sequence(240). These commands were performed using the native ExploreDTI toolbox plugins.

Location, size and microstructural properties of WMHs

White matter hyperintensities (WMHs) were segmented utilising the Lesion Prediction Algorithm (LPA)(241), implemented in the LST toolbox version 3.0.0 for SPM12 (www.statistical-modelling.de/lst.html). The LPA was applied to both FLAIR and T1 images. Meticulous visual image review ensured accurate and appropriate segmentation of only WMHs. Each segmented lesion received a unique lesion number, and an individualised atlas of lesions was created for each subject. To objectively localise each lesion, the SPM Anatomic Automatic Labelling extension was employed(242). Lesions were categorised based on their anatomical position in the periventricular or the deep white matter. Periventricular lesions were defined as those within 15mm of a ventricle(243), while deep white matter lesions were those outside this range. Atlas-based tractography was performed using the segmented lesions as regions of interest in each subject, utilising the native ExploreDTI plugin, and diffusion metrics (FA and MD) unique to each WMH were calculated.

WMHs phenotypes

Lesions were initially clustered based on both macrostructural properties (volume in mm3) and microstructural properties (FA and MD) using k-means clustering (cluster package in R version 4.0.3 with RStudio Version 1.4.1103). The optimal number of lesion phenotypes or clusters was determined using the elbow method. Three primary lesion phenotypes were identified. These phenotypes were further stratified based on their location (deep vs periventricular), resulting in a total of six lesion phenotypes. The frequency of each lesion phenotype per individual was calculated and used for subsequent analysis. Lesion phenotypes were assigned automatically by k-means clustering (based on lesion volume, FA and MD), no manual reassignment was involved and because k-means assigns each lesion to the nearest cluster centroid there were no unclassified borderline cases.

Cognitive function

Global cognitive function at each wave (Wave 3 to 6; MEAN ± SD-year follow-up; wave 3 - 28.8 (1.5), wave 4 - 28.6 (1.3) wave 5 - 27.9 (1.7) and wave 6 - 27.6 (1.8)) was assessed using a battery of neuropsychological tests, including 10-word immediate recall test (2 trials), 10-word delayed recall test, semantic verbal fluency (animal naming), and orientation (date, day, month, year). A composite score per participant and at each wave was derived by combining individual test scores to broadly reflect global cognitive function. The composite scores were generated based on an equally unit-weighted approach using standardised scores (z scores). The lower the composite score, the worse the cognitive function. For interpretability, it should be noted that the immediate recall test comprised two trials (maximum total score = 20), the delayed recall test had a maximum score of 10, semantic verbal fluency (animal naming) had no fixed upper limit but typically ranges between 10–30 items, and orientation (date, day, month, year) had a maximum score of 4. The composite cognitive z-scores and covariate data (e.g., age, sex, vascular risk factors) were already derived, standardised, and quality-checked as part of

the TILDA dataset. For this study, no additional cognitive or covariate data processing was undertaken; our role was limited to assessing WM lesions and linking these to the pre-existing dataset variables.

Covariates

Covariates included age, sex, education (none/primary, secondary, or tertiary/higher); smoking (never, past or current); problematic alcohol consumption (CAGE questionnaire; yes or no); physical activity (International Physical Activity Questionnaire - IPAQ; short-form; low, moderate or high); body mass index (BMI, continuous variable); pre-existing self-reported physician-diagnosed cardiovascular diseases and events (CVDEs, none or one or more of the following: angina, heart attack, congestive heart failure, stroke, transient ischemic attack, and atrial fibrillation); average systolic and diastolic blood pressure measurements obtained twice using an OMRON digital automatic blood pressure monitor (Model M10-IT); antihypertensive medication (Anatomical Therapeutic Chemical (ATC) codes C02 (antiadrenergic agents), C03 (diuretics), C07 (β blockers), C08 (calcium-channel blockers), and C09 (angiotensin- converting enzyme inhibitors)); antidepressant medication (ATC code N06A); and symptoms of depression (the Centre for Epidemiological Studies Depression Scale - CESD; continuous variable). Age, sex, and education were selected as baseline covariates because they are established determinants of WMH burden and cognitive decline, and are routinely adjusted for in dementia epidemiology.

Statistical Analysis

All statistical analyses were performed using R version 4.0.3 with RStudio Version 1.4.1103. The observed sample was first characterised using unadjusted means and standard deviations for continuous variables and percentages (%) for categorical variables. To estimate selection bias, the observed sample was compared to the total cohort including those excluded from analysis. Independent t-tests and chi-squared tests where appropriate were used to assess differences between the two groups. Linear mixed effect models were used to examine the relationship between lesion phenotypes (predictor) and cognitive function at waves 3, 4, 5 and 6 (outcome). Fixed effects included the number of lesion phenotypes in separate models and waves with an interaction term. The significance of the interaction was assessed using likelihood ratio tests. Participants constituted the random intercept. Baseline models included age, sex and education as covariates; further adjustment included smoking, alcohol consumption, physical activity, BMI, CVDEs, average systolic and diastolic blood pressure, depressive symptoms and antihypertensive and antidepressant medication.

CHAPTER 10: Results

Data Description

Table 1 provides descriptive statistics of the study sample (n=497) at Wave 3. Mean age of the study sample was 68.5 years (SD 7.56); 51.9% of the participants were female and 20.7% had a low (primary school) level of education. Mean MMSE (Mini Mental State Examination) at Wave 3 was 28.8 (SD=1.5).

A total of 11,933 individual white matter lesions were segmented and analysed from the cohort (n= 497) (Table 2). On average, each participant exhibited 24 white matter hyperintensities (WMHs) with a mean volume of 263.21 mm3.

Cluster analyses revealed three distinct lesion phenotypes (Figure 7): Type A (Low Volume, High FA/Low MD), Type B (Low Volume, Low FA/High MD) and Type C (High Volume, Low FA/High MD), and, each further categorised into periventricular and deep white matter lesions. We will omit the MD descriptor for simplicity from this point. 40% of lesions were Periventricular Type A (Low Volume, High FA), 26% were Periventricular Type B (Low Volume, Low FA), 19% were Periventricular Type C (High Volume, Low FA), 11% were Deep Type A (Low Volume, High FA), 3% were Deep Type C (High Volume, Low FA), and 1% were Deep Type B (Low Volume, Low FA). Descriptive characteristics of these six lesion phenotypes are presented in Table 3. It should be noted that no distinct High Volume/High FA phenotype emerged from the k-means analysis. While some lesions visually appeared close to this quadrant in the scatterplots, the clustering algorithm assigned each lesion to the nearest centroid, resulting in three main phenotypes only.

Comparisons among the lesion phenotypes, with the Periventricular low volume, high FA Type A (Low Volume, High FA) group as the reference, revealed notable demographic and clinical differences. Those with deep phenotypes (Type A, B, C) were older ($p<0.001$), more likely to be women (Type A (Low Volume, High FA) and C (High Volume, Low FA); $p<0.001$), and exhibited lower levels of education (Type A and C; $p<0.001$). Individuals in the Deep Phenotype groups were more likely to have two or more cardiovascular conditions (Type A (Low Volume, High FA) and C (High Volume, Low FA); $p<0.001$, Type B (Low Volume, Low FA) $p<0.05$), higher systolic blood pressure (Type A (Low Volume, High FA) $p<0.05$, Type B (Low Volume, Low FA) $p<0.001$), current smoking habits (Type A (Low Volume, High FA); $p<0.001$, Type C (High Volume, Low FA); $p<0.01$), problematic alcohol consumption (Type A (Low Volume, High FA); $p<0.01$, Type B (Low Volume, Low FA); $p<0.001$), lower levels of physical activity (Type A (Low Volume, High FA); $p<0.001$, Type C (High Volume, Low FA); $p<0.05$), and higher levels of depressive symptoms (Type C (High Volume, Low FA); $p<0.01$, Type A (Low Volume, High FA); $p<0.1$). Similar trends were observed in the Periventricular Type B (Low Volume, Low FA) group.

The association between lesion phenotypes and 6-year cognitive decline

Results are presented for the fully adjusted models (including vascular and lifestyle covariates). For context, models adjusted only for age, sex, and education yielded the same direction and magnitude of associations, with slightly wider confidence intervals.

Baseline Linear Mixed Effects (LME) models revealed that a higher number of deep (X=7.3; p=.05) and periventricular (X=12.9, p=.004) high volume, low fractional anisotropy lesion phenotypes (Type C) were associated with accelerated cognitive decline from Wave 4 to Wave 6 (Figures 3 and 4), compared to the reference group with periventricular low volume, high FA (Type A) lesions. Additionally, a higher number of deep low volume, high FA (Type A) lesions were also linked to accelerated cognitive decline (X=10.5; p=.01) (Figure 10).

The phenotype by Wave correlation did not reach significance for the number of periventricular low volume, high FA (Type A) lesions, deep and periventricular low volume, low FA (Type B) lesions (p>.05). There were no significant associations between the number of periventricular Type A (low volume, high FA) lesions (p=0.46) or deep Type B (low volume, low FA) lesions (p=0.48) and cognitive decline. In contrast, the number of periventricular low volume, low FA (Type B) lesions was overall positively associated with cognitive function (B=0.04; 95% CI= 0.00, 0.09; p=.02) (Figure 11).

These findings remained robust to adjustments for smoking, alcohol consumption, physical activity, body mass index (BMI), cardiovascular diseases (CVDEs), average systolic and diastolic blood pressure, antihypertensive and antidepressant medication, and of depression.

CHAPTER 11: Discussion

Our study sought to elucidate the combined impact of white matter hyperintensity (WMH) volume, microstructure, and location on cognitive decline over six years in a large MRI sample of community-dwelling older adults from a nationally representative population-based study of aging. Our hypothesis that WMHs manifest as variable phenotypes is supported by the identification of three potential groups of lesions based on MRI-defined macro and microstructural white matter characteristics. Additionally, our analysis confirms that deep white matter, large volume hyperintensities with significantly lower average fractional anisotropy (FA) and higher mean diffusivity (MD) are associated with accelerated cognitive decline over time. We present a novel approach to classifying WMHs based on a combination of location, macro- and microstructural properties and describe the associations of these phenotypes with longitudinal cognitive decline.

Using a data-driven approach, we identified three distinct groups of lesions based on their macro and microstructural white matter characteristics (Low Volume/High FA, Low Volume/Low FA, and High Volume/Low FA). These groups were further stratified into periventricular and deep white matter lesions, resulting in six distinct WMH phenotypes. We found that WMHs characterised by low volume and relatively high average FA in the periventricular region, resembling normal appearing white matter microstructural properties, were the most frequently identified phenotype.

Our observations highlight the relationship between MRI phenotypes and various demographic and clinical factors. Lesions in the deep white matter, as well as those of low volume and low FA in the periventricular white matter (Type B), are associated with increased age, female gender, lower education levels, higher cardiovascular risk factors, antihypertensive medication use, smoking, problematic alcohol use, and a sedentary lifestyle aligning with existing literature detailing the relationship between lifestyle, vascular disease, and brain health.

Deep WMHs Types A (low volume, high FA) and C (high volume, low FA) and Periventricular Type C (high volume, low FA) lesions were associated with accelerated cognitive decline over six years, indicating that lesions in the deep white matter and higher volume lesions, regardless of distribution, are more likely to be linked with cognitive decline. While this lesion-load dependent relationship aligns with existing literature, the observation that lesions located beyond the periventricular region in the deep white matter are also associated with cognitive decline is poorly appreciated, providing potential insights into the significance of WMHs.

The most robust association with cognitive decline was found in Periventricular Type C lesions (high volume, low FA), representing lesions with architectural values furthest removed from normal appearing white matter ($p=0.004$). This aligns with previous observations of decreased FA in various brain regions in individuals with mild cognitive impairment(244–246). Our findings support an association between microstructural damage and cognitive impairment, providing evidence for a lesion-burden dependent relationship.

Of note, we did not identify a subtype of WMH which demonstrated high volume and high FA, which suggests that as lesion size increases, microstructural integrity decreases. The absence of high-volume, high-FA lesions in our analysis precluded the opportunity to

explore differential associations based on microstructural properties. The absence of these lesions suggests that as WMHs increase in volume, their microstructural integrity declines, as evidenced by reduced FA values. This finding supports the progressive and pathological nature of WMHs, underscoring that lesion growth likely correlates with progressive axonal disruption, loss of myelin integrity and white matter connectivity.

Our observation that Periventricular Type B (low volume, low FA) lesions appear to be protective against cognitive decline raises questions and invites a deeper exploration of the underlying vascular dynamics in the periventricular regions. The periventricular white matter, situated in proximity to the lateral ventricles, is known to be particularly vulnerable to changes in cerebral blood flow due to its unique vascular supply. The periventricular white matter is primarily nourished by small perforating arteries arising from larger vessels, such as the anterior, middle, and posterior cerebral arteries. These penetrating arteries course through the periventricular region, supplying the adjacent white matter.

The propensity for periventricular white matter ischemic insult is well established and multifactorial, culminating in white matter (ischaemic) lesions in the setting of vascular risk factors. The disposition of the arterial supply results in a watershed area in the periventricular white matter, which is highly sensitive to changes in perfusion pressure making it susceptible to hypoperfusion-related damage. Hypoxia has been described in the pathogenesis of WMHs using specific markers for vascular morphology and tissue hypoxia(247). Increased vessel wall thickness and larger perivascular spaces have been observed in white matter disease(248). Particularly in the setting of deep white matter disease, capillary endothelial cells have been observed to be activated with increased arteriolar tuberosity and decreased vessel density(249).

These factors contribute to the underlying vulnerability of the periventricular white matter. The recognised mechanisms of damage to the periventricular white matter may be a slow or chronic process, that might allow the brain to adapt over time. A compensatory adaption could explain why some periventricular lesions do not significantly impact cognitive function. The periventricular regions are notably less densely packed neuronal pathways(157), therefore damage to the periventricular region may primarily affect less critical pathways. It remains unclear if small periventricular lesions can be classified as a normal part of the aging process, rather than a specific pathological hallmark and in isolation these may not correlate with significant cognitive impairment. Our finding relating to the protective nature of periventricular Type B lesions (low volume and low FA), may relate to factors not accounted in our cognitive testing combined with subjects' compensatory mechanisms. As the affected periventricular area may not significantly impact global cognition, particularly when dealing with low volume lesions, there may be deficits in processing speed or executive function which are not captured in broad cognitive testing.

Our study draws parallels with a recent article by Li et al, which concludes that WMHs are non-specific lesions associated with amyloid-beta deposition, cognitive decline and multiple vascular risk factors(250). Our findings are in line with Li's findings in that we state, as already established in the literature, WMHs are more prevalent in subjects with two or more cardiovascular conditions, higher levels of systolic blood pressure, positive smoking history and lower levels of physical activity. However, while this recent article posits that WMHs are non-specific lesions in terms of underlying aetiology, we offer that

WMHs may be defined as separate phenotypes, which can specifically serve as markers predictive of longitudinal cognitive decline, as we have shown that individuals who possess large volume lesions with diffusion metrics furthest removed from normal (i.e. Type C lesions with large volume and low FA), demonstrated accelerated cognitive decline over a six year period compared to others.

With regard to the underlying aetiology of WMHs, evidence in the literature has trended toward a prevalent vascular or ischaemic aetiology. Other factors have been described and likely play a role, though probably not to the same extent as primarily vascular insults. Blood-brain barrier dysfunction and decreased vascular integrity have been described in white matter disease(251). Microglial cell activation, related to the phagocytosis of myelin breakdown products, has also been described and is more active in periventricular white matter lesions, rather than deep white matter lesions(252). It is possible that periventricular lesions are characterised by greater inflammatory activity while deep lesions reflect more advanced small vessel ischaemia and axonal destruction, processes which may have a more adverse effect cognition. Our findings do not necessarily contradict the literature but instead suggest that distinct pathological processes may underlie periventricular and deep white matter lesions with differing consequences for cognition. Toxic effects on vascular permeability secondary to amyloid deposits and cerebral blood flow autoregulation have also been described in the pathogenesis of WMH(253).

Systemic vascular disorders and risk factors such as hypertension, diabetes and smoking are closely associated with WMHs and likely contribute to the above processes leading to their development. These risk factors and their biomechanical effects contribute to a multifactorial pathogenesis with visible lesions on imaging representing only the “tip of the iceberg”. This concept suggests that the hyperintensities on FLAIR sequences reflect just the most overt manifestation of underlying white matter damage, while a larger, diffuse burden of microstructural damage exists in the surrounding normal-appearing white matter, undetectable by conventional imaging. Studies have shown that structural damage often extends beyond the visible WMH boundaries. For instance, O’Sullivan et al. identified reduced cerebral blood flow and structural damage in normal appearing white matter surrounding WMHs, suggesting hypoperfusion as an early feature in WMH development(254). Other studies have similarly reported microstructural changes radiating into peri-WMH tissue, indicating that white matter alterations are part of a diffuse process(230,255,256).

Our most commonly observed WMHs were in the periventricular region with FA values most closely resembling normal appearing white matter, compared to lesions seen in the deep white matter. If a linear or progressive pattern of white matter disease is accepted, our finding supports the theory that periventricular white matter is more susceptible to microangiopathy. Our observation that deep white matter hyperintensities, both type A (low volume and high FA) and type C (high volume and low FA) were associated with poorer cognitive outcomes, supports the theory that deep white matter disease represents a more severe form of disease.

While our study sheds light on the complex relationship between WMH characteristics and cognitive outcomes, the vascular intricacies of the periventricular region warrant further investigation. Future studies exploring the hemodynamic aspects and perfusion dynamics specific to periventricular white matter are warranted and longitudinal studies

with serial neuroimaging are needed to monitor the progression of WMHs and determine if lesions may regress with intervention.

SECTION FOUR: CONCLUSION

CHAPTER 12: Conclusion

Our study provides insights into the complex relationship between WMH characteristics and cognitive decline, shedding light on potential novel phenotypes associated with differential cognitive outcomes, but the vascular intricacies of the periventricular region warrant further investigation. The identification of six distinct WMH phenotypes, coupled with a comprehensive consideration of demographic and health factors, improves understanding of the predictors of cognitive decline. Future longitudinal studies with serial neuroimaging are warranted to monitor the natural progression of WMHs and determine if interventions may lead to lesion regression with appropriate treatment and how this interacts with longitudinal cognitive outcomes.

While acknowledging inherent limitations, our findings contribute valuable insights into the multifaceted relationships between white matter integrity and cognitive outcomes, and paves the way for future efforts aimed at deciphering and mitigating the impact of WMHs on cognitive health in aging populations.

CHAPTER 13: Limitations

Our study, while offering valuable insights into the intricate relationship between white matter hyperintensity (WMH) phenotypes and cognitive decline, is characterised by both strengths and limitations that collectively contribute to the overall integrity of our findings.

Strengths:

Large, Representative Sample: The inclusion of a substantial MRI sample from a nationally representative population-based study enhances the external validity of our findings, allowing for broader generalisability to diverse groups of community-dwelling older adults.

Longitudinal Design: The longitudinal nature of our study spanning six years provides a temporal dimension to our analyses, enabling the exploration of cognitive decline over time and capturing changes in WMH phenotypes.

Advanced Lesion Phenotyping: Employing a data-driven approach for lesion phenotyping, considering both macrostructural and microstructural properties, adds depth to our characterisation of WMH subtypes. This nuanced approach enhances our understanding of the heterogeneity within WMHs.

Limitations:

Cross-Sectional Nature of Lesion Phenotyping: The identification of WMH phenotypes was based on cross-sectional analyses, limiting our ability to capture dynamic changes in lesion characteristics over time. Longitudinal studies with repeated imaging sessions could provide a more comprehensive understanding of the evolving nature of WMHs.

Generalisability and Population Characteristics: Our study focused on a specific cohort of community-dwelling older adults from a nationally representative population-based study. Generalisability to other demographic groups or clinical populations may be limited, and caution is advised when extrapolating findings to broader populations.

Absence of a Control Group: The absence of a control group composed of individuals without WMHs or with low lesion burden is a limitation of our study. Inclusion of a control group would have allowed for direct comparison between individuals with varied degrees of WMH burden and those with normal appearing white matter, lending strength to the subsequent findings and improving the validity of the study. In the absence of a control group it is difficult to isolate the effects of WMHs with regards to cognitive decline from other age-related factors or comorbidities that could independently affect outcomes. In addition, a control group would have provided a baseline trajectory of cognitive outcomes. Future research should incorporate an appropriately matched control group to enhance the outcomes and strengthen the causal relationship between WMH and cognitive decline.

MR Acquisition Technique: Our MR acquisition protocol utilises a slice thickness of 4mm for both the FLAIR and diffusion sequences which represents a limitation of our study. A thickness of 4mm reduces our spatial resolution and limits segmentation of

smaller white matter lesions, and may contribute to partial volume effects (mixing of signals from adjacent tissue), compromising the ability to distinguish between smaller lesions. Thinner slices (2-3mm ideally) would provide more accurate lesion segmentation. In addition, the implementation of a multi-shell sequence would allow for more detailed characterisation of white matter microstructure through utilisation of multiple B value acquisitions. This would allow for diffusion kurtosis imaging and more complex analysis of white matter microstructure, enhancing the differentiation of our described white matter phenotypes. Furthermore, multi-shell imaging would mitigate the effect of partial volume errors. Adopting higher resolution images and a multi-shell technique would result in more accurate data.

Absence of Volumetric Brain Atrophy Measures: Our analysis did not include quantitative measures of global or regional brain atrophy. This is an important limitation because WMH association with cognition may be confounded or mediated by neurodegenerative change. Brain atrophy captures a partly distinct biological pathway (neuronal and synaptic loss) which may coexist with, result from, or perhaps be independent of, small vessel disease. Without volumetric data we cannot apportion variance in cognition between WMHs and neurodegeneration or atrophy. Similarly, we could not determine whether brain atrophy mediates the effect of WMH on cognition and could not determine if higher WMH burden had a more significant effect on cognition in individuals with lower brain reserve. This limitation is of particular significance given the cognitive endpoints of the study and the link of medial temporal and cortical atrophy with cognitive decline. From a practical standpoint, the inclusion of a synchronous analysis pipeline including volumetric data to derive measures of brain volume as well as lesion segmentation could enable multivariable models that adjust for or specifically test mediation by, brain atrophy.

Limited Cortical Sensitivity of FLAIR and Absence of Cortex-Specific Measures: Our imaging protocol relied on FLAIR, which is well suited to detecting periventricular and deep white-matter lesions but has limited sensitivity to cortical pathology. The thin cortical ribbon is prone to partial-volume averaging with CSF, flow/susceptibility artefacts in sulci, and lower SNR at gyral crowns; as a result, cortical microinfarcts, focal cortical gliosis/demyelination, and subtle laminar changes are often invisible or equivocal on conventional FLAIR. Given that ageing and cognition were central to this study, this is a meaningful constraint: cortical measures (e.g., cortical thickness/surface area as proxies for brain ageing; detection of cortical lesions that disrupt associative networks) could confound or mediate WMH–cognition associations. Without cortex-specific metrics we cannot determine whether observed cognitive effects are driven by white-matter damage alone or by co-existing cortical degeneration. Future work could include Double Inversion Recovery (DIR) sequences to suppress CSF and white matter highlighting intracortical lesions. Phase-Sensitive Inversion Recovery (PSIR) could be used to enhance grey-white matter contrast, aiding the detection of subtle cortical lesions and improving cortical thickness estimation.

Acknowledging both strengths and limitations, our study offers a nuanced exploration of the complex relationships between WMH characteristics and cognitive decline. The comprehensive approach, from advanced lesion phenotyping to consideration of diverse factors, contributes to a balanced interpretation of our findings. While our observations provide valuable insights, the identified limitations underscore the need for continued research refinement and external validation. Striking a balance between the strengths and

limitations enhances the reliability and applicability of our study, paving the way for future investigations in this evolving field.

CHAPTER 14: Implications for Future Research

To my knowledge, this is the largest Irish study to date and may serve as a population wide reference to help clinicians understand the pathophysiology underlying age related cerebral white matter hyperintensities, inform their clinical and radiological interpretation and potentially lead to more patient specific medical care.

The comprehensive study presented in this thesis has explored the complexities of WMHs, delving into their historical context, imaging features, and associations with aging and cognitive decline. Through a combination of advanced neuroimaging techniques, including Diffusion Tensor Imaging, this work has contributed to our understanding of WMH heterogeneity and its impact on brain function.

WMHs are increasingly recognised as significant biomarkers of cerebral small vessel disease, reflecting both macrostructural and microstructural alterations in brain tissue. The findings from this thesis support the notion that WMHs are not uniform entities but rather exhibit heterogeneous phenotypes that correlate with different clinical outcomes. Specifically, WMH burden, as measured by volume, location, and microstructural properties (e.g. reduced fractional anisotropy and increased mean diffusivity), is linked to accelerated cognitive decline in older adults.

The key findings of this thesis include the identification of distinct white matter hyperintensity phenotypes based on location and microstructural properties. These differences in WMH characteristics have implications for predicting which individuals will progress to demonstrate preserved cognition versus cognitive impairment. Increased volume of WMHs combined with low FA and high MD is strongly associated with poorer cognitive function over time. This implies that assessment of diffusion properties using DTI is integral to understanding the implication of these lesions. Use of such advanced techniques offer a potential avenue to detect patients at risk of dementia. Early identification of these individuals with high risk WMHs could enable targeted interventions aimed at reducing the rate of progression of cognitive decline. The findings underscore the importance of implementing advanced imaging techniques in specialised clinical assessments of ageing patients.

We should consider doing further research into the pathogenesis and natural history of cerebral WHMs and ageing. Further study of the longitudinal implications of these lesions and their relationship with neuropsychological diseases is likely to yield tangible outcomes. Future research could consider the association of WMH burden, including WMH phenotypes and the relationship with entities including depression, autonomic dysfunction, falls and incident diseases.

The investigation of these lesions is heavily rooted in image acquisition and currently the field of radiology is seeing rapid growth in artificial intelligence. As lesion segmentation technologies and artificial intelligence techniques become more widely available, the ability to more accurately isolate pathology and process the vast quantities of information produced will become streamlined. In tandem to improvements in software, hardware improvements are also ever present, with the advent of 7T MRI scanners becoming more commercially available. The increase in field strength allows even higher levels of fidelity of MR images.

Future studies should avail of PET imaging of microglial activation to interrogate the inflammatory component of WMH pathophysiology. Translocator protein (TSPO) PET provides an in-vivo index of glial activation in normal appearing white matter and WMHs. Analysis of TSPO PET in conjunction with MRI and longitudinal cognitive data would provide new avenues of research including topographical mapping of TSPO signal relative to WMH burden, potential longitudinal analysis to determine if TSPO activation predicts subsequent WMH growth and microstructural damage and whether these changes mediate cognitive decline.

The longitudinal nature of study invites continued analysis as TILDA continues to collect data on patients in our cohort. Because MRI yields model-based signals rather than direct histology, brain banking is essential to resolve the biological heterogeneity underpinning WMHs and to validate imaging biomarkers. Prospective consent for brain donation (via the Dublin Brain Bank) would allow for lesion targeted sampling enabling quantification of biomarkers and histological correlation. The development of a linked MRI/PET/Cognitive/Histological dataset would enable rigorous validation of these biomarkers and provide a clear account of the pathogenesis of WMHs in ageing. Ultimately comparing our findings with histopathological specimens may prove to be instrumental in the goal of one day converting MRI scanners into an in-vivo microscope.

BIBLIOGRAPHY

1. Hachinski VC, Potter P, Merskey H. Leuko-araiosis. Arch Neurol. 1987 Jan;44(1):21–3.
2. Moody DM, Bell MA, Challa VR. The corpus callosum, a unique white-matter tract: anatomic features that may explain sparing in Binswanger disease and resistance to flow of fluid masses. AJNR Am J Neuroradiol. 1988;9(6):1051–9.
3. Caplan LR. Binswanger's disease--revisited. Neurology. 1995 Apr;45(4):626–33.
4. Rosenberg GA. Binswanger's disease. Arch Neurol. 1986 July;43(7):641–2.
5. Blass JP, Hoyer S, Nitsch R. A translation of Otto Binswanger's article, "The delineation of the generalized progressive paralyses". 1894. Arch Neurol. 1991 Sept;48(9):961–72.
6. Xiong YY, Mok V. Age-Related White Matter Changes. J Aging Res. 2011;2011:617927.
7. Bohnen NI, Bogan CW, Müller MLTM. Frontal and periventricular brain white matter lesions and cortical deafferentation of cholinergic and other neuromodulatory axonal projections. Eur Neurol J. 2009 Sept;1(1):33–50.
8. Wardlaw JM, Smith EE, Biessels GJ, Cordonnier C, Fazekas F, Frayne R, et al. Neuroimaging standards for research into small vessel disease and its contribution to ageing and neurodegeneration. Lancet Neurol. 2013 Aug;12(8):822–38.
9. Wardlaw JM, Valdés Hernández MC, Muñoz-Maniega S. What are white matter hyperintensities made of? Relevance to vascular cognitive impairment. J Am Heart Assoc. 2015 June 23;4(6):001140.
10. Hadley DM, Teasdale GM. Magnetic resonance imaging of the brain and spine. J Neurol. 1988 Mar;235(4):193–206.
11. Verny M, Duyckaerts C, Pierot L, Hauw JJ. Leuko-araiosis. Dev Neurosci. 1991;13(4–5):245–50.
12. Wahlund LO. Brain imaging and vascular dementia. Dementia. 1994;5(3–4):193–6.
13. Yanagisawa M, Kitahama T. [Clinical differences between multiple cerebral infarcts with and without dementia]. Nihon Rinsho. 1993 Dec;51 Suppl:457–63.
14. Le Bihan D, Breton E, Lallemand D, Grenier P, Cabanis E, Laval-Jeantet M. MR imaging of intravoxel incoherent motions: application to diffusion and perfusion in neurologic disorders. Radiology. 1986 Nov;161(2):401–7.
15. Pierpaoli C, Jezzard P, Basser PJ, Barnett A, Di Chiro G. Diffusion tensor MR imaging of the human brain. Radiology. 1996 Dec;201(3):637–48.
16. Munoz DG, Hastak SM, Harper B, Lee D, Hachinski VC. Pathologic correlates of increased signals of the centrum ovale on magnetic resonance imaging. Arch Neurol. 1993 May;50(5):492–7.
17. Fazekas F, Kleinert R, Offenbacher H, Schmidt R, Kleinert G, Payer F, et al. Pathologic correlates of incidental MRI white matter signal hyperintensities. Neurology. 1993 Sept;43(9):1683–9.
18. Fisher CM. Lacunar strokes and infarcts: a review. Neurology. 1982 Aug;32(8):871–6.
19. Fisher CM. LACUNES: SMALL, DEEP CEREBRAL INFARCTS. Neurology. 1965 Aug;15:774–84.
20. Fernando MS, O'Brien JT, Perry RH, English P, Forster G, McMeekin W, et al. Comparison of the pathology of cerebral white matter with post-mortem magnetic

resonance imaging (MRI) in the elderly brain. Neuropathol Appl Neurobiol. 2004 Aug;30(4):385–95.
21. Lee DY, Fletcher E, Martinez O, Ortega M, Zozulya N, Kim J, et al. Regional pattern of white matter microstructural changes in normal aging, MCI, and AD. Neurology. 2009 Nov 24;73(21):1722–8.
22. van Walderveen MA, Kamphorst W, Scheltens P, van Waesberghe JH, Ravid R, Valk J, et al. Histopathologic correlate of hypointense lesions on T1-weighted spin-echo MRI in multiple sclerosis. Neurology. 1998 May;50(5):1282–8.
23. Kozachuk WE, DeCarli C, Schapiro MB, Wagner EE, Rapoport SI, Horwitz B. White matter hyperintensities in dementia of Alzheimer's type and in healthy subjects without cerebrovascular risk factors. A magnetic resonance imaging study. Arch Neurol. 1990 Dec;47(12):1306–10.
24. Ylikoski A, Erkinjuntti T, Raininko R, Sarna S, Sulkava R, Tilvis R. White matter hyperintensities on MRI in the neurologically nondiseased elderly. Analysis of cohorts of consecutive subjects aged 55 to 85 years living at home. Stroke. 1995 July;26(7):1171–7.
25. Guttmann CR, Jolesz FA, Kikinis R, Killiany RJ, Moss MB, Sandor T, et al. White matter changes with normal aging. Neurology. 1998 Apr;50(4):972–8.
26. Sharma R, Sekhon S, Lui F, Cascella M. White Matter Lesions. In: StatPearls [Internet]. Treasure Island (FL): StatPearls Publishing; 2025 [cited 2025 Jan 11]. Available from: http://www.ncbi.nlm.nih.gov/books/NBK562167/
27. Smith EE, Saposnik G, Biessels GJ, Doubal FN, Fornage M, Gorelick PB, et al. Prevention of Stroke in Patients With Silent Cerebrovascular Disease: A Scientific Statement for Healthcare Professionals From the American Heart Association/American Stroke Association. Stroke. 2017 Feb;48(2):e44–71.
28. Zhuang FJ, Chen Y, He WB, Cai ZY. Prevalence of white matter hyperintensities increases with age. Neural Regen Res. 2018 Dec;13(12):2141–6.
29. Misquitta K, Dadar M, Louis Collins D, Tartaglia MC, Alzheimer's Disease Neuroimaging Initiative. White matter hyperintensities and neuropsychiatric symptoms in mild cognitive impairment and Alzheimer's disease. Neuroimage Clin. 2020;28:102367.
30. Fennema-Notestine C, McEvoy LK, Notestine R, Panizzon MS, Yau WYW, Franz CE, et al. White matter disease in midlife is heritable, related to hypertension, and shares some genetic influence with systolic blood pressure. Neuroimage Clin. 2016;12:737–45.
31. Fornage M, Debette S, Bis JC, Schmidt H, Ikram MA, Dufouil C, et al. Genome-wide association studies of cerebral white matter lesion burden: the CHARGE consortium. Ann Neurol. 2011 June;69(6):928–39.
32. Lin J, Wang D, Lan L, Fan Y. Multiple Factors Involved in the Pathogenesis of White Matter Lesions. Biomed Res Int. 2017;2017:9372050.
33. Kim KW, MacFall JR, Payne ME. Classification of white matter lesions on magnetic resonance imaging in elderly persons. Biol Psychiatry. 2008 Aug 15;64(4):273–80.
34. Ducros A, Boukobza M, Porcher R, Sarov M, Valade D, Bousser MG. The clinical and radiological spectrum of reversible cerebral vasoconstriction syndrome. A prospective series of 67 patients. Brain. 2007 Dec;130(Pt 12):3091–101.
35. Schiffmann R, van der Knaap MS. Invited article: an MRI-based approach to the diagnosis of white matter disorders. Neurology. 2009 Feb 24;72(8):750–9.
36. van Straaten ECW, Fazekas F, Rostrup E, Scheltens P, Schmidt R, Pantoni L, et al. Impact of white matter hyperintensities scoring method on correlations with clinical data: the LADIS study. Stroke. 2006 Mar;37(3):836–40.

37. Rostrup E, Gouw AA, Vrenken H, van Straaten ECW, Ropele S, Pantoni L, et al. The spatial distribution of age-related white matter changes as a function of vascular risk factors--results from the LADIS study. Neuroimage. 2012 Apr 15;60(3):1597–607.
38. Rowbotham GF, Little E. CIRCULATIONS OF THE CEREBRAL HEMISPHERES. Br J Surg. 1965 Jan;52:8–21.
39. Ravens JR, Toole JF, Hasegawa T. Anastomoses in the vascular bed of the human cerebrum. J Neuropathol Exp Neurol. 1968 Jan;27(1):123–4.
40. Yao H, Sadoshima S, Ibayashi S, Kuwabara Y, Ichiya Y, Fujishima M. Leukoaraiosis and dementia in hypertensive patients. Stroke. 1992 Nov;23(11):1673–7.
41. Wakita H, Tomimoto H, Akiguchi I, Kimura J. Glial activation and white matter changes in the rat brain induced by chronic cerebral hypoperfusion: an immunohistochemical study. Acta Neuropathol. 1994;87(5):484–92.
42. Birns J, Jarosz J, Markus HS, Kalra L. Cerebrovascular reactivity and dynamic autoregulation in ischaemic subcortical white matter disease. J Neurol Neurosurg Psychiatry. 2009 Oct;80(10):1093–8.
43. Cerebrovascular dysfunction and microcirculation rarefaction precede white matter lesions in a mouse genetic model of cerebral ischemic small vessel disease - PubMed [Internet]. [cited 2025 Jan 11]. Available from: https://pubmed.ncbi.nlm.nih.gov/20071773/
44. Mok V, Ding D, Fu J, Xiong Y, Chu WWC, Wang D, et al. Transcranial Doppler ultrasound for screening cerebral small vessel disease: a community study. Stroke. 2012 Oct;43(10):2791–3.
45. Poels MMF, Zaccai K, Verwoert GC, Vernooij MW, Hofman A, van der Lugt A, et al. Arterial stiffness and cerebral small vessel disease: the Rotterdam Scan Study. Stroke. 2012 Oct;43(10):2637–42.
46. Joutel A, Monet-Leprêtre M, Gosele C, Baron-Menguy C, Hammes A, Schmidt S, et al. Cerebrovascular dysfunction and microcirculation rarefaction precede white matter lesions in a mouse genetic model of cerebral ischemic small vessel disease. J Clin Invest. 2010 Feb;120(2):433–45.
47. Guo ZN, Liu J, Xing Y, Yan S, Lv C, Jin H, et al. Dynamic cerebral autoregulation is heterogeneous in different subtypes of acute ischemic stroke. PLoS One. 2014;9(3):e93213.
48. White RP, Markus HS. Impaired dynamic cerebral autoregulation in carotid artery stenosis. Stroke. 1997 July;28(7):1340–4.
49. Immink RV, van Montfrans GA, Stam J, Karemaker JM, Diamant M, van Lieshout JJ. Dynamic cerebral autoregulation in acute lacunar and middle cerebral artery territory ischemic stroke. Stroke. 2005 Dec;36(12):2595–600.
50. Reinhard M, Roth M, Müller T, Guschlbauer B, Timmer J, Czosnyka M, et al. Effect of carotid endarterectomy or stenting on impairment of dynamic cerebral autoregulation. Stroke. 2004 June;35(6):1381–7.
51. Pantoni L. Cerebral small vessel disease: from pathogenesis and clinical characteristics to therapeutic challenges. Lancet Neurol. 2010 July;9(7):689–701.
52. Lee HY, Oh BH. Aging and arterial stiffness. Circ J. 2010 Nov;74(11):2257–62.
53. Diehl RR. Cerebral autoregulation studies in clinical practice. Eur J Ultrasound. 2002 Nov;16(1–2):31–6.
54. Caplan LR, Hennerici M. Impaired clearance of emboli (washout) is an important link between hypoperfusion, embolism, and ischemic stroke. Arch Neurol. 1998 Nov;55(11):1475–82.

55. Guo ZN, Xing Y, Wang S, Ma H, Liu J, Yang Y. Characteristics of dynamic cerebral autoregulation in cerebral small vessel disease: Diffuse and sustained. Sci Rep. 2015 Oct 15;5:15269.
56. Brickman AM, Honig LS, Scarmeas N, Tatarina O, Sanders L, Albert MS, et al. Measuring cerebral atrophy and white matter hyperintensity burden to predict the rate of cognitive decline in Alzheimer disease. Arch Neurol. 2008 Sept;65(9):1202–8.
57. Luchsinger JA, Brickman AM, Reitz C, Cho SJ, Schupf N, Manly JJ, et al. Subclinical cerebrovascular disease in mild cognitive impairment. Neurology. 2009 Aug 11;73(6):450–6.
58. LaFerla FM, Green KN, Oddo S. Intracellular amyloid-beta in Alzheimer's disease. Nat Rev Neurosci. 2007 July;8(7):499–509.
59. Kalaria RN. Linking cerebrovascular defense mechanisms in brain ageing and Alzheimer's disease. Neurobiol Aging. 2009 Sept;30(9):1512–4.
60. Austin SA, Santhanam AV, Katusic ZS. Endothelial nitric oxide modulates expression and processing of amyloid precursor protein. Circ Res. 2010 Dec 10;107(12):1498–502.
61. van Beek AH, Claassen JA, Rikkert MGO, Jansen RW. Cerebral autoregulation: an overview of current concepts and methodology with special focus on the elderly. J Cereb Blood Flow Metab. 2008 June;28(6):1071–85.
62. Chow N, Bell RD, Deane R, Streb JW, Chen J, Brooks A, et al. Serum response factor and myocardin mediate arterial hypercontractility and cerebral blood flow dysregulation in Alzheimer's phenotype. Proc Natl Acad Sci U S A. 2007 Jan 16;104(3):823–8.
63. Wang YL, Chen W, Cai WJ, Hu H, Xu W, Wang ZT, et al. Associations of White Matter Hyperintensities with Cognitive Decline: A Longitudinal Study. J Alzheimers Dis. 2020;73(2):759–68.
64. Garnier-Crussard A, Bougacha S, Wirth M, Dautricourt S, Sherif S, Landeau B, et al. White matter hyperintensity topography in Alzheimer's disease and links to cognition. Alzheimers Dement. 2022 Mar;18(3):422–33.
65. Andeweg J. The anatomy of collateral venous flow from the brain and its value in aetiological interpretation of intracranial pathology. Neuroradiology. 1996 Oct;38(7):621–8.
66. Schaller B, Graf R. Cerebral venous infarction: the pathophysiological concept. Cerebrovasc Dis. 2004;18(3):179–88.
67. Schaller B. Physiology of cerebral venous blood flow: from experimental data in animals to normal function in humans. Brain Res Brain Res Rev. 2004 Nov;46(3):243–60.
68. Fisher J, Vaghaiwalla F, Tsitlik J, Levin H, Brinker J, Weisfeldt M, et al. Determinants and clinical significance of jugular venous valve competence. Circulation. 1982 Jan;65(1):188–96.
69. Chung CP, Hsu HY, Chao AC, Chang FC, Sheng WY, Hu HH. Detection of intracranial venous reflux in patients of transient global amnesia. Neurology. 2006 June 27;66(12):1873–7.
70. Nakase H, Kempski OS, Heimann A, Takeshima T, Tintera J. Microcirculation after cerebral venous occlusions as assessed by laser Doppler scanning. J Neurosurg. 1997 Aug;87(2):307–14.
71. Nakase H, Nagata K, Otsuka H, Sakaki T, Kempski O. Local cerebral blood flow autoregulation following "asymptomatic" cerebral venous occlusion in the rat. J Neurosurg. 1998 July;89(1):118–24.

72. Morgan MK, Johnston I, Besser M, Baines D. Cerebral arteriovenous malformations, steal, and the hypertensive breakthrough threshold. An experimental study in rats. J Neurosurg. 1987 Apr;66(4):563–7.
73. Henry-Feugeas MC. Intracranial MR dynamics in clinically diagnosed Alzheimer's disease: the emerging concept of "pulse wave encephalopathy." Curr Alzheimer Res. 2009 Dec;6(6):488–502.
74. Abbott NJ, Rönnbäck L, Hansson E. Astrocyte-endothelial interactions at the blood-brain barrier. Nat Rev Neurosci. 2006 Jan;7(1):41–53.
75. Starr JM, Wardlaw J, Ferguson K, MacLullich A, Deary IJ, Marshall I. Increased blood-brain barrier permeability in type II diabetes demonstrated by gadolinium magnetic resonance imaging. J Neurol Neurosurg Psychiatry. 2003 Jan;74(1):70–6.
76. Tibbling G, Link H, Ohman S. Principles of albumin and IgG analyses in neurological disorders. I. Establishment of reference values. Scand J Clin Lab Invest. 1977 Sept;37(5):385–90.
77. Wallin A, Blennow K, Fredman P, Gottfries CG, Karlsson I, Svennerholm L. Blood brain barrier function in vascular dementia. Acta Neurol Scand. 1990 Apr;81(4):318–22.
78. Young VG, Halliday GM, Kril JJ. Neuropathologic correlates of white matter hyperintensities. Neurology. 2008 Sept 9;71(11):804–11.
79. Jalal FY, Yang Y, Thompson J, Lopez AC, Rosenberg GA. Myelin loss associated with neuroinflammation in hypertensive rats. Stroke. 2012 Apr;43(4):1115–22.
80. Maillard P, Seshadri S, Beiser A, Himali JJ, Au R, Fletcher E, et al. Effects of systolic blood pressure on white-matter integrity in young adults in the Framingham Heart Study: a cross-sectional study. Lancet Neurol. 2012 Dec;11(12):1039–47.
81. Mills KT, Stefanescu A, He J. The global epidemiology of hypertension. Nat Rev Nephrol. 2020 Apr;16(4):223–37.
82. Dufouil C, de Kersaint-Gilly A, Besançon V, Levy C, Auffray E, Brunnereau L, et al. Longitudinal study of blood pressure and white matter hyperintensities: the EVA MRI Cohort. Neurology. 2001 Apr 10;56(7):921–6.
83. Seshadri S, Wolf PA, Beiser A, Elias MF, Au R, Kase CS, et al. Stroke risk profile, brain volume, and cognitive function: the Framingham Offspring Study. Neurology. 2004 Nov 9;63(9):1591–9.
84. Swan GE, DeCarli C, Miller BL, Reed T, Wolf PA, Jack LM, et al. Association of midlife blood pressure to late-life cognitive decline and brain morphology. Neurology. 1998 Oct;51(4):986–93.
85. Kennedy KM, Raz N. Pattern of normal age-related regional differences in white matter microstructure is modified by vascular risk. Brain Res. 2009 Nov 10;1297:41–56.
86. Lee DY, Fletcher E, Martinez O, Ortega M, Zozulya N, Kim J, et al. Regional pattern of white matter microstructural changes in normal aging, MCI, and AD. Neurology. 2009 Nov 24;73(21):1722–8.
87. Salat DH, Williams VJ, Leritz EC, Schnyer DM, Rudolph JL, Lipsitz LA, et al. INTERINDIVIDUAL VARIATION IN BLOOD PRESSURE IS ASSOCIATED WITH REGIONAL WHITE MATTER INTEGRITY IN GENERALLY HEALTHY OLDER ADULTS. Neuroimage. 2012 Jan 2;59(1):181–92.
88. Atwood LD, Wolf PA, Heard-Costa NL, Massaro JM, Beiser A, D'Agostino RB, et al. Genetic variation in white matter hyperintensity volume in the Framingham Study. Stroke. 2004 July;35(7):1609–13.
89. Kochunov P, Glahn D, Winkler A, Duggirala R, Olvera RL, Cole S, et al. Analysis of genetic variability and whole genome linkage of whole-brain, subcortical, and ependymal hyperintense white matter volume. Stroke. 2009 Dec;40(12):3685–90.

90. DeStefano AL, Atwood LD, Massaro JM, Heard-Costa N, Beiser A, Au R, et al. Genome-wide scan for white matter hyperintensity: the Framingham Heart Study. Stroke. 2006 Jan;37(1):77–81.
91. Turner ST, Fornage M, Jack CR, Mosley TH, Kardia SLR, Boerwinkle E, et al. Genomic susceptibility loci for brain atrophy in hypertensive sibships from the GENOA study. Hypertension. 2005 Apr;45(4):793–8.
92. Lan LF, Zheng L, Yang X, Ji XT, Fan YH, Zeng JS. Peroxisome proliferator-activated receptor-γ agonist pioglitazone ameliorates white matter lesion and cognitive impairment in hypertensive rats. CNS Neurosci Ther. 2015 May;21(5):410–6.
93. Nebes RD, Vora IJ, Meltzer CC, Fukui MB, Williams RL, Kamboh MI, et al. Relationship of deep white matter hyperintensities and apolipoprotein E genotype to depressive symptoms in older adults without clinical depression. Am J Psychiatry. 2001 June;158(6):878–84.
94. van Rijn MJE, Bos MJ, Isaacs A, Yazdanpanah M, Arias-Vásquez A, Stricker BHC, et al. Polymorphisms of the renin-angiotensin system are associated with blood pressure, atherosclerosis and cerebral white matter pathology. J Neurol Neurosurg Psychiatry. 2007 Oct;78(10):1083–7.
95. Hassan A, Lansbury A, Catto AJ, Guthrie A, Spencer J, Craven C, et al. Angiotensin converting enzyme insertion/deletion genotype is associated with leukoaraiosis in lacunar syndromes. J Neurol Neurosurg Psychiatry. 2002 Mar;72(3):343–6.
96. Ozato K, Shin DM, Chang TH, Morse HC. TRIM family proteins and their emerging roles in innate immunity. Nat Rev Immunol. 2008 Nov;8(11):849–60.
97. Li Y, Huang X, Guo F, Lei T, Li S, Monaghan-Nichols P, et al. TRIM65 E3 ligase targets VCAM-1 degradation to limit LPS-induced lung inflammation. J Mol Cell Biol. 2020 Apr 24;12(3):190–201.
98. Haacke EM, Makki M, Ge Y, Maheshwari M, Sehgal V, Hu J, et al. Characterizing iron deposition in multiple sclerosis lesions using susceptibility weighted imaging. J Magn Reson Imaging. 2009 Mar;29(3):537–44.
99. Kleinschmidt-DeMasters BK, Norenberg MD. Rapid correction of hyponatremia causes demyelination: relation to central pontine myelinolysis. Science. 1981 Mar 6;211(4486):1068–70.
100. Redmond J, Cruse B, Kiers L. Nitrous oxide-induced neurological disorders: an increasing public health concern. Intern Med J. 2022 May;52(5):740–4.
101. Scaravilli F, Bazille C, Gray F. Neuropathologic contributions to understanding AIDS and the central nervous system. Brain Pathol. 2007 Apr;17(2):197–208.
102. Huang S, de Jong D, Das JP, Widemon RS, Braumuller B, Paily J, et al. Imaging the Side Effects of CAR T Cell Therapy: A Primer for the Practicing Radiologist. Acad Radiol. 2023 Nov;30(11):2712–27.
103. Smith DA, Kikano E, Tirumani SH, de Lima M, Caimi P, Ramaiya NH. Imaging-based Toxicity and Response Pattern Assessment Following CAR T-Cell Therapy. Radiology. 2022 Feb;302(2):438–45.
104. Martino M, Macheda S, Aguglia U, Arcudi L, Pucci G, Martino B, et al. Identifying and managing CAR T-cell-mediated toxicities: on behalf of an Italian CAR-T multidisciplinary team. Expert Opin Biol Ther. 2022 Mar;22(3):407–21.
105. Eckstein C, Saidha S, Levy M. A differential diagnosis of central nervous system demyelination: beyond multiple sclerosis. J Neurol. 2012 May;259(5):801–16.
106. Shah R, Bag AK, Chapman PR, Curé JK. Imaging manifestations of progressive multifocal leukoencephalopathy. Clin Radiol. 2010 June;65(6):431–9.

107. Ferreira S, D'Cruz DP, Hughes GRV. Multiple sclerosis, neuropsychiatric lupus and antiphospholipid syndrome: where do we stand? Rheumatology (Oxford). 2005 Apr;44(4):434–42.
108. Vitali P, Migliaccio R, Agosta F, Rosen HJ, Geschwind MD. Neuroimaging in dementia. Semin Neurol. 2008 Sept;28(4):467–83.
109. Ding XQ, Bley A, Ohlenbusch A, Kohlschütter A, Fiehler J, Zhu W, et al. Imaging evidence of early brain tissue degeneration in patients with vanishing white matter disease: a multimodal MR study. J Magn Reson Imaging. 2012 Apr;35(4):926–32.
110. Young NP, Weinshenker BG, Lucchinetti CF. Acute disseminated encephalomyelitis: current understanding and controversies. Semin Neurol. 2008 Feb;28(1):84–94.
111. Ashrafian H, Davey P. A review of the causes of central pontine myelinosis: yet another apoptotic illness? Eur J Neurol. 2001 Mar;8(2):103–9.
112. Huang D, Cossoy M, Li M, Choi D, Taege A, Staugaitis SM, et al. Inflammatory progressive multifocal leukoencephalopathy in human immunodeficiency virus-negative patients. Ann Neurol. 2007 July;62(1):34–9.
113. Seewann A, Enzinger C, Filippi M, Barkhof F, Rovira A, Gass A, et al. MRI characteristics of atypical idiopathic inflammatory demyelinating lesions of the brain : A review of reported findings. J Neurol. 2008 Jan;255(1):1–10.
114. Li J, Huang W, Luo X, Wen Y, Cho J, Kovanlikaya I, et al. The central vein sign in multiple sclerosis lesions: Susceptibility relaxation optimization from a routine MRI multiecho gradient echo sequence. J Neuroimaging. 2022 Jan;32(1):48–56.
115. Clarke MA, Cheek R, Kazimuddin HF, Hernandez B, Clarke R, McKnight CD, et al. Paramagnetic rim lesions and the central vein sign: Characterizing multiple sclerosis imaging markers. J Neuroimaging. 2024;34(1):86–94.
116. Black S, Gao F, Bilbao J. Understanding white matter disease: imaging-pathological correlations in vascular cognitive impairment. Stroke. 2009 Mar;40(3 Suppl):S48-52.
117. Jagust WJ, Zheng L, Harvey DJ, Mack WJ, Vinters HV, Weiner MW, et al. Neuropathological basis of magnetic resonance images in aging and dementia. Ann Neurol. 2008 Jan;63(1):72–80.
118. Erten-Lyons D, Woltjer R, Kaye J, Mattek N, Dodge HH, Green S, et al. Neuropathologic basis of white matter hyperintensity accumulation with advanced age. Neurology. 2013 Sept 10;81(11):977–83.
119. Braak H, Braak E, Grundke-Iqbal I, Iqbal K. Occurrence of neuropil threads in the senile human brain and in Alzheimer's disease: a third location of paired helical filaments outside of neurofibrillary tangles and neuritic plaques. Neurosci Lett. 1986 Apr 24;65(3):351–5.
120. Kidd M. Paired helical filaments in electron microscopy of Alzheimer's disease. Nature. 1963 Jan 12;197:192–3.
121. Brion JP. Neurofibrillary tangles and Alzheimer's disease. Eur Neurol. 1998 Oct;40(3):130–40.
122. Gavett BE, Stern RA, McKee AC. Chronic traumatic encephalopathy: a potential late effect of sport-related concussive and subconcussive head trauma. Clin Sports Med. 2011 Jan;30(1):179–88, xi.
123. Zlokovic BV. Neurovascular pathways to neurodegeneration in Alzheimer's disease and other disorders. Nat Rev Neurosci. 2011 Nov 3;12(12):723–38.
124. Brion JP, Anderton BH, Authelet M, Dayanandan R, Leroy K, Lovestone S, et al. Neurofibrillary tangles and tau phosphorylation. Biochem Soc Symp. 2001;(67):81–8.

125. Wang X, Xing A, Xu C, Cai Q, Liu H, Li L. Cerebrovascular hypoperfusion induces spatial memory impairment, synaptic changes, and amyloid-β oligomerization in rats. J Alzheimers Dis. 2010;21(3):813–22.
126. Knopman DS, Roberts R. Vascular risk factors: imaging and neuropathologic correlates. J Alzheimers Dis. 2010;20(3):699–709.
127. Choi J, Kim JY, Kwon HJ, Choi HJ, Kim SH, Kim S, et al. Association of cerebral white matter hyperintensities with coronary artery calcium in a healthy population: a cross-sectional study. Sci Rep. 2022 Dec 13;12(1):21562.
128. Yarchoan M, Xie SX, Kling MA, Toledo JB, Wolk DA, Lee EB, et al. Cerebrovascular atherosclerosis correlates with Alzheimer pathology in neurodegenerative dementias. Brain. 2012 Dec;135(Pt 12):3749–56.
129. van Beek JHGM, Kirkwood TBL, Bassingthwaighte JB. Understanding the physiology of the ageing individual: computational modelling of changes in metabolism and endurance. Interface Focus. 2016 Apr 6;6(2):20150079.
130. Weinert BT, Timiras PS. Invited review: Theories of aging. J Appl Physiol (1985). 2003 Oct;95(4):1706–16.
131. Dai X, Hummel SL, Salazar JB, Taffet GE, Zieman S, Schwartz JB. Cardiovascular physiology in the older adults. J Geriatr Cardiol. 2015 May;12(3):196–201.
132. Barnett K, Mercer SW, Norbury M, Watt G, Wyke S, Guthrie B. Epidemiology of multimorbidity and implications for health care, research, and medical education: a cross-sectional study. Lancet. 2012 July 7;380(9836):37–43.
133. Franklin SS, Gustin W, Wong ND, Larson MG, Weber MA, Kannel WB, et al. Hemodynamic patterns of age-related changes in blood pressure. The Framingham Heart Study. Circulation. 1997 July 1;96(1):308–15.
134. Doubal FN, MacLullich AMJ, Ferguson KJ, Dennis MS, Wardlaw JM. Enlarged perivascular spaces on MRI are a feature of cerebral small vessel disease. Stroke. 2010 Mar;41(3):450–4.
135. Jurcau MC, Jurcau A, Cristian A, Hogea VO, Diaconu RG, Nunkoo VS. Inflammaging and Brain Aging. Int J Mol Sci. 2024 Sept 30;25(19):10535.
136. López-Otín C, Blasco MA, Partridge L, Serrano M, Kroemer G. The hallmarks of aging. Cell. 2013 June 6;153(6):1194–217.
137. López-Otín C, Blasco MA, Partridge L, Serrano M, Kroemer G. Hallmarks of aging: An expanding universe. Cell. 2023 Jan 19;186(2):243–78.
138. Liddelow SA, Guttenplan KA, Clarke LE, Bennett FC, Bohlen CJ, Schirmer L, et al. Neurotoxic reactive astrocytes are induced by activated microglia. Nature. 2017 Jan 26;541(7638):481–7.
139. Gautam J, Cao Y, Yao Y. Pericytic Laminin Maintains Blood-Brain Barrier Integrity in an Age-Dependent Manner. Transl Stroke Res. 2020 Apr;11(2):228–42.
140. Rahimian R, Cordeau P, Kriz J. Brain Response to Injuries: When Microglia Go Sexist. Neuroscience. 2019 May 1;405:14–23.
141. Chen D, Huang Y, Shi Z, Li J, Zhang Y, Wang K, et al. Demyelinating processes in aging and stroke in the central nervous system and the prospect of treatment strategy. CNS Neurosci Ther. 2020 Dec;26(12):1219–29.
142. Shibao C, Grijalva CG, Raj SR, Biaggioni I, Griffin MR. Orthostatic hypotension-related hospitalizations in the United States. Am J Med. 2007 Nov;120(11):975–80.
143. Sprung J, Knopman DS, Petersen RC, Mielke MM, Weingarten TN, Vassilaki M, et al. Association of Hospitalization with Long-Term Cognitive Trajectories in Older Adults. J Am Geriatr Soc. 2021 Mar;69(3):660–8.

144. Debette S, Beiser A, DeCarli C, Au R, Himali JJ, Kelly-Hayes M, et al. Association of MRI markers of vascular brain injury with incident stroke, mild cognitive impairment, dementia, and mortality: the Framingham Offspring Study. Stroke. 2010 Apr;41(4):600–6.
145. Ghaznawi R, Geerlings MI, Jaarsma-Coes M, Hendrikse J, de Bresser J, UCC-Smart Study Group. Association of White Matter Hyperintensity Markers on MRI and Long-term Risk of Mortality and Ischemic Stroke: The SMART-MR Study. Neurology. 2021 Apr 27;96(17):e2172–83.
146. Tavares-Júnior JWL, de Souza ACC, Alves GS, Bonfadini J de C, Siqueira-Neto JI, Braga-Neto P. Cognitive Assessment Tools for Screening Older Adults With Low Levels of Education: A Critical Review. Front Psychiatry. 2019;10:878.
147. Molnar FJ, Benjamin S, Hawkins SA, Briscoe M, Ehsan S. One Size Does Not Fit All: Choosing Practical Cognitive Screening Tools for Your Practice. J Am Geriatr Soc. 2020 Oct;68(10):2207–13.
148. Parikh S, Bernard G, Leventer RJ, van der Knaap MS, van Hove J, Pizzino A, et al. A clinical approach to the diagnosis of patients with leukodystrophies and genetic leukoencephelopathies. Mol Genet Metab. 2015 Apr;114(4):501–15.
149. Hu HY, Ou YN, Shen XN, Qu Y, Ma YH, Wang ZT, et al. White matter hyperintensities and risks of cognitive impairment and dementia: A systematic review and meta-analysis of 36 prospective studies. Neurosci Biobehav Rev. 2021 Jan;120:16–27.
150. Filley CM, Fields RD. White matter and cognition: making the connection. J Neurophysiol. 2016 Nov 1;116(5):2093–104.
151. Wardlaw JM, Chappell FM, Valdés Hernández MDC, Makin SDJ, Staals J, Shuler K, et al. White matter hyperintensity reduction and outcomes after minor stroke. Neurology. 2017 Sept 5;89(10):1003–10.
152. Ngandu T, Lehtisalo J, Solomon A, Levälahti E, Ahtiluoto S, Antikainen R, et al. A 2 year multidomain intervention of diet, exercise, cognitive training, and vascular risk monitoring versus control to prevent cognitive decline in at-risk elderly people (FINGER): a randomised controlled trial. Lancet. 2015 June 6;385(9984):2255–63.
153. Medana IM, Esiri MM. Axonal damage: a key predictor of outcome in human CNS diseases. Brain. 2003 Mar;126(Pt 3):515–30.
154. Hase Y, Horsburgh K, Ihara M, Kalaria RN. White matter degeneration in vascular and other ageing-related dementias. J Neurochem. 2018 Mar;144(5):617–33.
155. Fields RD. A new mechanism of nervous system plasticity: activity-dependent myelination. Nat Rev Neurosci. 2015 Dec;16(12):756–67.
156. Sampaio-Baptista C, Johansen-Berg H. White Matter Plasticity in the Adult Brain. Neuron. 2017 Dec 20;96(6):1239–51.
157. Zatorre RJ, Fields RD, Johansen-Berg H. Plasticity in gray and white: neuroimaging changes in brain structure during learning. Nat Neurosci. 2012 Mar 18;15(4):528–36.
158. Sorond FA, Gorelick PB. Brain White Matter: A Substrate for Resilience and a Substance for Subcortical Small Vessel Disease. Brain Sci. 2019 Aug 8;9(8):193.
159. Hofstetter S, Tavor I, Tzur Moryosef S, Assaf Y. Short-term learning induces white matter plasticity in the fornix. J Neurosci. 2013 July 31;33(31):12844–50.
160. Schlaug G, Marchina S, Norton A. Evidence for plasticity in white-matter tracts of patients with chronic Broca's aphasia undergoing intense intonation-based speech therapy. Ann N Y Acad Sci. 2009 July;1169:385–94.
161. Filley CM. Cognitive Dysfunction in White Matter Disorders: New Perspectives in Treatment and Recovery. J Neuropsychiatry Clin Neurosci. 2021;33(4):349–55.

162. Al-Janabi OM, Bauer CE, Goldstein LB, Murphy RR, Bahrani AA, Smith CD, et al. White Matter Hyperintensity Regression: Comparison of Brain Atrophy and Cognitive Profiles with Progression and Stable Groups. Brain Sci. 2019 July 19;9(7):170.
163. Firbank MJ, Wiseman RM, Burton EJ, Saxby BK, O'Brien JT, Ford GA. Brain atrophy and white matter hyperintensity change in older adults and relationship to blood pressure. Brain atrophy, WMH change and blood pressure. J Neurol. 2007 June;254(6):713–21.
164. Verhaaren BFJ, Vernooij MW, de Boer R, Hofman A, Niessen WJ, van der Lugt A, et al. High blood pressure and cerebral white matter lesion progression in the general population. Hypertension. 2013 June;61(6):1354–9.
165. Prabhakaran S. Blood Pressure, Brain Volume and White Matter Hyperintensities, and Dementia Risk. JAMA. 2019 Aug 13;322(6):512–3.
166. Lauterbur PC. Image formation by induced local interactions. Examples employing nuclear magnetic resonance. 1973. Clin Orthop Relat Res. 1989 July;(244):3–6.
167. Röntgen WC. ON A NEW KIND OF RAYS. Science. 1896 Feb 14;3(59):227–31.
168. Manbachi A, Cobbold RSC. Development and Application of Piezoelectric Materials for Ultrasound Generation and Detection. Ultrasound. 2011 Nov;19(4):187–96.
169. Thomas AMK, Busch U. Sir Godfrey Hounsfield at 100. Z Med Phys. 2019 Dec;29(4):299–301.
170. Rabi II, Zacharias JR, Millman S, Kusch P. Milestones in magnetic resonance: "a new method of measuring nuclear magnetic moment" . 1938. J Magn Reson Imaging. 1992;2(2):131–3.
171. Roy TL, Forbes TL, Dueck AD, Wright GA. MRI for peripheral artery disease: Introductory physics for vascular physicians. Vasc Med. 2018 Apr;23(2):153–62.
172. Soher BJ, Dale BM, Merkle EM. A review of MR physics: 3T versus 1.5T. Magn Reson Imaging Clin N Am. 2007 Aug;15(3):277–90, v.
173. Viard A, Eustache F, Segobin S. History of Magnetic Resonance Imaging: A Trip Down Memory Lane. Neuroscience. 2021 Oct 15;474:3–13.
174. Chavhan GB, Babyn PS, Thomas B, Shroff MM, Haacke EM. Principles, techniques, and applications of T2*-based MR imaging and its special applications. Radiographics. 2009;29(5):1433–49.
175. De Coene B, Hajnal JV, Gatehouse P, Longmore DB, White SJ, Oatridge A, et al. MR of the brain using fluid-attenuated inversion recovery (FLAIR) pulse sequences. AJNR Am J Neuroradiol. 1992;13(6):1555–64.
176. Okuda T, Korogi Y, Shigematsu Y, Sugahara T, Hirai T, Ikushima I, et al. Brain lesions: when should fluid-attenuated inversion-recovery sequences be used in MR evaluation? Radiology. 1999 Sept;212(3):793–8.
177. Hajnal JV, Bryant DJ, Kasuboski L, Pattany PM, De Coene B, Lewis PD, et al. Use of fluid attenuated inversion recovery (FLAIR) pulse sequences in MRI of the brain. J Comput Assist Tomogr. 1992;16(6):841–4.
178. Le Bihan D. Diffusion, confusion and functional MRI. Neuroimage. 2012 Aug 15;62(2):1131–6.
179. Novikov DS. The present and the future of microstructure MRI: From a paradigm shift to normal science. J Neurosci Methods. 2021 Mar 1;351:108947.
180. Naraghi AM, Awdeh H, Wadhwa V, Andreisek G, Chhabra A. Diffusion tensor imaging of peripheral nerves. Semin Musculoskelet Radiol. 2015 Apr;19(2):191–200.
181. Moseley ME, Kucharczyk J, Mintorovitch J, Cohen Y, Kurhanewicz J, Derugin N, et al. Diffusion-weighted MR imaging of acute stroke: correlation with T2-weighted

and magnetic susceptibility-enhanced MR imaging in cats. AJNR Am J Neuroradiol. 1990 May;11(3):423–9.
182. Balyasnikova S, Löfgren J, de Nijs R, Zamogilnaya Y, Højgaard L, Fischer BM. PET/MR in oncology: an introduction with focus on MR and future perspectives for hybrid imaging. Am J Nucl Med Mol Imaging. 2012;2(4):458–74.
183. Alexander AL, Lee JE, Lazar M, Field AS. Diffusion tensor imaging of the brain. Neurotherapeutics. 2007 July;4(3):316–29.
184. Horsfield MA, Jones DK. Applications of diffusion-weighted and diffusion tensor MRI to white matter diseases - a review. NMR Biomed. 2002;15(7–8):570–7.
185. Skare S, Andersson JL. On the effects of gating in diffusion imaging of the brain using single shot EPI. Magn Reson Imaging. 2001 Oct;19(8):1125–8.
186. Conturo TE, Lori NF, Cull TS, Akbudak E, Snyder AZ, Shimony JS, et al. Tracking neuronal fiber pathways in the living human brain. Proc Natl Acad Sci U S A. 1999 Aug 31;96(18):10422–7.
187. Hagmann P, Jonasson L, Maeder P, Thiran JP, Wedeen VJ, Meuli R. Understanding diffusion MR imaging techniques: from scalar diffusion-weighted imaging to diffusion tensor imaging and beyond. Radiographics. 2006 Oct;26 Suppl 1:S205-223.
188. Ozturk A, Sasson AD, Farrell J a. D, Landman BA, da Motta ACBS, Aralasmak A, et al. Regional differences in diffusion tensor imaging measurements: assessment of intrarater and interrater variability. AJNR Am J Neuroradiol. 2008 June;29(6):1124–7.
189. Beaulieu C. The basis of anisotropic water diffusion in the nervous system - a technical review. NMR Biomed. 2002;15(7–8):435–55.
190. Hasan KM, Walimuni IS, Abid H, Hahn KR. A review of diffusion tensor magnetic resonance imaging computational methods and software tools. Comput Biol Med. 2011 Dec;41(12):1062–72.
191. Polders DL, Leemans A, Hendrikse J, Donahue MJ, Luijten PR, Hoogduin JM. Signal to noise ratio and uncertainty in diffusion tensor imaging at 1.5, 3.0, and 7.0 Tesla. J Magn Reson Imaging. 2011 June;33(6):1456–63.
192. Nana R, Zhao T, Hu X. Single-shot multiecho parallel echo-planar imaging (EPI) for diffusion tensor imaging (DTI) with improved signal-to-noise ratio (SNR) and reduced distortion. Magn Reson Med. 2008 Dec;60(6):1512–7.
193. Bammer R, Holdsworth SJ, Veldhuis WB, Skare ST. New methods in diffusion-weighted and diffusion tensor imaging. Magn Reson Imaging Clin N Am. 2009 May;17(2):175–204.
194. Jones DK, Cercignani M. Twenty-five pitfalls in the analysis of diffusion MRI data. NMR Biomed. 2010 Aug;23(7):803–20.
195. Johnson G, Jung KJ, Wu EX, Hilal SK. Self-correction of proton spectroscopic images for gradient eddy current distortions and static field inhomogeneities. Magn Reson Med. 1993 Aug;30(2):255–61.
196. Mohammadi S, Möller HE, Kugel H, Müller DK, Deppe M. Correcting eddy current and motion effects by affine whole-brain registrations: evaluation of three-dimensional distortions and comparison with slicewise correction. Magn Reson Med. 2010 Oct;64(4):1047–56.
197. Truong TK, Chen N kuei, Song AW. Dynamic correction of artifacts due to susceptibility effects and time-varying eddy currents in diffusion tensor imaging. Neuroimage. 2011 Aug 15;57(4):1343–7.
198. Kober T, Gruetter R, Krueger G. Prospective and retrospective motion correction in diffusion magnetic resonance imaging of the human brain. Neuroimage. 2012 Jan 2;59(1):389–98.

199. Gallichan D, Scholz J, Bartsch A, Behrens TE, Robson MD, Miller KL. Addressing a systematic vibration artifact in diffusion-weighted MRI. Hum Brain Mapp. 2010 Feb;31(2):193–202.
200. Liu Z, Wang Y, Gerig G, Gouttard S, Tao R, Fletcher T, et al. Quality Control of Diffusion Weighted Images. Proc SPIE Int Soc Opt Eng. 2010 Mar 11;7628:76280J-.
201. Yoshita M, Fletcher E, DeCarli C. Current concepts of analysis of cerebral white matter hyperintensities on magnetic resonance imaging. Top Magn Reson Imaging. 2005 Dec;16(6):399–407.
202. Fazekas F, Chawluk JB, Alavi A, Hurtig HI, Zimmerman RA. MR signal abnormalities at 1.5 T in Alzheimer's dementia and normal aging. AJR Am J Roentgenol. 1987 Aug;149(2):351–6.
203. de Leeuw FE, de Groot JC, Achten E, Oudkerk M, Ramos LM, Heijboer R, et al. Prevalence of cerebral white matter lesions in elderly people: a population based magnetic resonance imaging study. The Rotterdam Scan Study. J Neurol Neurosurg Psychiatry. 2001 Jan;70(1):9–14.
204. Scheltens P, Barkhof F, Leys D, Pruvo JP, Nauta JJ, Vermersch P, et al. A semiquantative rating scale for the assessment of signal hyperintensities on magnetic resonance imaging. J Neurol Sci. 1993 Jan;114(1):7–12.
205. Liao D, Cooper L, Cai J, Toole JF, Bryan NR, Hutchinson RG, et al. Presence and severity of cerebral white matter lesions and hypertension, its treatment, and its control. The ARIC Study. Atherosclerosis Risk in Communities Study. Stroke. 1996 Dec;27(12):2262–70.
206. Prins ND, van Straaten ECW, van Dijk EJ, Simoni M, van Schijndel RA, Vrooman HA, et al. Measuring progression of cerebral white matter lesions on MRI: visual rating and volumetrics. Neurology. 2004 May 11;62(9):1533–9.
207. Mäntylä R, Erkinjuntti T, Salonen O, Aronen HJ, Peltonen T, Pohjasvaara T, et al. Variable agreement between visual rating scales for white matter hyperintensities on MRI. Comparison of 13 rating scales in a poststroke cohort. Stroke. 1997 Aug;28(8):1614–23.
208. Leys D, Soetaert G, Petit H, Fauquette A, Pruvo JP, Steinling M. Periventricular and white matter magnetic resonance imaging hyperintensities do not differ between Alzheimer's disease and normal aging. Arch Neurol. 1990 May;47(5):524–7.
209. Grimaud J, Lai M, Thorpe J, Adeleine P, Wang L, Barker GJ, et al. Quantification of MRI lesion load in multiple sclerosis: a comparison of three computer-assisted techniques. Magn Reson Imaging. 1996;14(5):495–505.
210. Tubi MA, Feingold FW, Kothapalli D, Hare ET, King KS, Thompson PM, et al. White matter hyperintensities and their relationship to cognition: Effects of segmentation algorithm. Neuroimage. 2020 Feb 1;206:116327.
211. van den Heuvel DMJ, ten Dam VH, de Craen AJM, Admiraal-Behloul F, van Es ACGM, Palm WM, et al. Measuring longitudinal white matter changes: comparison of a visual rating scale with a volumetric measurement. AJNR Am J Neuroradiol. 2006 Apr;27(4):875–8.
212. Davis Garrett K, Cohen RA, Paul RH, Moser DJ, Malloy PF, Shah P, et al. Computer-mediated measurement and subjective ratings of white matter hyperintensities in vascular dementia: relationships to neuropsychological performance. Clin Neuropsychol. 2004 Feb;18(1):50–62.
213. Meier DS, Weiner HL, Guttmann CRG. Time-series modeling of multiple sclerosis disease activity: a promising window on disease progression and repair potential? Neurotherapeutics. 2007 July;4(3):485–98.

214. Mikol DD, Barkhof F, Chang P, Coyle PK, Jeffery DR, Schwid SR, et al. Comparison of subcutaneous interferon beta-1a with glatiramer acetate in patients with relapsing multiple sclerosis (the REbif vs Glatiramer Acetate in Relapsing MS Disease [REGARD] study): a multicentre, randomised, parallel, open-label trial. Lancet Neurol. 2008 Oct;7(10):903–14.
215. Tran P, Thoprakarn U, Gourieux E, Dos Santos CL, Cavedo E, Guizard N, et al. Automatic segmentation of white matter hyperintensities: validation and comparison with state-of-the-art methods on both Multiple Sclerosis and elderly subjects. Neuroimage Clin. 2022;33:102940.
216. Heinen R, Steenwijk MD, Barkhof F, Biesbroek JM, van der Flier WM, Kuijf HJ, et al. Performance of five automated white matter hyperintensity segmentation methods in a multicenter dataset. Sci Rep. 2019 Nov 14;9(1):16742.
217. Frangi AF, Niessen WJ, Viergever MA. Three-dimensional modeling for functional analysis of cardiac images: a review. IEEE Trans Med Imaging. 2001 Jan;20(1):2–25.
218. Sato Y, Nakajima S, Shiraga N, Atsumi H, Yoshida S, Koller T, et al. Three-dimensional multi-scale line filter for segmentation and visualization of curvilinear structures in medical images. Med Image Anal. 1998 June;2(2):143–68.
219. Ashburner J, Friston KJ. Voxel-based morphometry--the methods. Neuroimage. 2000 June;11(6 Pt 1):805–21.
220. Schmidt P, Gaser C, Arsic M, Buck D, Förschler A, Berthele A, et al. An automated tool for detection of FLAIR-hyperintense white-matter lesions in Multiple Sclerosis. Neuroimage. 2012 Feb 15;59(4):3774–83.
221. The Irish Longitudinal Study on Ageing (TILDA) - Trinity College Dublin [Internet]. [cited 2025 Jan 14]. Available from: https://tilda.tcd.ie/
222. Whelan BJ, Savva GM. Design and methodology of the Irish Longitudinal Study on Ageing. J Am Geriatr Soc. 2013 May;61 Suppl 2:S265-268.
223. Donoghue O, Foley M, Kenny RA. Cohort maintenance strategies used by The Irish Longitudinal Study on Ageing (TILDA). 2017 May 1 [cited 2025 Jan 14]; Available from: https://tilda.tcd.ie/publications/reports/CohortMaintenance/
224. Where Are We Now? - The Irish Longitudinal Study on Ageing (TILDA) - Trinity College Dublin [Internet]. [cited 2025 Jan 14]. Available from: https://tilda.tcd.ie/about/where-are-we-now/
225. Kenny RA, Whelan BJ, Cronin H, Kamiya Y, Kearney P, O'Regan C, et al. The Design of The Irish Longitudinal Study on Ageing. 2010 Feb 2 [cited 2025 Jan 14]; Available from: https://tilda.tcd.ie/publications/reports/DesignReport/index.php
226. Herrmann LL, Le Masurier M, Ebmeier KP. White matter hyperintensities in late life depression: a systematic review. J Neurol Neurosurg Psychiatry. 2008 June;79(6):619–24.
227. Debette S, Markus HS. The clinical importance of white matter hyperintensities on brain magnetic resonance imaging: systematic review and meta-analysis. BMJ. 2010 July 26;341:c3666.
228. Prins ND, Scheltens P. White matter hyperintensities, cognitive impairment and dementia: an update. Nat Rev Neurol. 2015 Mar;11(3):157–65.
229. Prins ND, van Dijk EJ, den Heijer T, Vermeer SE, Koudstaal PJ, Oudkerk M, et al. Cerebral white matter lesions and the risk of dementia. Arch Neurol. 2004 Oct;61(10):1531–4.
230. Maniega SM, Valdés Hernández MC, Clayden JD, Royle NA, Murray C, Morris Z, et al. White matter hyperintensities and normal-appearing white matter integrity in the aging brain. Neurobiol Aging. 2015 Feb;36(2):909–18.

231. Bastin ME, Clayden JD, Pattie A, Gerrish IF, Wardlaw JM, Deary IJ. Diffusion tensor and magnetization transfer MRI measurements of periventricular white matter hyperintensities in old age. Neurobiol Aging. 2009 Jan;30(1):125–36.
232. Pantoni L, Simoni M. Pathophysiology of cerebral small vessels in vascular cognitive impairment. Int Psychogeriatr. 2003;15 Suppl 1:59–65.
233. Gouw AA, Seewann A, van der Flier WM, Barkhof F, Rozemuller AM, Scheltens P, et al. Heterogeneity of small vessel disease: a systematic review of MRI and histopathology correlations. J Neurol Neurosurg Psychiatry. 2011 Feb;82(2):126–35.
234. Moody DM, Brown WR, Challa VR, Anderson RL. Periventricular venous collagenosis: association with leukoaraiosis. Radiology. 1995 Feb;194(2):469–76.
235. De Looze C, Williamson W, Hirst R, O'Connor J, Knight S, McCrory C, et al. Impaired orthostatic heart rate recovery is associated with smaller thalamic volume: Results from The Irish Longitudinal Study on Aging (TILDA). Hum Brain Mapp. 2020 Aug 15;41(12):3370–8.
236. ExploreDTI - General Info [Internet]. [cited 2025 Jan 15]. Available from: https://exploredti.com/generalinfo.htm
237. Vos SB, Tax CMW, Luijten PR, Ourselin S, Leemans A, Froeling M. The importance of correcting for signal drift in diffusion MRI. Magn Reson Med. 2017 Jan;77(1):285–99.
238. Perrone D, Aelterman J, Pižurica A, Jeurissen B, Philips W, Leemans A. The effect of Gibbs ringing artifacts on measures derived from diffusion MRI. Neuroimage. 2015 Oct 15;120:441–55.
239. Soares JM, Marques P, Alves V, Sousa N. A hitchhiker's guide to diffusion tensor imaging. Front Neurosci. 2013;7:31.
240. Irfanoglu MO, Walker L, Sarlls J, Marenco S, Pierpaoli C. Effects of image distortions originating from susceptibility variations and concomitant fields on diffusion MRI tractography results. Neuroimage. 2012 May 15;61(1):275–88.
241. Schmidt P. Bayesian inference for structured additive regression models for large-scale problems with applications to medical imaging. In 2017 [cited 2025 Jan 15]. Available from: https://www.semanticscholar.org/paper/Bayesian-inference-for-structured-additive-models-Schmidt/edc315de56ff336b75f36b30bad74fab231d39ca
242. Rolls ET, Joliot M, Tzourio-Mazoyer N. Implementation of a new parcellation of the orbitofrontal cortex in the automated anatomical labeling atlas. Neuroimage. 2015 Nov 15;122:1–5.
243. Nyquist PA, Bilgel M, Gottesman R, Yanek LR, Moy TF, Becker LC, et al. Age differences in periventricular and deep white matter lesions. Neurobiol Aging. 2015 Apr;36(4):1653–8.
244. Bozoki AC, Korolev IO, Davis NC, Hoisington LA, Berger KL. Disruption of limbic white matter pathways in mild cognitive impairment and Alzheimer's disease: a DTI/FDG-PET study. Hum Brain Mapp. 2012 Aug;33(8):1792–802.
245. Cherubini A, Péran P, Spoletini I, Di Paola M, Di Iulio F, Hagberg GE, et al. Combined volumetry and DTI in subcortical structures of mild cognitive impairment and Alzheimer's disease patients. J Alzheimers Dis. 2010;19(4):1273–82.
246. Bai F, Zhang Z, Watson DR, Yu H, Shi Y, Yuan Y, et al. Abnormal integrity of association fiber tracts in amnestic mild cognitive impairment. J Neurol Sci. 2009 Mar 15;278(1–2):102–6.
247. Fernando MS, Simpson JE, Matthews F, Brayne C, Lewis CE, Barber R, et al. White matter lesions in an unselected cohort of the elderly: molecular pathology suggests origin from chronic hypoperfusion injury. Stroke. 2006 June;37(6):1391–8.

248. Moody DM, Thore CR, Anstrom JA, Challa VR, Langefeld CD, Brown WR. Quantification of afferent vessels shows reduced brain vascular density in subjects with leukoaraiosis. Radiology. 2004 Dec;233(3):883–90.
249. Brown WR, Moody DM, Challa VR, Thore CR, Anstrom JA. Venous collagenosis and arteriolar tortuosity in leukoaraiosis. J Neurol Sci. 2002 Nov 15;203–204:159–63.
250. Li TR, Li BL, Xu XR, Zhong J, Wang TS, Liu FQ, et al. Association of white matter hyperintensities with cognitive decline and neurodegeneration. Front Aging Neurosci. 2024;16:1412735.
251. Sahlas DJ, Bilbao JM, Swartz RH, Black SE. Clasmatodendrosis correlating with periventricular hyperintensity in mixed dementia. Ann Neurol. 2002 Sept;52(3):378–81.
252. Simpson JE, Ince PG, Higham CE, Gelsthorpe CH, Fernando MS, Matthews F, et al. Microglial activation in white matter lesions and nonlesional white matter of ageing brains. Neuropathol Appl Neurobiol. 2007 Dec;33(6):670–83.
253. O'Sullivan M, Lythgoe DJ, Pereira AC, Summers PE, Jarosz JM, Williams SCR, et al. Patterns of cerebral blood flow reduction in patients with ischemic leukoaraiosis. Neurology. 2002 Aug 13;59(3):321–6.
254. O'Sullivan M, Summers PE, Jones DK, Jarosz JM, Williams SC, Markus HS. Normal-appearing white matter in ischemic leukoaraiosis: a diffusion tensor MRI study. Neurology. 2001 Dec 26;57(12):2307–10.
255. Leritz EC, Shepel J, Williams VJ, Lipsitz LA, McGlinchey RE, Milberg WP, et al. Associations between T1 white matter lesion volume and regional white matter microstructure in aging. Hum Brain Mapp. 2014 Mar;35(3):1085–100.
256. Maillard P, Fletcher E, Lockhart SN, Roach AE, Reed B, Mungas D, et al. White matter hyperintensities and their penumbra lie along a continuum of injury in the aging brain. Stroke. 2014 June;45(6):1721–6.

APPENDIX

TABLES

Table 1. Demographic descriptive statistics of the sample population

Descriptor	N = 497
Age (mean, sd)	68.5 (7.5)
Sex (Female, %)	51.9
Education (Low, %)	20.7
CVD conditions (>1, %)	29.7
Systolic/ Diastolic BP (mean, sd)	134.3 (18.3) / 79.9 (10.3)
Hypertension (on meds, %)	15.7
BMI (mean, sd)	28.0 (4.3)
Smoking (Present, %)	6.8
Physical activity (low, %)	33.8
Problematic alcohol (%, missing %)	8.8, 11.2
Depression symptoms (mean, sd)	3.5 (3.4)

Table 2. Descriptive statistics of the sample population's segmented white matter hyperintensities and cognitive testing.

Descriptor	**N = 497**
Number of White Matter Lesions (mean(sd), [min, max])	24.0 (12.6), [4,141]
Lesion Volume mm^3 (mean(sd), [min, max])	263.21 (1333.0), [0.72, 34653.58]
Lesion average FA (mean(sd), [min, max])	0.29 (0.10), [0.04, 0.78]
Lesion average MD (10^3) (mean(sd), [min, max])	1.10 (0.35) [0.36, 2.94]
Lesion average RD (10^3) (mean(sd), [min, max])	0.94 (0.34), [0.26, 2.83]
Lesion average AD (10^3) (mean(sd), [min, max])	1.43 (0.40), [0.47, 3.31]
Location (Deep, %)	14.6
MMSE (mean, sd)	28.8 (1.5)
Immediate Recall, 2 trials (mean, sd)	14.2 (2.9)
Delayed Recall (mean, sd)	6.2 (2.4)
Animal Naming (mean, sd)	19.4 (5.4)

Table 3. Lesion phenotypes and descriptive characteristics. Where SD values are 0.00, this means p<0.001.

Characteristic	Low Volume-High FA (N=6056)		Low Volume-Low FA (N=3193)		High Volume-Low FA (N=2684)	
Locations	Deep (N=1295) (11%)	PVT (N=4761) (40%)	Deep (N=119) (1%)	PVT (N=3074) (26%)	Deep (N=336) (3%)	PVT (N=2348) (19%)
Volume (mean, sd)	24.7 (23.0)	24.4 (28.1)	20.9 (18.6)	28.6 (41.1)	248.6 (623.2)	1200.4 (2806.0)
Average FA (mean, sd)	0.30 (0.07)	0.35 (0.09)	0.16 (0.05)	0.20 (0.07)	0.24 (0.05)	0.27 (0.07)
Average MD (mean, sd)^3	0.83 (0.00)	0.87 (0.00)	1.19 (0.00)	1.55 (0.00)	0.96 (0.00)	1.14 (0.00)
Average RD (mean, sd)^3	0.69 (0.00)	0.70 (0.00)	1.08 (0.00)	1.39 (0.00)	0.84 (0.00)	0.98 (0.00)
Average AD (mean, sd)^3	1.11 (0.13)	1.22 (0.24)	1.39 (0.42)	1.88 (0.41)	1.20 (0.13)	1.47 (0.21)
Age (mean, sd)	71.1 (7.5)	69.1 (7.6)	71.6 (6.8)	67.1 (7.7)	71.7 (7.3)	69.3 (7.1)
Sex (female, %)	56.2	46.9	57.9	46.3	62.2	49.5
Education (low, %)	27.3	22.2	21.0	19.8	32.4	23.2
CVD conditions (2+)	43.6	31.8	42.8	26.8	52.1	32.1
Systolic BP (mean, sd)	136.2 (17.8)	135.0 (17.5)	142.3 (17.2)	133.8 (18.4)	135.5 (17.5)	134.7 (17.8)

Hypertension (on meds, %)	22.5	17.4	31.9	14.8	27.6	16.4
BMI (mean, sd)	28.36 (4.4)	28.41 (4.2)	27.84 (4.5)	28.12 (4.3)	28.35 (4.6)	27.95 (4.3)
Smoking (current, %)	10.3	7.7	5.0	6.3	13.9	8.7
Problematic Alcohol (yes, %)	11.5	9.0	19.3	10.1	10.1	7.4
Physical Activity (low, %)	40.3	34.4	36.9	33.8	38.6	33.9
Depression (mean, sd)	3.56 (3.42)	3.37 (3.3)	3.06 (3.16)	3.46 (3.39)	3.94 (3.78)	3.56 (3.47)

FIGURES

Figure 1. Spin: Spin alignment and precession around B0.. In a static field B0, slightly more spins occupy the low-energy (parallel) state, creating a net longitudinal magnetization M_0. Proton magnetic moments precess at the Larmor frequency around B0.

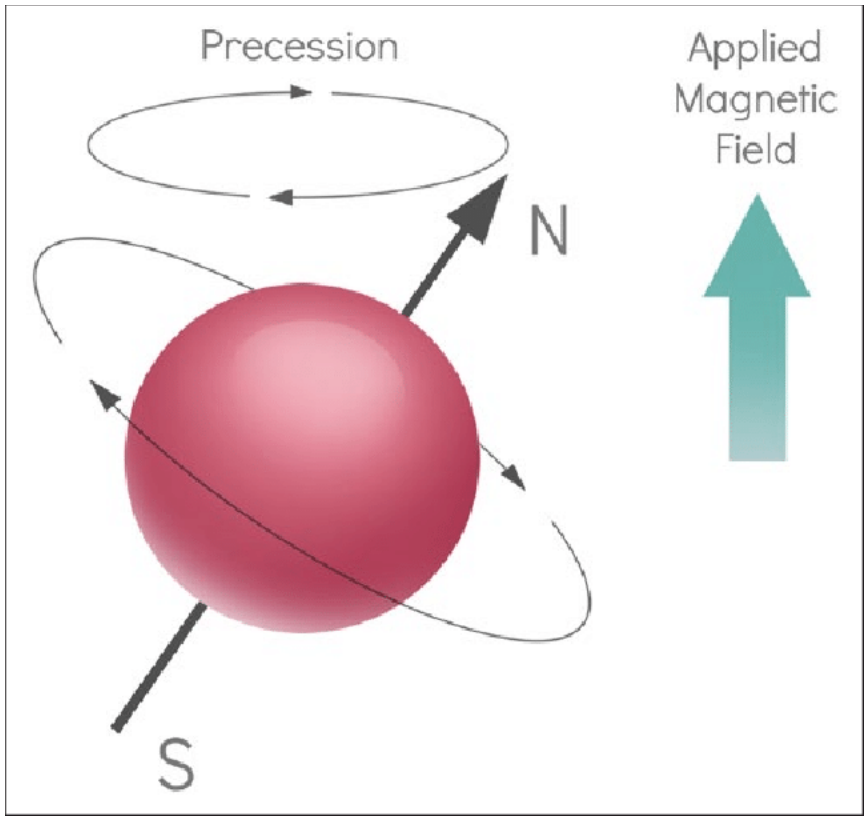

Figure 2. T1 and T2 Relaxation: Illustration of longitudinal (T1) and transverse (T2) relaxation. The upper graph shows the recovery of longitudinal magnetization over time, characterised by the T1 relaxation time. A shorter T1 (blue curve) indicated faster recovery of M(z) towards the equilibrium, while a longer T1 (red curve) indicates slower recovery. The lower graph illustrates the decay of transverse magnetization over time, characterised by the T2 relaxation time. The shorter (blue curve) indicates faster signal decay over time.

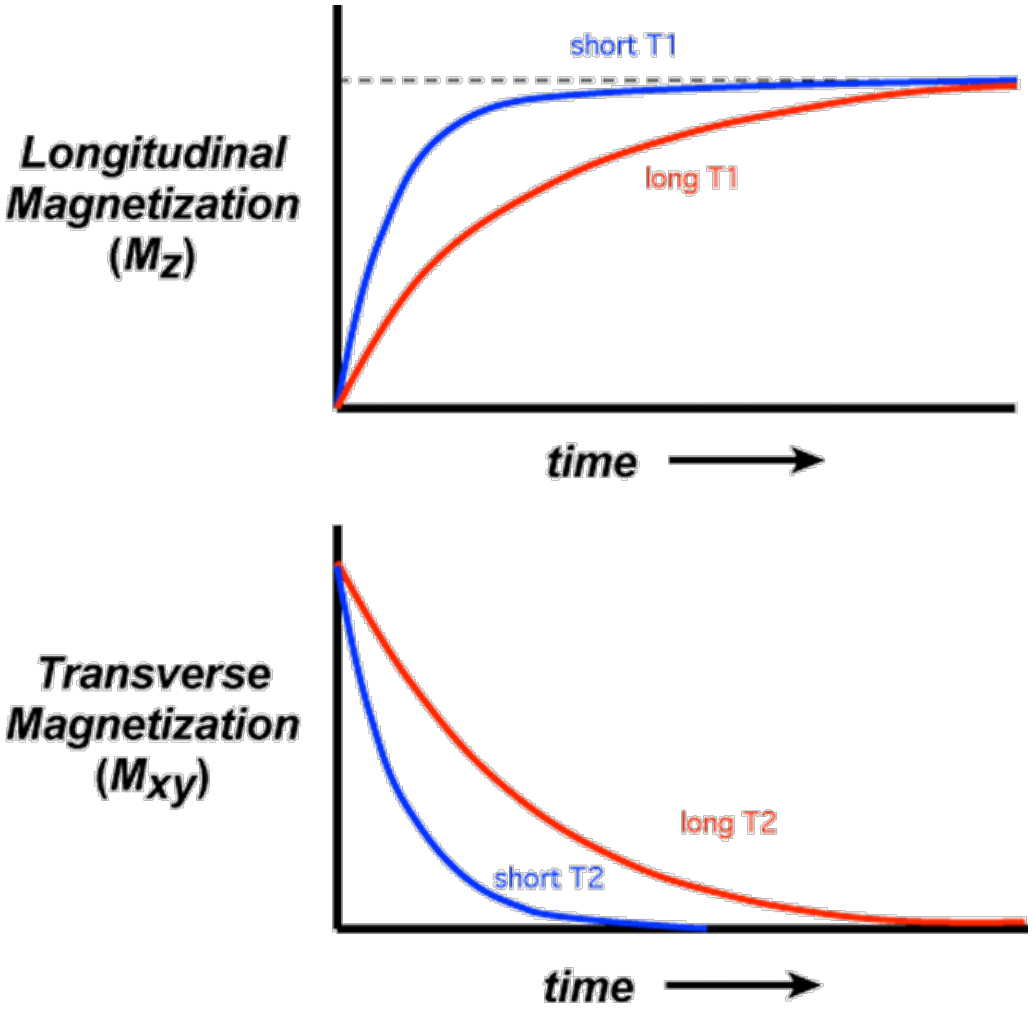

Figure 3. FLAIR Sequence: Timing diagram illustrating the Fluid Inversion Recovery (FLAIR) sequence, with specific reference to the magnetization recovery of different tissues following the 180 degree radiofrequency inversion pulse. Each tissue recovers at a predetermined rate depending on its characteristic T1 relaxation time. The longitudinal magnetization of each tissue crosses the zero point at a specific time known as its "null point". The 90 degree excitation pulse is applied at the null point of water (blue line), resulting in zero production of signal in the subsequent image.

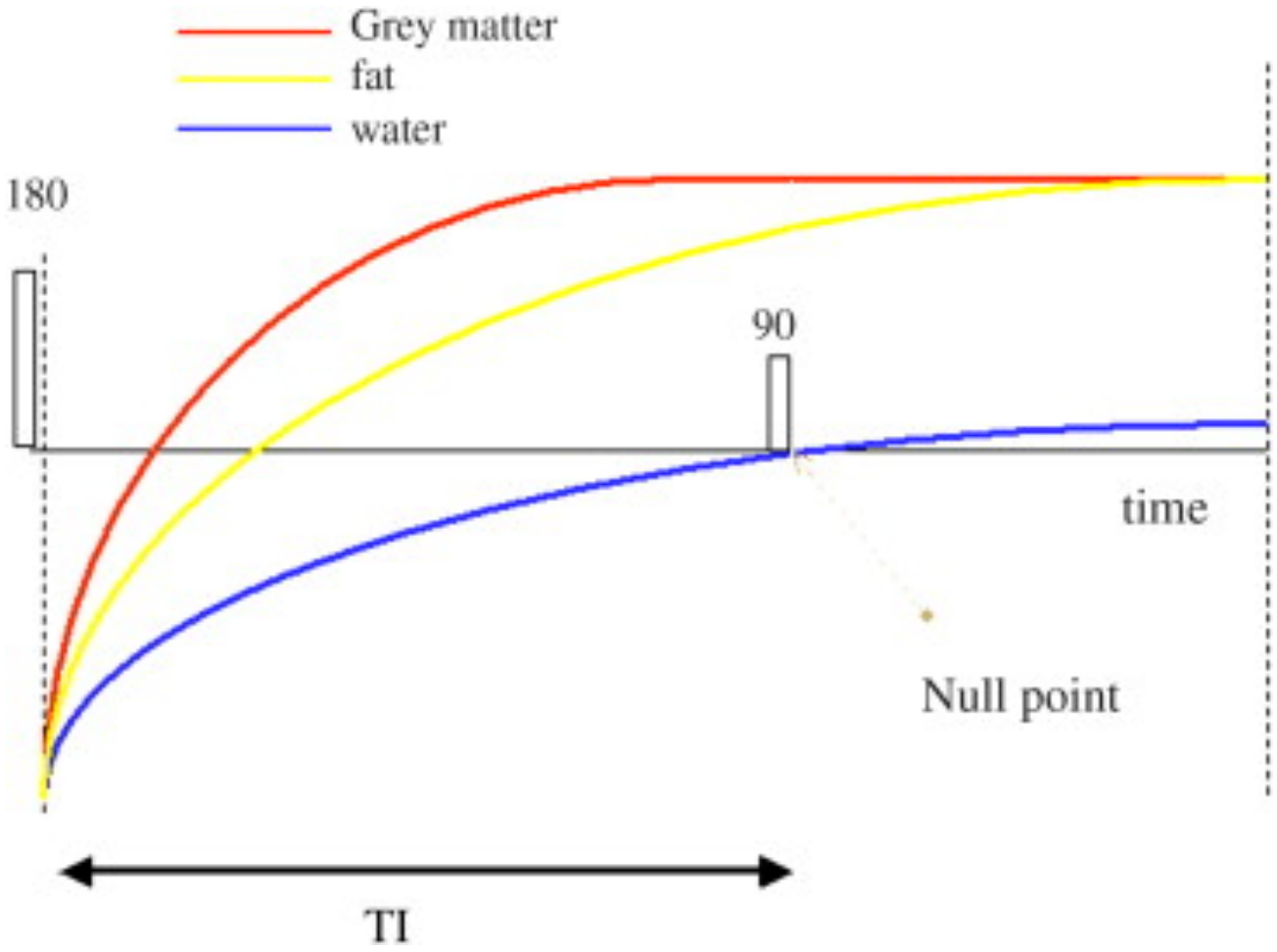

Figure 4. Isotropic and Anisotropic Diffusion: In an isotropic environment (a), water molecules diffuse equally in all directions resulting in a spherical representation of the diffusion tensor indicating low Fractional Anisotropy (FA). In this case, the eigenvalues are approximately equal leading to an FA close to zero. In anisotropic environments (b), such as white matter tracts, water diffusion is restricted and preferentially occurs along specific directions I.e. the orientation of the fibers. This directional preference results in an ellipsoidal representation of the diffusion tensor, the principal eigenvector corresponding to the direction of water diffusion within the tract. This is termed high Fractional Anisotropy, indicating a strong directional diffusion and potentially varying MD depending on overall diffusivity.

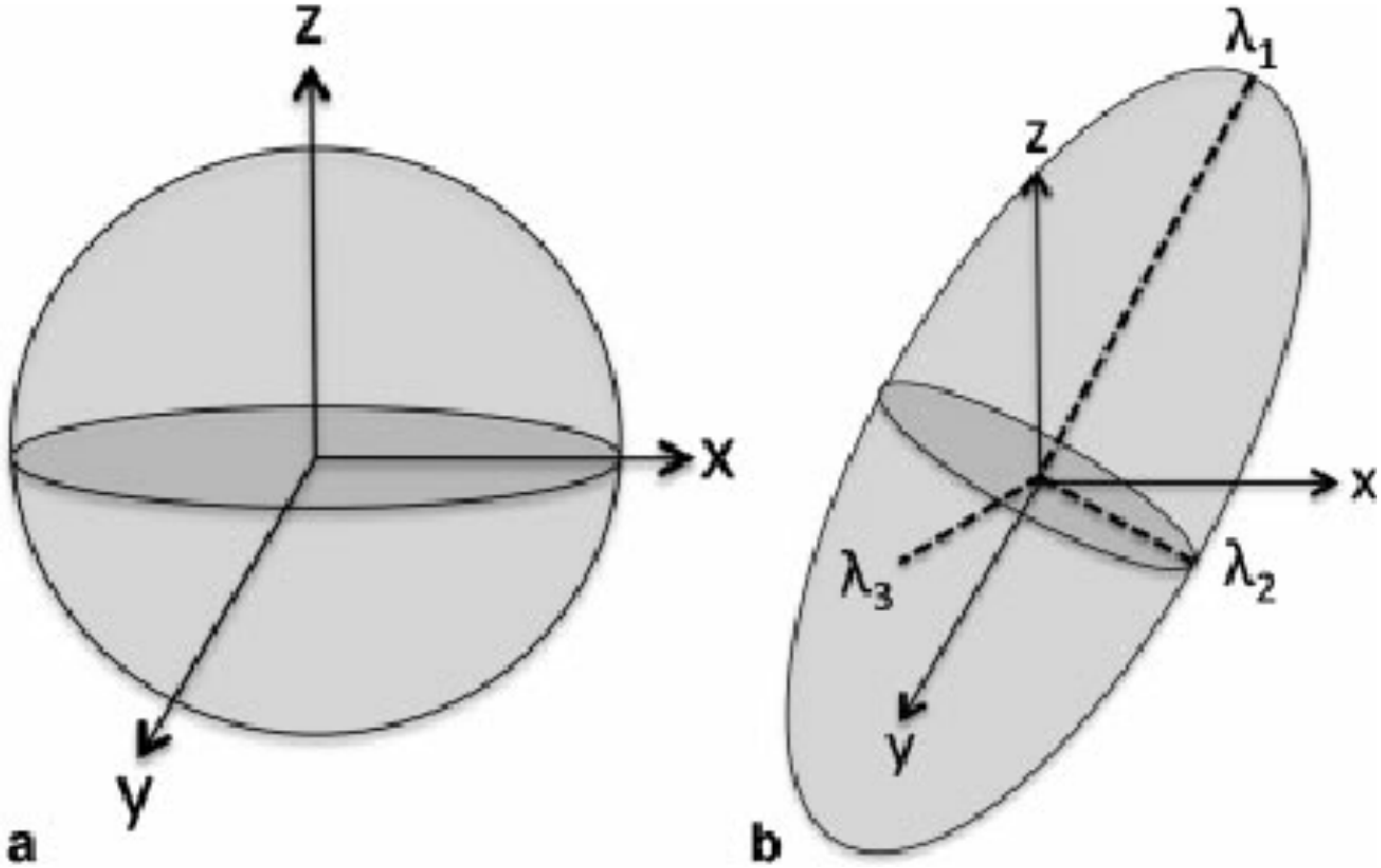

Figure 5. Illustration of the principle of DWI: Differentiating normal from pathological tissues by exploiting the differences in water molecule diffusion. Restricted diffusion (pathology) appears bright, while free diffusion (normal tissue) appears dark on high b-value images.

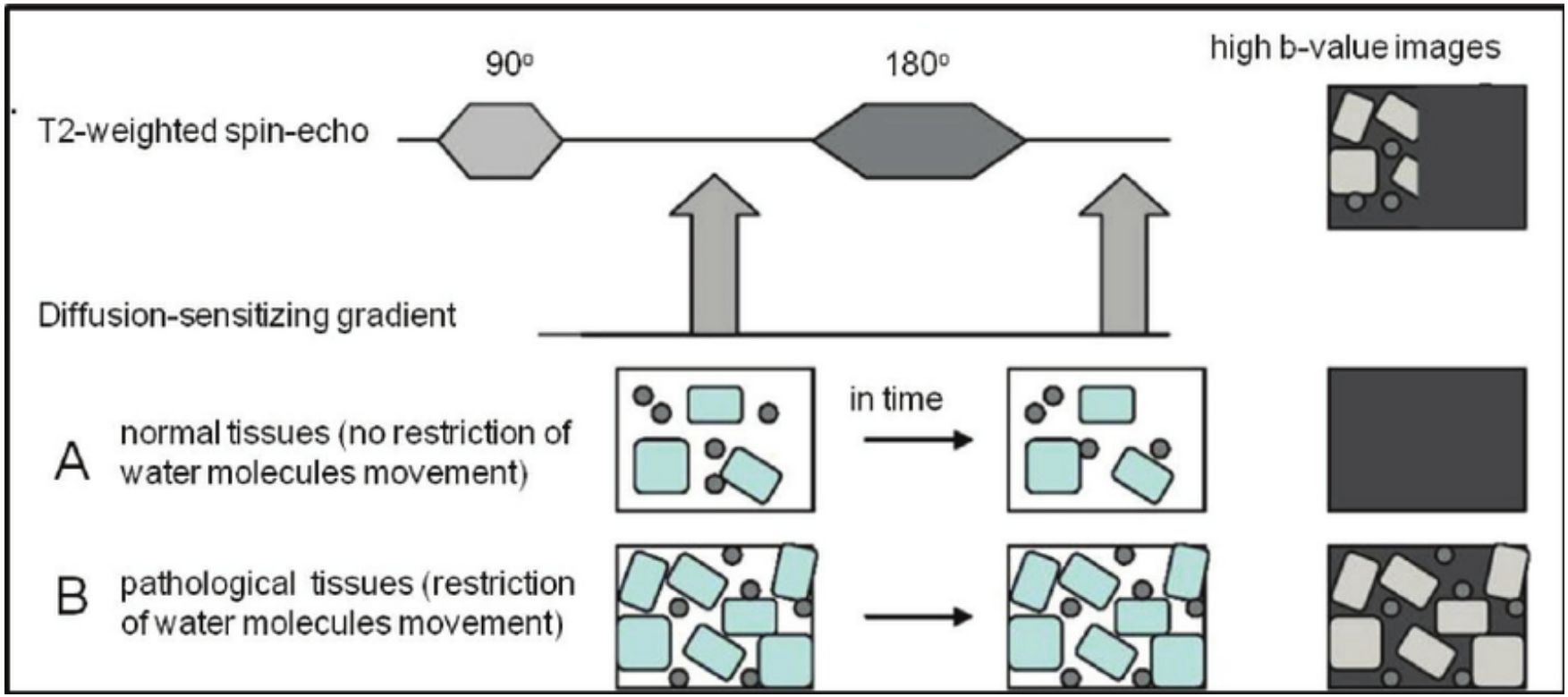

Figure 6. Cohort demographics analysis.

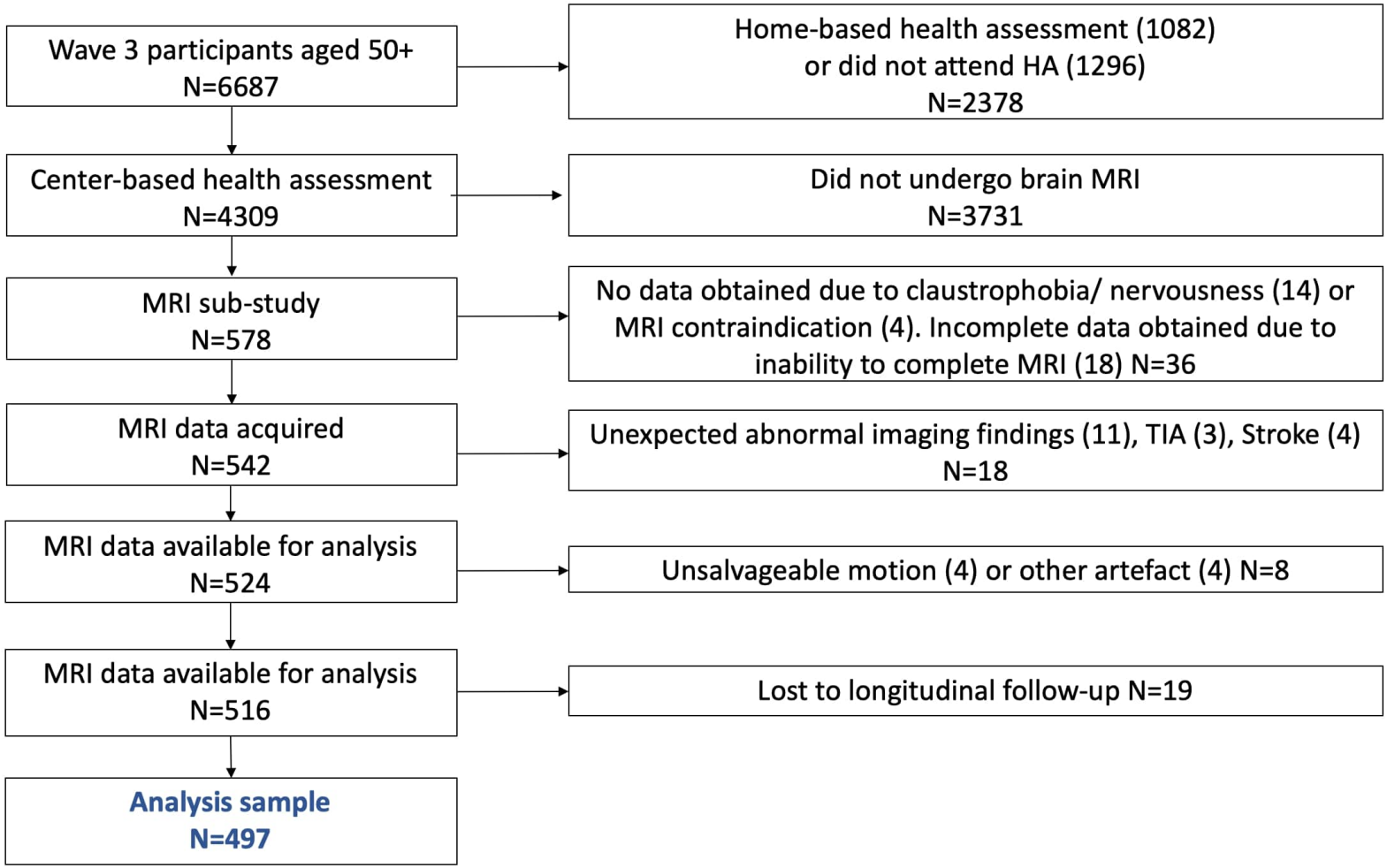

Figure 7. Lesion phenotype cluster analysis.

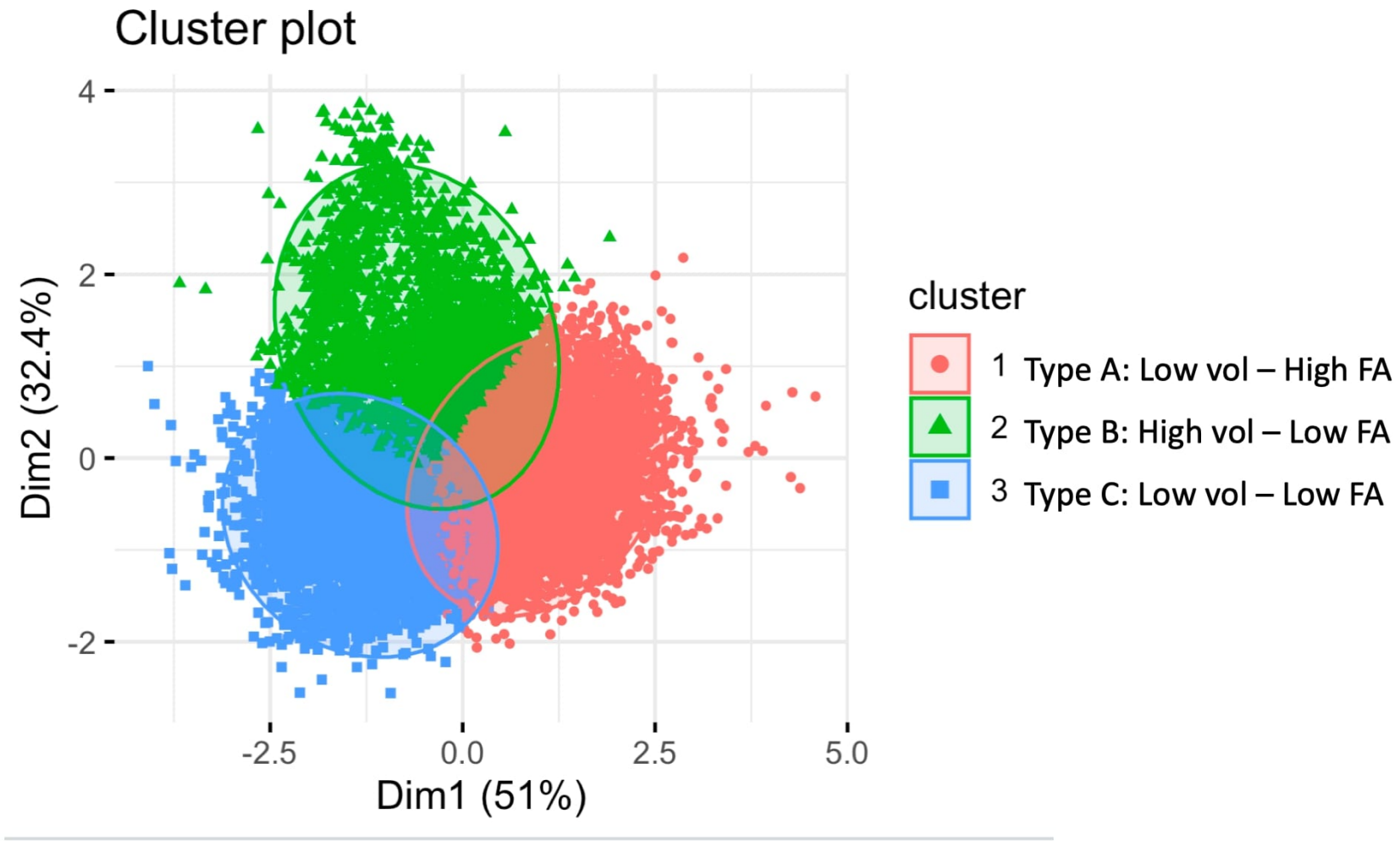

Figure 8. Baseline linear mixed effects models for Deep High Volume, Low FA Lesions at waves 3, 4, 5 and 6.

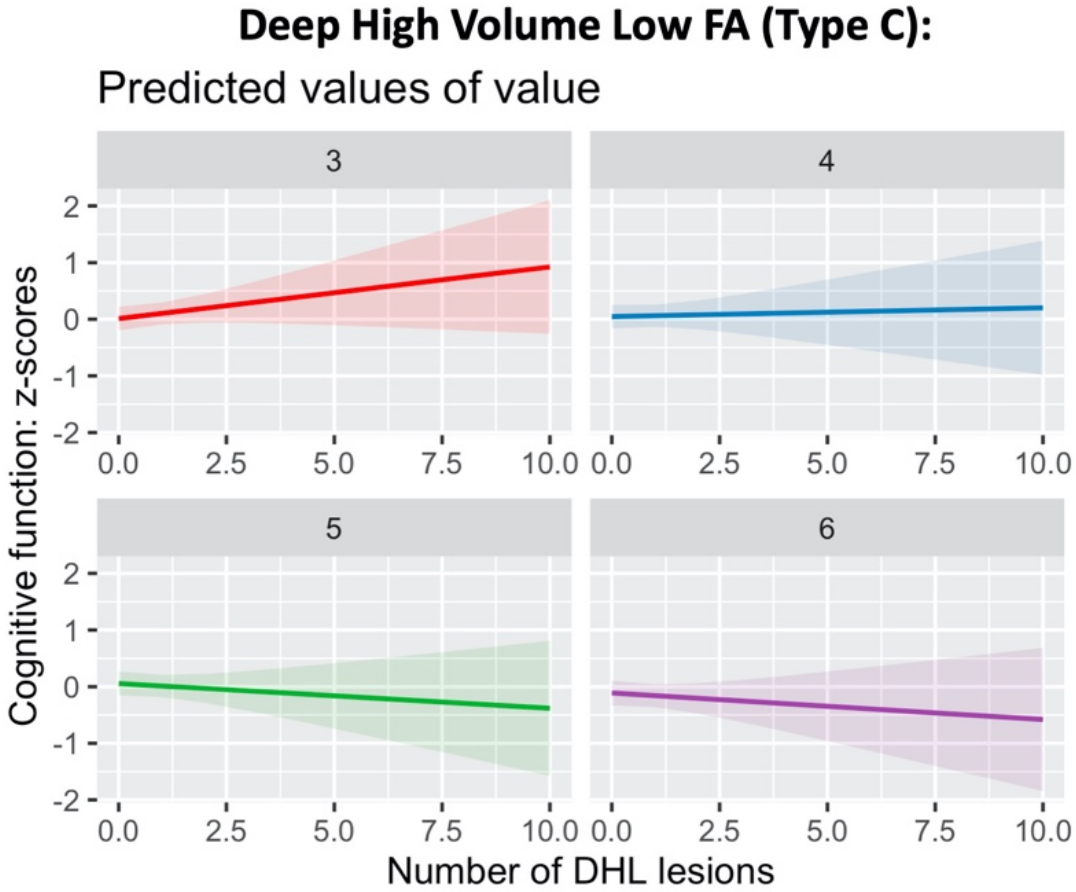

Fixed effects.	Coeff.	P-value
DHL lesions: Wave 4	-0.07562	0.18368
DHL lesions: Wave 5	-0.13505	0.01856 *
DHL lesions: Wave 6	-0.13792	0.02551 *

Adjusted for age, sex and education

Remained significant when further adjusted for CVD, hypertension, bmi, smoking, alcohol consumption, physical activity and depression

Figure 9. Baseline linear mixed effects models for Periventricular High Volume, Low FA Lesions at waves 3, 4, 5 and 6.

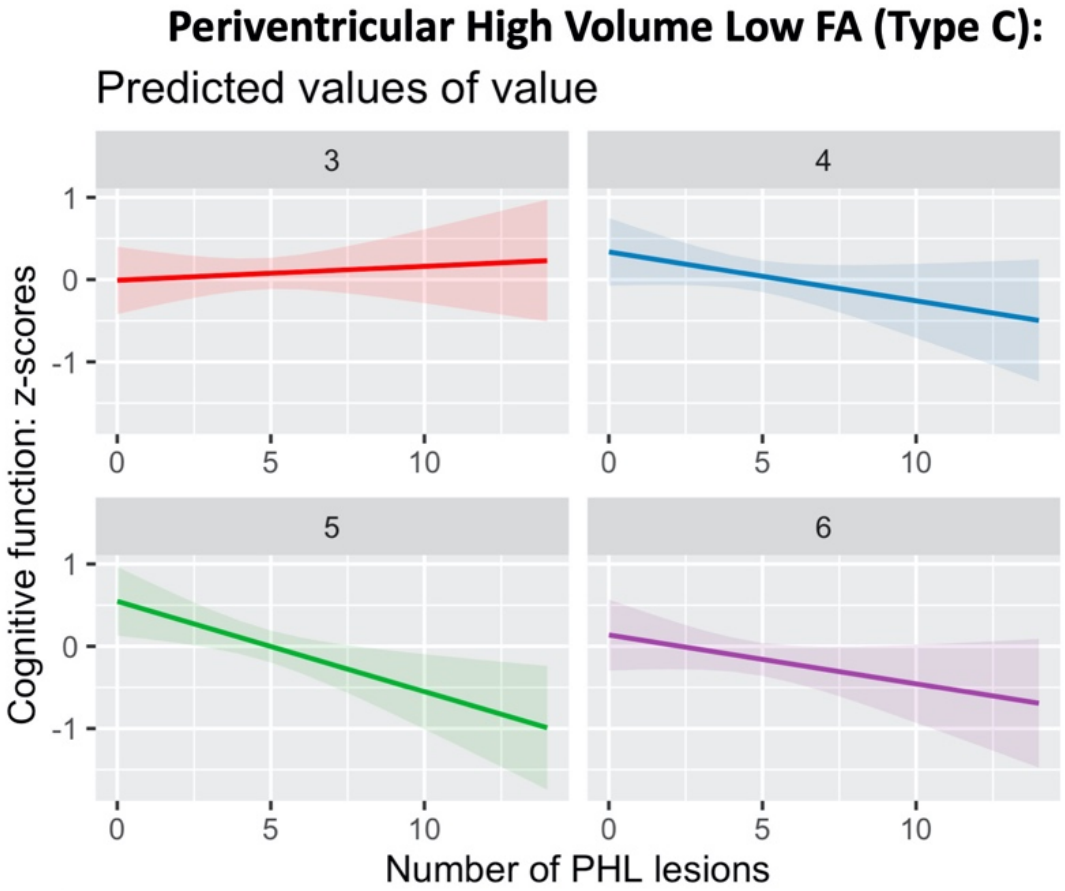

Fixed effects.	Coeff.	P-value
PHL lesions: Wave 4	-0.07676	0.029282 *
PHL lesions: Wave 5	-0.12707	0.000394 ***
PHL lesions: Wave 6	-0.07654	0.041460 *

Adjusted for age, sex and education

Remained significant when further adjusted for CVD, hypertension, bmi, smoking, alcohol consumption, physical activity and depression

Figure 10. Baseline linear mixed effects models for Deep Low Volume, High FA Lesions at waves 3, 4, 5 and 6.

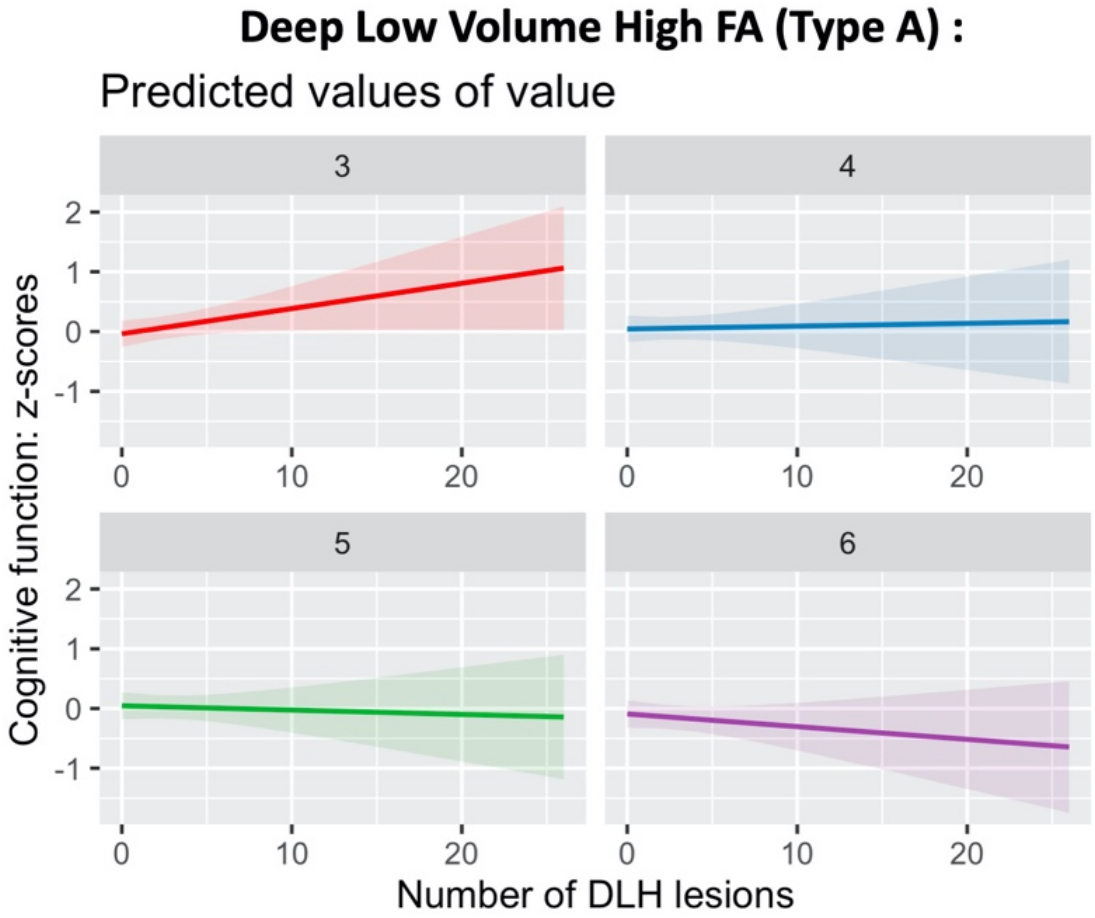

Fixed effects.	Coeff.	P-value
DLH lesions: Wave 4	-0.03755	0.05741 .
DLH lesions: Wave 5	-0.04945	0.01330 *
DLH lesions: Wave 6	-0.06347	0.00290 **

Adjusted for age, sex and education
Remained significant when further adjusted for CVD, hypertension, bmi, smoking, alcohol consumption, physical activity and depression

Figure 11. Association of Periventricular Low Volume Low FA lesions with Cognitive Decline.

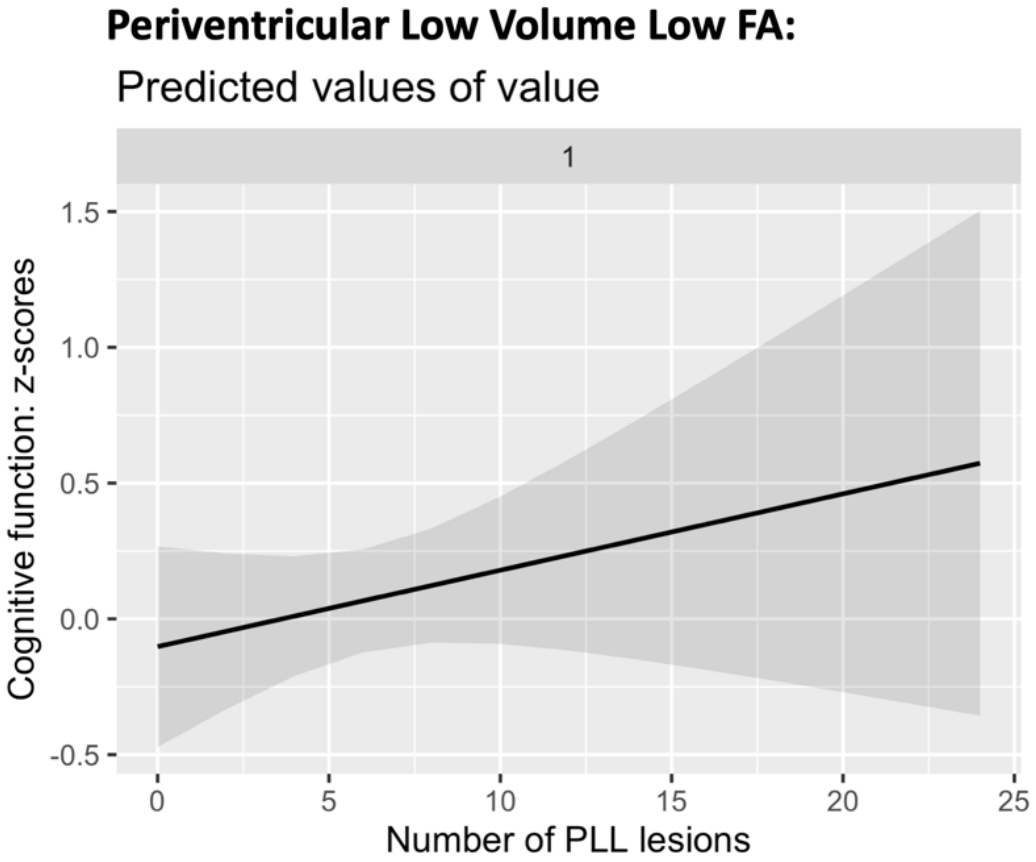

The higher the N of periventricular low volume, low FA lesions, the better the cognitive function (B=0.04; p=.02)